

Stereoselective Synthesis of Allele-Specific BET Inhibitors

Adam Bond, Andrea Testa, [Alessio Ciulli](#)

Submitted date: 16/05/2020 • Posted date: 18/05/2020

Licence: CC BY-NC-ND 4.0

Citation information: Bond, Adam; Testa, Andrea; Ciulli, Alessio (2020): Stereoselective Synthesis of Allele-Specific BET Inhibitors. ChemRxiv. Preprint. <https://doi.org/10.26434/chemrxiv.12317354.v1>

Developing stereoselective synthetic routes that are efficient and cost-effective is important to allow easy access to biologically active molecules. Our previous syntheses of allele-selective bumped inhibitors of the Bromo and Extra-Terminal (BET) bromodomain proteins, Brd2, Brd3, Brd4 and BrdT, required a wasteful, late-stage alkylation step and expensive chiral separation. To circumvent these limitations, we developed a route based on stereocontrolled alkylation of an aspartic acid derivative that was used in a divergent, racemisation-free protocol to yield structurally diverse and enantiopure triazolodiazepines. With this approach, we synthesized bumped thienodiazepine-based BET inhibitor, ET-JQ1-OMe, in five steps and 99% ee without the need for chiral chromatography. Exquisite selectivity of ET-JQ1-OMe for Leu-Ala and Leu-Val mutants over wild-type bromodomain was confirmed by isothermal titration calorimetry and X-ray crystallography. Our new approach provides unambiguous chemical evidence for the absolute stereochemistry of the active, allele-specific BET inhibitor and a viable route that will facilitate wider access to this compound class.

File list (2)

Bond manuscript for ChemRxiv.pdf (571.31 KiB)

[view on ChemRxiv](#) • [download file](#)

Merged Supporting Information 2.pdf (3.41 MiB)

[view on ChemRxiv](#) • [download file](#)

Stereoselective synthesis of allele-specific BET inhibitors

Adam G. Bond, Andrea Testa,† Alessio Ciulli*

Author's affiliation: Division of Biological Chemistry and Drug Discovery, School of Life Sciences, University of Dundee, James Black Centre, Dow Street, Dundee DD1 5EH, United Kingdom

Abstract:

Developing stereoselective synthetic routes that are efficient and cost-effective is important to allow easy access to biologically active molecules. Our previous syntheses of allele-selective bumped inhibitors of the Bromo and Extra-Terminal (BET) bromodomain proteins, Brd2, Brd3, Brd4 and BrdT, required a wasteful, late-stage alkylation step and expensive chiral separation. To circumvent these limitations, we developed a route based on stereocontrolled alkylation of an aspartic acid derivative that was used in a divergent, racemisation-free protocol to yield structurally diverse and enantiopure triazolodiazepines. With this approach, we synthesized bumped thienodiazepine-based BET inhibitor, ET-JQ1-OMe, in five steps and 99% ee without the need for chiral chromatography. Exquisite selectivity of ET-JQ1-OMe for Leu-Ala and Leu-Val mutants over wild-type bromodomain was confirmed by isothermal titration calorimetry and X-ray crystallography. Our new approach provides unambiguous chemical evidence for the absolute stereochemistry of the active, allele-specific BET inhibitor and a viable route that will facilitate wider access to this compound class.

Chemical biology and therapeutic development rely on the design or discovery of biologically active compounds that typically contain one or more stereocenters. Amongst the different stereoisomers for a given compound, it is often the case that only one (so-called eutomer) exhibits the desired biological activity, while the other(s) (distomers) may be inactive or have toxic and off-target effects.¹ Studying and testing diastereomeric or racemic mixtures have limitations and could lead to unwanted or artefactual results, it is therefore important to develop stereoselective routes and processes which yield solely the desired biologically active molecule.²⁻⁵

The four Bromo and Extra-Terminal (BET) proteins, Brd2, Brd3, Brd4 and BrdT, play a crucial role in transcriptional regulation and other processes such as cell proliferation and cell cycle progression.⁶⁻⁸ BET proteins have become attractive therapeutic targets as their misregulation has been linked to diseases such as cancer, neurological disorders and inflammation.⁹⁻¹⁰ Association to disease has fuelled great interest in the field to develop small molecule BET inhibitors, many of which are in the clinic.¹¹⁻¹⁴ Many BET inhibitors include a triazolodiazepine scaffold, including JQ1 (ref. ¹⁵) and I-BET762 (ref. ¹⁶) (Fig. 1). Due to the high conservation of BET bromodomains at the acetyl-lysine binding pocket, these inhibitors are pan-selective so do

not significantly discriminate between the bromodomains within and across the BET family.¹⁷⁻¹⁸ More recently, compounds have been reported to show selective inhibition for the first bromodomains (BD1), or for the second bromodomains (BD2), of the BET family.¹⁹⁻²² Although these compounds can discriminate between the two bromodomains, they still lack the ability to discriminate between the bromodomains of the four BET proteins.

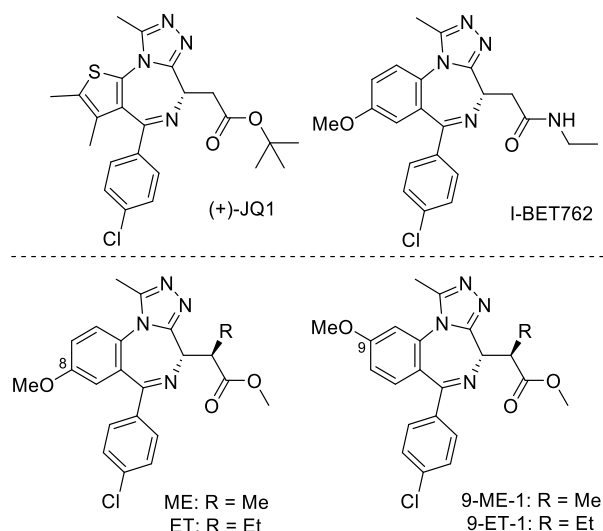


Figure 1. Pan and allele-selective BET inhibitors. Pan-selective inhibitors (+)-JQ1 and I-BET762 (top) and allele selective probes ME, ET, 9-ME-1 and 9-ET-1 (bottom).

To aid individual intra-BET selectivity, we previously developed a chemical genetics approach to engineer orthogonal protein/ligand pairs between the BET proteins and selective inhibitors.²³ Our “bump & hole” approach involved the introduction of a single point mutation to the target BET bromodomain by replacing a leucine residue that is conserved across all BET bromodomains, with a smaller residue (e.g. alanine) to generate a “hole”.²⁴ Simultaneously, an alkyl “bump” is incorporated at a diastereotopic, methylene group on the parent scaffold based on the I-BET762 inhibitor, aimed to both complement the size of the “hole” and provide a steric clash to the wild-type protein. This approach led to the generation of allele specific chemical probes ET (ref. ²⁴) and 9-ME-1 (ref. ²⁵) (Fig. 1) targeting the leucine to alanine (L/A) or the less disruptive, leucine to valine (L/V) mutation, respectively. We used this new system to dissect individual roles of BD1 vs BD2 in Brd4 and the other BET proteins and showed that while the BD1 is necessary and sufficient for chromatin binding, the BD2 plays a role in transcriptional regulation.²⁴⁻²⁵

Our previous approaches for incorporation of an alkyl “bump” into the I-BET scaffold involved alkylation of a potassium enolate to afford bumped I-BET derivatives with undesired diastereoselectivity and in low yields (Fig. 2A). Epimerisation was required to enhance the amount

of desired diastereomer, and further separation by high performance liquid chromatography (HPLC) to isolate the desired isomer. Due to the use of potassium hexamethyldisilazide (KHMDs) for the enolization, and the need of an epimerisation step at such a late stage of the synthesis, the products are racemic and require chiral separation to isolate the enantiomers.²⁴⁻²⁶ Separation of the enantiomers can be costly (up to £1000 for <150 mg of racemate) and leads to loss of material during the separation.

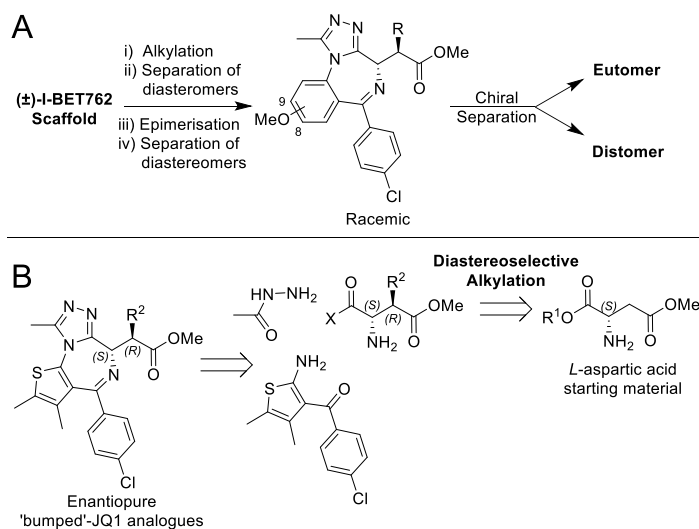


Figure 2. Synthetic routes to bumped BET inhibitors. (A) Previous synthetic strategy for bumped I-BET762 derivatives. (B) Retrosynthetic analysis for enantiopure bumped JQ1 derivatives.

We sought to address these problems by developing a new stereoselective synthetic strategy. We hypothesised that incorporating the “bump” earlier in the synthesis via a diastereoselective alkylation of an aspartic acid derivative would allow circumventing the limitations of the original route (Fig. 2B). Here, we describe a new synthetic route that allows the preparation of both novel and previously described bumped BET inhibitors stereoselectively in 99% ee. We also provide unambiguous chemical evidence to the absolute stereochemistry of the active allele-specific ligand, previously only assumed based on co-crystal structures.²⁵

Our first efforts to alkylate (+)-JQ1 directly proved unsuccessful, likely due to the steric hindrance caused by the *tert*-butyl ester. Conversion from the *tert*-butyl to a methyl ester was required to allow for the introduction of the bump. Alkylation with KHMDs and alkyl iodides proceeded with undesired diastereoselectivity towards the (S,S) diastereomer over the (S,R) diastereomer in overall alkylation yields of approx. 20%. Epimerisation of the major (S,S) isomer with sodium methoxide allows access to the desired (S,R) isomer in a 1:1 ratio with the starting

(S,S) isomer. However, the use of strong bases during alkylation and additional epimerisation steps may lead to complete racemisation of both stereocentres as previously reported,²⁴⁻²⁶ (see Scheme S1 in SI). With enantiopure (+)-JQ1 costing >\$750 per gram, and its derivatives e.g. (+)-JQ1 carboxylic acid being even more expensive, this wasteful approach is not a viable strategy for the preparation of enantiopure bumped JQ1.

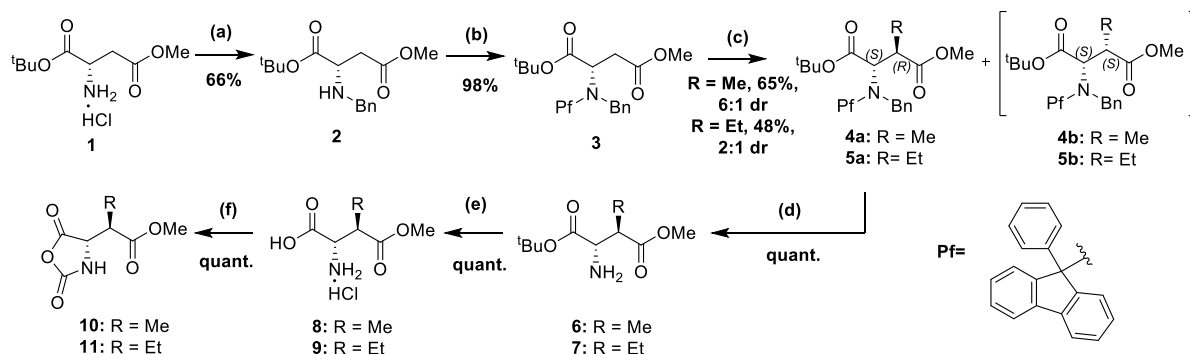
To efficiently prepare the desired bumped JQ1 derivatives as single enantiomers, we sought to stereoselectively introduce the “bump” earlier in the synthesis. Our synthetic methodology was based on previously reported stereoselective alkylation of *L*-aspartic acid diester derivatives.²⁷⁻³⁰ It was demonstrated that protection of the amino group with both 9-phenyl-9-fluorenyl (Pf) and benzyl (Bn) groups can drive diastereoselective alkylation of the β -carbon to the nitrogen while protecting the α -proton from epimerisation.

L-aspartic acid derived diester **1** was first treated with benzaldehyde in dichloromethane (DCM) and the formation of the intermediate imine was monitored by ¹H-NMR. Reduction of the imine with sodium borohydride yielded the mono-benzyl protected amine **2**. Amine **2** was treated with 9-phenyl-9-fluorenyl bromide, lead (II) nitrate and tribasic potassium phosphate in acetonitrile to form the *N*-diprotected diester **3**. Deprotonation of diester **3** with lithium hexamethyldisilazide (LHMDS) at –78°C in tetrahydrofuran (THF) afforded the desired *E*-lithium enolate, which was reacted with methyl iodide at –40°C over 16 h. This yielded methylated diastereomers **4a** (*S,R*) and **4b** (*S,S*) in a 6:1 ratio respectively. Ethylated compounds **5a** and **5b** were prepared in a similar way by deprotonation of diester **3** with LHMDS at –78°C in THF followed by addition of ethyl iodide and stirring at –78°C for 16 h. This was left for a further 24 h at –23°C to yield diastereomers **5a** (*S,R*) and **5b** (*S,S*) in a 2:1 ratio respectively. The choice of LHMDS over the respective potassium base, KHMDS, was motivated by prior findings that switching between these bases can reverse the diastereoselectivity on a similar aspartate derived diester to compound **3**.²⁷ Using the potassium base leads to a chelate controlled enolate-ester intermediate which has the opposite geometry to the non-chelated, ‘open’ lithium enolate intermediate and influences facial selectivity to attack by the electrophile (alkyl iodide).

Removal of both Pf and Bn groups were performed by hydrogenation of alkylated diesters **4a** and **5a** with a suspension of 10% palladium on carbon (Pd/C) in acetic acid to give free amines **6** and **7** in high yields. The resulting free amines were dissolved in a 1:1 mixture of trifluoroacetic acid (TFA) and dichloromethane to achieve the *tert*-butyl ester deprotection and leave the free amino acid as a TFA salt. The TFA salts were then dissolved in 2 M HCl and freeze-dried to obtain the amino acids **8** and **9** as HCl salts. Conversion of salts posed crucial for the next step as any

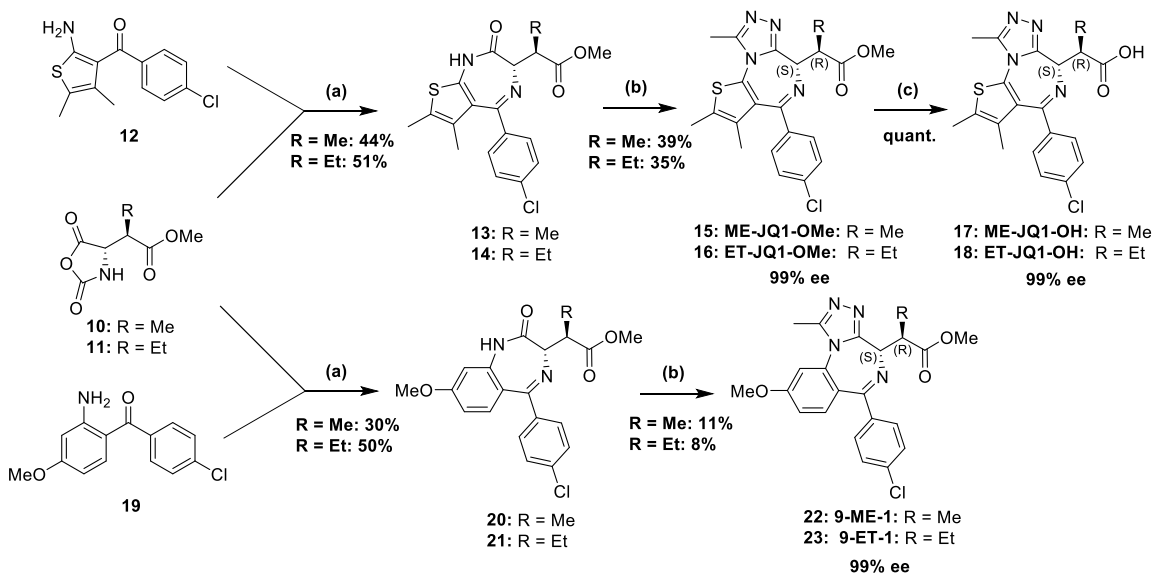
TFA present lead to the formation of trifluoroacetamide by-products. Amino acids **8** and **9** (HCl salts) were treated with triphosgene in THF over 16 h to yield the key *N*-carboxyanhydrides (NCAs) **10** and **11**, as precursors of the alkylated sidechain fragment. These were used in the next steps without the need for further purification (Scheme 1).

Scheme 1. Stereoselective synthesis of *N*-carboxyanhydrides **10 and **11**.**



Conditions: (a) i) Na₂CO₃, EtOAc, H₂O, ii) PhCHO, DCM, 2h, r.t., iii) NaBH₄, MeOH, 1 h, 0°C – r.t.; (b) PfbBr, K₃PO₄, Pb(NO₃)₂, MeCN, r.t., 4 h; (c) i) LHMDs, THF, –78°C, 1 h, ii) MeI/EtI, –78°C to –23°C, 48 h/96 h; (d) H₂, Pd/C, AcOH, r.t., 24 h; (e) i) TFA, DCM, r.t., 2 h, ii) 2 M HCl, freeze dry; (f) Triphosgene, THF, r.t., 16 h.

Scheme 2. Formation of thienodiazepines **15-18 and benzodiazepine derivatives **22** and **23**.**



Conditions: (a) i) TFA, Toluene, 60°C, 0.5 h, ii) TEA, 80°C, 16 h; (b) i) KO^tBu, THF, –78°C to –10°C, 0.5 h, ii) (OEt)₂P(O)Cl, –78°C to –10°C, 0.75 h, iii) AcNHNH₂, r.t., 1 h, iv) n-butanol, 90°C, 1 h; (c) LiOH, THF:H₂O 4:1, R = Me; r.t., 1 to 3 days; R = Et: 45°C, 1 wk.

Next, thienodiazepines **13** and **14** were formed in a condensation reaction between NCAs **10** and **11** and amino ketone **12** by heating in the presence of TFA and subsequently triethylamine (TEA) in toluene as reported by Fier et al.³¹ The use of this methodology for the benzodiazepine ring formation was crucial in our synthetic strategy as it was found to retain the stereochemistry of the amino acid derived NCA. Deprotonation of the lactam in both **13** and **14** with potassium *tert*-butoxide and addition of diethyl chlorophosphate, as described,³² gave the activated phosphorylimidate intermediate which was not isolated. This was subsequently reacted with acetylhydrazine which led to the formation of the triazole ring in the final compounds **15** (ME-JQ1-OMe) and **16** (ET-JQ1-OMe) with 99% ee determined with supercritical fluid chiral chromatography (Scheme 2, see SI for analytical details). Overall, we were able to achieve ~40 mg of enantiopure product in just five, yield limiting, steps from <£100 worth of starting materials. In comparison, our previous approach required six steps, including expensive chiral purification (~£1,000) and 1 g of JQ1 (\$750) to achieve the same amount of pure product.

Quantitative conversion to carboxylic acids **17** (ME-JQ1-OH) and **18** (ET-JQ1-OH) was achieved by treating esters **15** and **16** in a 4:1 mixture of THF to either a 0.54 M or 0.65 M lithium hydroxide (LiOH) solution respectfully. Heating to 45°C was required for ethyl bumped compound **16** due to the conversion being much slower in comparison to the methyl bumped compound **15**. These very mild conditions were essential to avoid epimerisation of the alkylated stereocenter adjacent to the carbonyl group. Using higher concentrations of LiOH and and/or higher temperatures resulted in an increased rate of hydrolysis but led to substantial epimerisation to the undesired (*S,S*) diastereomer. Access to these free acids allows the possibility for further functionalisation (e.g. via amide or ester bond formation).

Having achieved the novel bumped JQ1 derivatives, we next sought to demonstrate the versatility and scope of our new route by attempting to synthesise the I-BET-based bumped probes, 9-ME-1 and 9-ET-1.²⁵ By using NCA precursors **10** and **11**, and treating them with aminobenzophenone **19** in the same condensation reaction as described previously, yielded benzodiazepines **20** and **21**. Subsequent triazole ring formation via a similar phosphorylimidate intermediate as described above yielded the final ligands, **22** (9-ME-1) and **23** (9-ET-1), with 99% ee determined with supercritical fluid chiral chromatography (see SI for analytical details). We have also demonstrated the accessibility for the (*S,S*) diastereomer (reported as **16*** in the SI) of **16** using the minor ethylated diastereomer **5b** as the starting point. Stereoselective access to 'inactive' stereoisomers provides important negative controls to increase validity and robustness of findings in both biophysical and biological assays.

To further characterise our novel bumped compound, we studied the binding of **16** to Brd4(2) L387A, L387V and wild-type using isothermal titration calorimetry (ITC). We found undetectable/no binding of **16** to the wild-type protein, consistent with ethyl bumped compounds reported previously.²⁴⁻²⁵ Crucially, **16** demonstrated very high binding affinity to both L/A and L/V mutants with equipotent K_d values of 65 nM (Fig. 3A). To validate the binding mode, we solved a high resolution (1.56 Å) X-ray structure of Brd2(2)^{L383V} co-crystallised with **16** (Fig. 3B). We found that **16** adopts a similar binding mode to 9-ME-1 and 9-ET-1 (see SI Fig. S1), positioning the ethyl “bump” towards the “hole” formed by the L/V mutation.

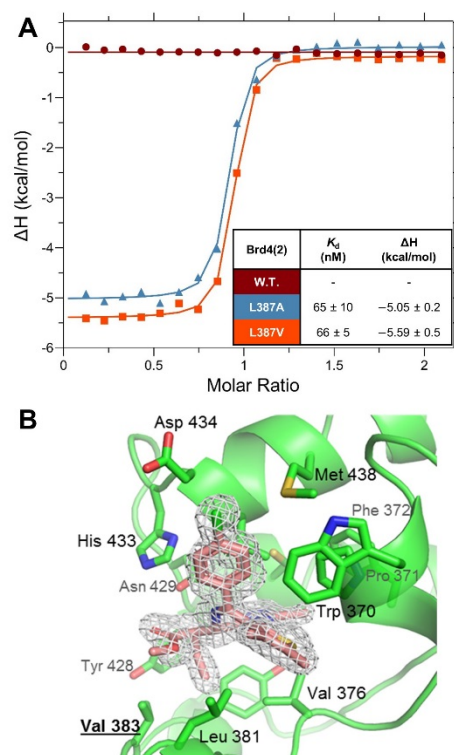


Figure 3. Biophysical and structural characterization of novel JQ1-based bumped inhibitor. (A) ITC titrations of ET-JQ1-OMe (**16**) against wild-type (W.T.) (maroon), L387A (blue) and L387V (red) constructs of Brd4(2). Table shows values taken as a mean and standard deviation from 3 replicates. (B) Co-crystal structure of **16** (pink carbons) with Fo-Fc omit map (grey mesh, contour: 3σ) bound to Brd2(2)^{L383V} mutant (green, cartoon representation; green carbons, binding site side chains) (PDB code: 6YTM). Bump and hole residue Val 383 is highlighted.

In summary, we describe a new stereoselective approach to successfully synthesise novel bumped JQ1 derivatives in 99% ee. Compared to the previous method, our new route achieves enantiopure product in one less step and without the need for chiral purification step, from widely available and relatively inexpensive starting materials. We validated the high allele-selectivity of

ET-JQ1-OMe over wild-type and provided unambiguous chemical evidence to the absolute stereochemistry of the eutomer. We have also demonstrated versatility and scope to synthesise previously reported bumped I-BET762 derivatives, 9-ME-1 and 9-ET-1 in 99% ee, providing a synthetic strategy to avoid wasteful, late-stage alkylation steps and chiral separation. Access to carboxylic acid derivatives retaining enantiomeric purity enables functionalisation into conjugates such as biotinylated and fluorescent probes and PROTACs,²³ which will further expand the scope and utility of this new synthetic strategy for chemical biology investigation.

Associated Content

Supporting Information. Supplementary results (Figures S1–S5 and Table S1); materials and methods section; supplementary references and NMR spectra. Atomic coordinates and structure factors for the crystal structure of Brd2(BD2)-L383V mutant in complex with ET-JQ1-OMe has been deposited in the protein databank (PDB) under accession number 6YTM.

AUTHOR INFORMATION

Corresponding Author

* Contact information for the author to whom correspondence should be addressed:

Alessio Ciulli, a.ciulli@dundee.ac.uk

Present Addresses

† Andrea Testa: Amphista Therapeutics Ltd, Bo'Ness Road, Newhouse, ML1 5UH, United Kingdom

Author Contributions

The manuscript was written through contributions of all authors, and all authors have given approval to the final version of the manuscript.

ORCID IDs:

Adam Bond: 0000-0002-1271-1032

Andrea Testa: 0000-0002-8973-9711

Alessio Ciulli: 0000-0002-8654-1670

Funding Sources

Research reported in this publication was supported by the Medical Research Scotland (PhD studentship 1170-2017 to A.B.). The A.C. lab was funded by awards from the UK Biotechnology

and Biological Sciences Research Council (BBSRC, grant BB/J001201/2) and the European Research Council (ERC, Starting Grant ERC-2012-StG-311460 DrugE3CRLs). Biophysics and drug discovery activities were supported by Wellcome Trust strategic awards to Dundee (100476/Z/12/Z and 094090/Z/10/Z, respectively).

Notes

The authors declare the following competing financial interest(s): The Ciulli laboratory receives or has received sponsored research support from Boehringer Ingelheim, Eisai, Nurix, Ono Pharmaceuticals, and Amphista Therapeutics.

A.C. is a scientific founder, shareholder, non-executive director and consultant of Amphista Therapeutics, a company that is developing targeted protein degradation therapeutic platforms. The remaining author reports no competing interests.

ACKNOWLEDGMENTS

We thank Kwok-Ho Chan for the gift of purified recombinant proteins; Angus Cowan for help with solving the crystal structure; Sarath Ramachandran and Ryan Casement for assisting with ITC and crystallography; Darryl McConnell (Boehringer Ingelheim) for discussions; Reach Separations for chiral analysis; and staff at Diamond Light Source for synchrotron access.

ABBREVIATIONS

AcNHNH₂, acetyl hydrazine; AcOH, acetic acid; BD1, first bromodomain; BD2, second bromodomain; BET, Bromo and extra-terminal; Brd, bromodomain; DCM, dichloromethane; ITC, isothermal titration calorimetry; KHMDs, potassium hexamethyldisilazide; LHMDs, lithium hexamethyldisilazide; NCA, N-carboxyanhydride; PfBr, phenylfluorenyl bromide; PROTACs, proteolysis targeting chimeras; TFA, trifluoroacetic acid; THF, tetrahydrofuran.

References

1. Nguyen, L. A.; He, H.; Pham-Huy, C., Chiral drugs: an overview. *Int J Biomed Sci.* **2006**, 2 (2), 85-100.
2. Nicolaou, K. C.; Chakraborty, T. K.; Piscopio, A. D.; Minowa, N.; Bertinato, P., Total synthesis of rapamycin. *J Am Chem Soc.* **1993**, 115 (10), 4419-4420.
3. Wu, X.; Stockdill, J. L.; Wang, P.; Danishefsky, S. J., Total Synthesis of Cyclosporine: Access to N-Methylated Peptides via Isonitrile Coupling Reactions. *J Am Chem Soc.* **2010**, 132 (12), 4098-4100.
4. Skotnitzki, J.; Spessert, L.; Knochel, P., Regio- and Stereoselective Allylic Substitutions of Chiral Secondary Alkylcopper Reagents: Total Synthesis of (+)-Lasiol, (+)-13-Norfaranal, and (+)-Faranal. *Angew Chem Int Ed Engl.* **2019**, 58 (5), 1509-1514.
5. Mitachi, K.; Aleiwi, B. A.; Schneider, C. M.; Siricilla, S.; Kurosu, M., Stereocontrolled Total Synthesis of Muraymycin D1 Having a Dual Mode of Action against Mycobacterium tuberculosis. *J Am Chem Soc.* **2016**, 138 (39), 12975-12980.
6. Baratta, M. G.; Schinzel, A. C.; Zwang, Y.; Bandopadhyay, P.; Bowman-Colin, C.; Kutt, J.; Curtis, J.; Piao, H.; Wong, L. C.; Kung, A. L.; Beroukhim, R.; Bradner, J. E.; Drapkin, R.; Hahn, W. C.; Liu, J. F.; Livingston, D. M., An in-tumor genetic screen reveals that the BET bromodomain protein, BRD4, is a potential therapeutic target in ovarian carcinoma. *Proc Natl Acad Sci U S A.* **2015**, 112 (1), 232-7.
7. Fujisawa, T.; Filippakopoulos, P., Functions of bromodomain-containing proteins and their roles in homeostasis and cancer. *Nat Rev Mol Cell Biol.* **2017**, 18 (4), 246-262.
8. Taniguchi, Y., The Bromodomain and Extra-Terminal Domain (BET) Family: Functional Anatomy of BET Paralogous Proteins. *Int J Mol Sci.* **2016**, 17 (11), 1849.
9. Belkina, A. C.; Denis, G. V., BET domain co-regulators in obesity, inflammation and cancer. *Nat Rev Cancer.* **2012**, 12 (7), 465-477.
10. Cochran, A. G.; Conery, A. R.; Sims, R. J., Bromodomains: a new target class for drug development. *Nat Rev Drug Discov.* **2019**, 18 (8), 609-628.
11. Massard, C.; Soria, J.; Stathis, A.; Delord, J.; Awada, A.; Peters, S.; Lewin, J.; Bekradda, M.; Rezai, K.; Zeng, Z., A phase Ib trial with MK-8628/OTX015, a small molecule inhibitor of bromodomain (BRD) and extra-terminal (BET) proteins, in patients with selected advanced solid tumors. *Eur J Cancer.* **2016**, 69, S2-S3.
12. Piha-Paul, S. A.; Sachdev, J. C.; Barve, M.; LoRusso, P.; Szmulewitz, R.; Patel, S. P.; Lara, P. N.; Chen, X.; Hu, B.; Freise, K. J.; Modi, D.; Sood, A.; Hutti, J. E.; Wolff, J.; Neil, B. H., First-in-Human Study of Mivebresib (ABBV-075), an Oral Pan-Inhibitor of Bromodomain and Extra

- Terminal Proteins, in Patients with Relapsed/Refractory Solid Tumors. *Clin Cancer Res.* **2019**, 25 (21), 6309-6319.
13. Alqahtani, A.; Choucair, K.; Ashraf, M.; Hammouda, D. M.; Alloghbi, A.; Khan, T.; Senzer, N.; Nemunaitis, J., Bromodomain and extra-terminal motif inhibitors: a review of preclinical and clinical advances in cancer therapy. *Future Sci OA.* **2019**, 5 (3), FSO372.
 14. Filippakopoulos, P.; Knapp, S., Targeting bromodomains: epigenetic readers of lysine acetylation. *Nat Rev Drug Discov.* **2014**, 13 (5), 337-356.
 15. Filippakopoulos, P.; Qi, J.; Picaud, S.; Shen, Y.; Smith, W. B.; Fedorov, O.; Morse, E. M.; Keates, T.; Hickman, T. T.; Felletar, I.; Philpott, M.; Munro, S.; McKeown, M. R.; Wang, Y.; Christie, A. L.; West, N.; Cameron, M. J.; Schwartz, B.; Heightman, T. D.; La Thangue, N.; French, C. A.; Wiest, O.; Kung, A. L.; Knapp, S.; Bradner, J. E., Selective inhibition of BET bromodomains. *Nature* **2010**, 468, 1067-73.
 16. Chung, C.-w.; Coste, H.; White, J. H.; Mirguet, O.; Wilde, J.; Gosmini, R. L.; Delves, C.; Magny, S. M.; Woodward, R.; Hughes, S. A.; Boursier, E. V.; Flynn, H.; Bouillot, A. M.; Bamborough, P.; Brusq, J.-M. G.; Gellibert, F. J.; Jones, E. J.; Riou, A. M.; Homes, P.; Martin, S. L.; Uings, I. J.; Tourn, J.; Clément, C. A.; Boullay, A.-B.; Grimley, R. L.; Blandel, F. M.; Prinjha, R. K.; Lee, K.; Kirilovsky, J.; Nicodeme, E., Discovery and Characterization of Small Molecule Inhibitors of the BET Family Bromodomains. *J Med Chem.* **2011**, 54 (11), 3827-3838.
 17. Galdeano, C.; Ciulli, A., Selectivity on-target of bromodomain chemical probes by structure-guided medicinal chemistry and chemical biology. *Future Med Chem.* **2016**, 8 (13), 1655-1680.
 18. Li, X.; Wu, Y.; Tian, G.; Jiang, Y.; Liu, Z.; Meng, X.; Bao, X.; Feng, L.; Sun, H.; Deng, H.; Li, X. D., Chemical Proteomic Profiling of Bromodomains Enables the Wide-Spectrum Evaluation of Bromodomain Inhibitors in Living Cells. *J Am Chem Soc.* **2019**, 141 (29), 11497-11505.
 19. Cheung, K.; Lu, G.; Sharma, R.; Vincek, A.; Zhang, R.; Plotnikov, A. N.; Zhang, F.; Zhang, Q.; Ju, Y.; Hu, Y.; Zhao, L.; Han, X.; Meslamani, J.; Xu, F.; Jaganathan, A.; Shen, T.; Zhu, H.; Rusinova, E.; Zeng, L.; Zhou, J.; Yang, J.; Peng, L.; Ohlmeyer, M.; Walsh, M. J.; Zhang, D. Y.; Xiong, H.; Zhou, M.-M., BET N-terminal bromodomain inhibition selectively blocks Th17 cell differentiation and ameliorates colitis in mice. *Proc Natl Acad Sci U S A.* **2017**, 2952-2957.
 20. Faivre, E. J.; McDaniel, K. F.; Albert, D. H.; Mantena, S. R.; Plotnik, J. P.; Wilcox, D.; Zhang, L.; Bui, M. H.; Sheppard, G. S.; Wang, L.; Sehgal, V.; Lin, X.; Huang, X.; Lu, X.; Uziel, T.; Hessler, P.; Lam, L. T.; Bellin, R. J.; Mehta, G.; Fidanze, S.; Pratt, J. K.; Liu, D.; Hasvold, L. A.; Sun, C.; Panchal, S. C.; Nicolette, J. J.; Fossey, S. L.; Park, C. H.; Longenecker, K.; Bigelow, L.; Torrent, M.; Rosenberg, S. H.; Kati, W. M.; Shen, Y., Selective inhibition of the BD2 bromodomain of BET proteins in prostate cancer. *Nature* **2020**, 578 (7794), 306-310.

21. Picaud, S.; Wells, C.; Felletar, I.; Brotherton, D.; Martin, S.; Savitsky, P.; Diez-Dacal, B.; Philpott, M.; Bountra, C.; Lingard, H.; Fedorov, O.; Müller, S.; Brennan, P. E.; Knapp, S.; Filippakopoulos, P., RVX-208, an inhibitor of BET transcriptional regulators with selectivity for the second bromodomain. *Proc Natl Acad Sci U S A*. **2013**, *110* (49), 19754.
22. Gilan, O.; Rioja, I.; Knezevic, K.; Bell, M. J.; Yeung, M. M.; Harker, N. R.; Lam, E. Y. N.; Chung, C.-w.; Bamborough, P.; Petretich, M.; Urh, M.; Atkinson, S. J.; Bassil, A. K.; Roberts, E. J.; Vassiliadis, D.; Burr, M. L.; Preston, A. G. S.; Wellaway, C.; Werner, T.; Gray, J. R.; Michon, A.-M.; Gobetti, T.; Kumar, V.; Soden, P. E.; Haynes, A.; Vappiani, J.; Tough, D. F.; Taylor, S.; Dawson, S.-J.; Bantscheff, M.; Lindon, M.; Drewes, G.; Demont, E. H.; Daniels, D. L.; Grandi, P.; Prinjha, R. K.; Dawson, M. A., Selective targeting of BD1 and BD2 of the BET proteins in cancer and immunoinflammation. *Science* **2020**, *368* (6489), 387-394.
23. Runcie, A. C.; Chan, K.-H.; Zengerle, M.; Ciulli, A., Chemical genetics approaches for selective intervention in epigenetics. *Curr Opin Chem Biol*. **2016**, *33*, 186-194.
24. Baud, M. G. J.; Lin-Shiao, E.; Cardote, T.; Tallant, C.; Pschibul, A.; Chan, K.-H.; Zengerle, M.; Garcia, J. R.; Kwan, T. T.-L.; Ferguson, F. M.; Ciulli, A., A bump-and-hole approach to engineer controlled selectivity of BET bromodomain chemical probes. *Science* **2014**, *346* (6209), 638-641.
25. Runcie, A. C.; Zengerle, M.; Chan, K. H.; Testa, A.; van Beurden, L.; Baud, M. G. J.; Epemolu, O.; Ellis, L. C. J.; Read, K. D.; Coulthard, V.; Brien, A.; Ciulli, A., Optimization of a "bump-and-hole" approach to allele-selective BET bromodomain inhibition. *Chem Sci*. **2018**, *9* (9), 2452-2468.
26. Baud, M. G. J.; Lin-Shiao, E.; Zengerle, M.; Tallant, C.; Ciulli, A., New Synthetic Routes to Triazolo-benzodiazepine Analogues: Expanding the Scope of the Bump-and-Hole Approach for Selective Bromo and Extra-Terminal (BET) Bromodomain Inhibition. *J Med Chem*. **2016**, *59* (4), 1492-1500.
27. Humphrey, J. M.; Bridges, R. J.; Hart, J. A.; Chamberlin, A. R., 2, 3-Pyrrolidinedicarboxylates as neurotransmitter conformer mimics: Enantioselective synthesis via chelation-controlled enolate alkylation. *J Org Chem*. **1994**, *59* (9), 2467-2472.
28. Dunn, P. J.; Haener, R.; Rapoport, H., Stereoselective synthesis of 2, 3-diamino acids. 2, 3-Diamino-4-phenylbutanoic acid. *J Org Chem*. **1990**, *55* (17), 5017-5025.
29. Nishida, H.; Eguchi, T.; Kakinuma, K., Amino acid starter unit in the biosynthesis of macrolactam polyketide antitumor antibiotic vicenistatin. *Tetrahedron* **2001**, *57* (39), 8237-8242.

30. Yoshida, T.; Takeshita, M.; Orita, H.; Kado, N.; Yasuda, S.; Kato, H.; Itoh, Y., A Large-Scale Preparation of (3S, 4S)-3-(tert-Butoxycarbonyl)amino-4-methylpyrrolidine and Its Analogs from L-Aspartic Acid. *Chem Pharm Bull.* **1996**, *44* (5), 1128-1131.
31. Fier, P. S.; Whittaker, A. M., An Atom-Economical Method To Prepare Enantiopure Benzodiazepines with N-Carboxyanhydrides. *Org Lett.* **2017**, *19* (6), 1454-1457.
32. Walser, A.; Flynn, T.; Mason, C.; Crowley, H.; Maresca, C.; Yaremko, B.; O'Donnell, M., Triazolobenzo- and triazolothienodiazepines as potent antagonists of platelet activating factor. *J Med Chem.* **1991**, *34* (3), 1209-1221.

Bond manuscript for ChemRxiv.pdf (571.31 KiB)

[view on ChemRxiv](#) • [download file](#)

Stereoselective synthesis of allele-specific BET inhibitors

Adam G. Bond, Andrea Testa, Alessio Ciulli

Supporting Information

Contents

Supplementary Figures	2
ITC Data	4
Table S1. X-ray data collection and refinement statistics.	7
Biophysical Methods	9
Chemistry – Materials and Methods	10
Chemistry – Experimental	11
Chiral HPLC Chromatograms.....	31
References	36
NMR Spectra	37

Supplementary Figures

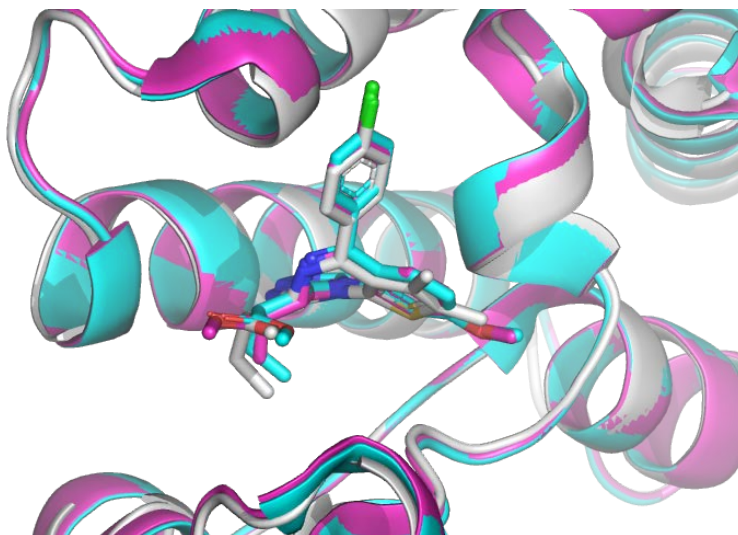


Figure S1. Co-crystal structure of Brd2(2)^{L383V} (grey cartoon representation) in complex with ET-JQ1-OMe (stick representation, grey carbons) superimposed with co-crystal structures of Brd2(2)^{L383V} (magenta (PDB code 5O3C)¹ and cyan (PDB code 5O3D)¹ cartoon representations) in complex with 9-ME-1 (stick representation, magenta carbons (5O3C)) and 9-ET-1 (stick representation, cyan carbons (5O3D)).

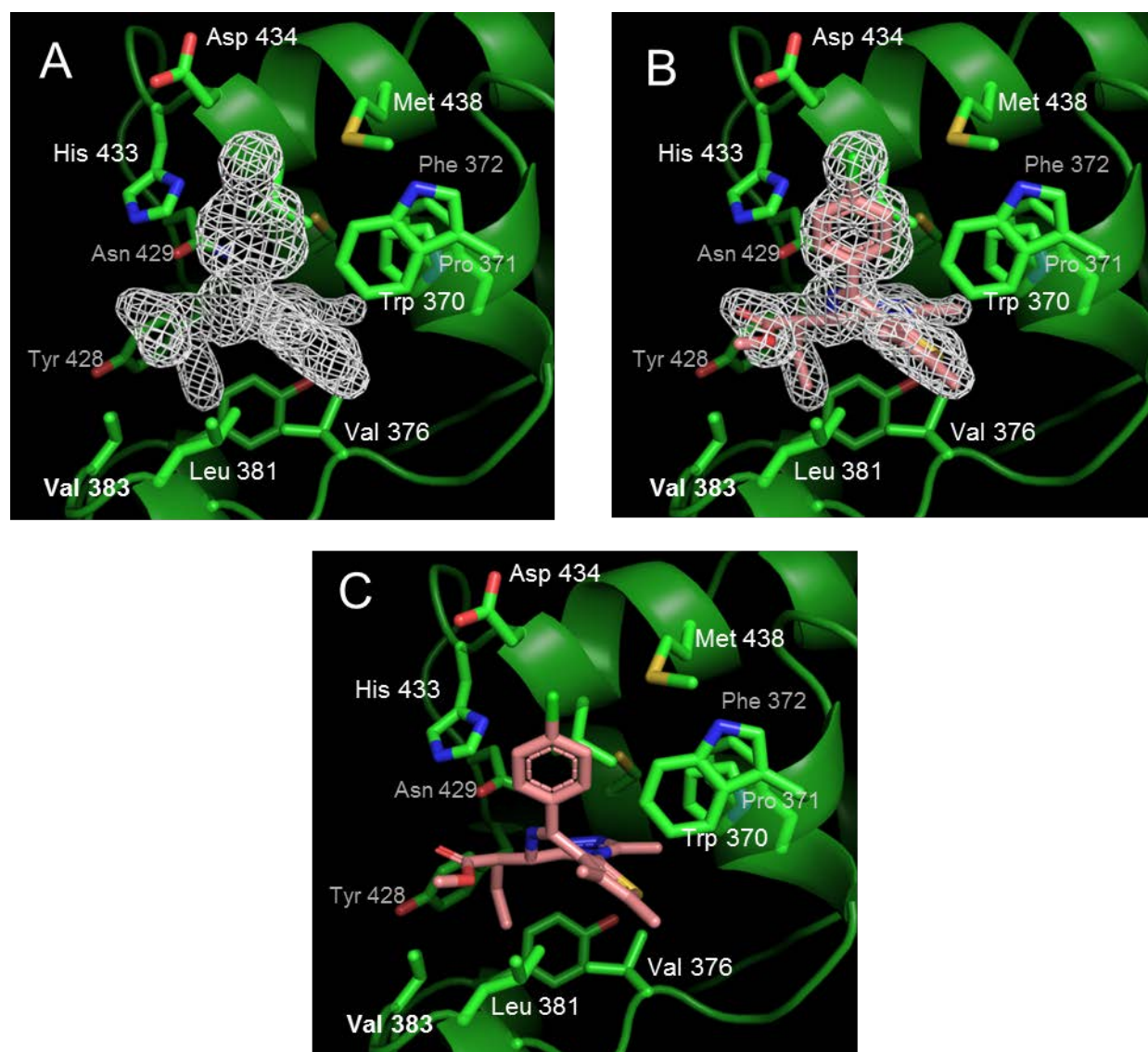


Figure S2. X-ray structure of Brd2(2)^{L383V} (green) co-crystallised with ET-JQ1-OMe (pink carbons). (A) Fo-Fc omit map (white mesh, contour: 3 σ); (B) Fo-Fc omit map with ET-JQ1-OMe (pink carbons); (C) ET-JQ1-OMe (pink carbons) with no omit map.

ITC Data

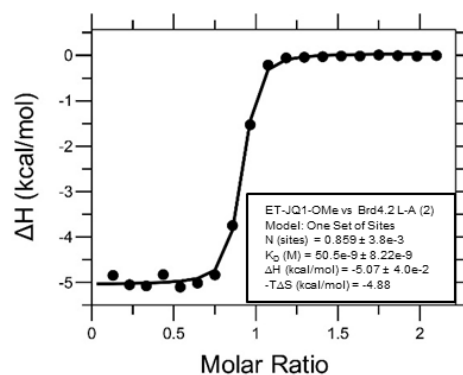
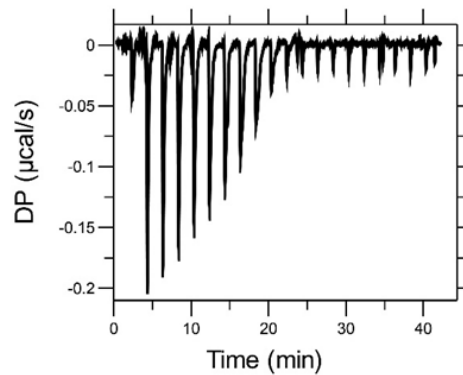
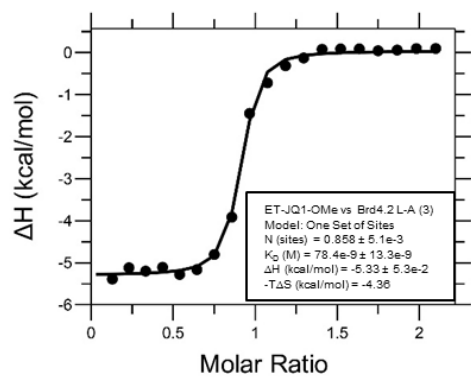
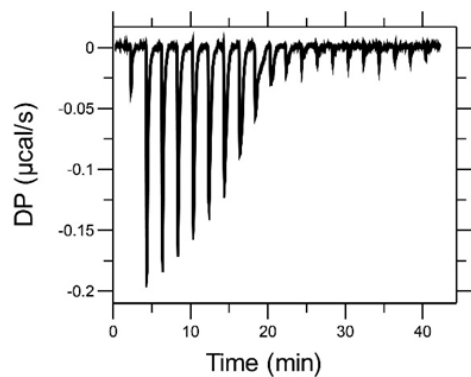
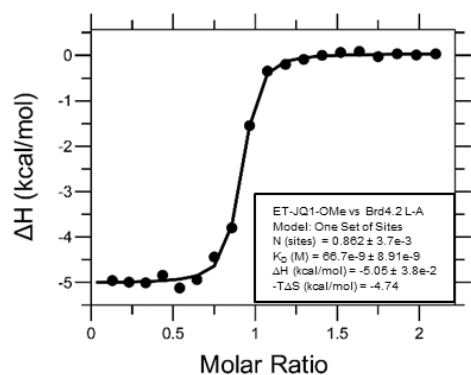
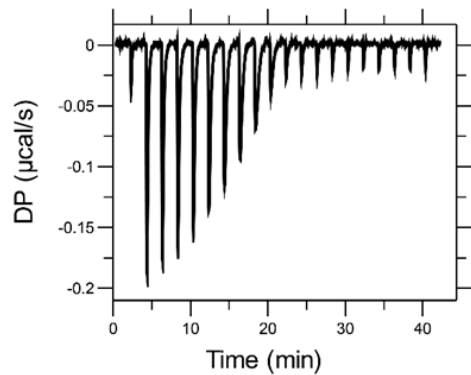


Figure S3. Titrations of ET-JQ1-OMe (**16**) into Brd4(2) L/A mutant construct. The experiment was performed in triplicate, each replicate is shown.

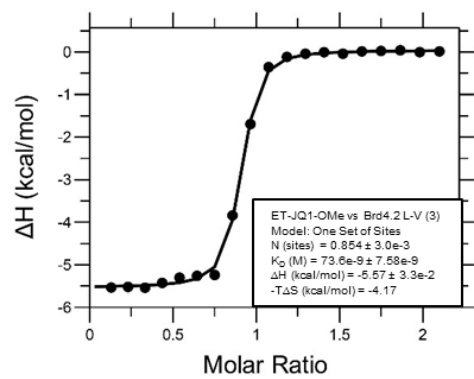
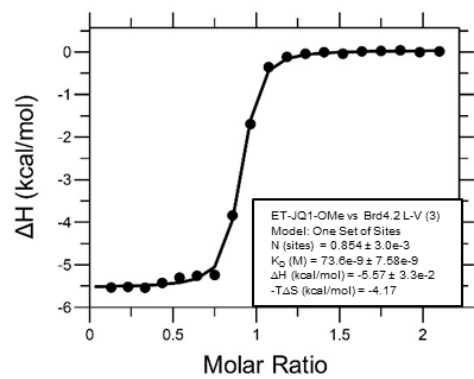
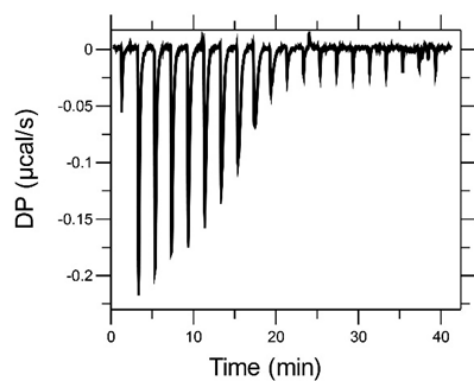
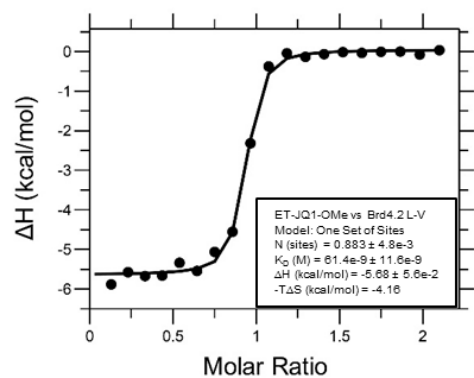
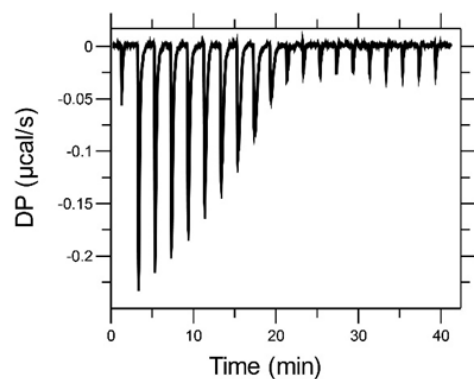


Figure S4. Titrations of ET-JQ1-OMe (**16**) into Brd4(2) L/V mutant construct. The experiment was performed in triplicate, each replicate is shown.

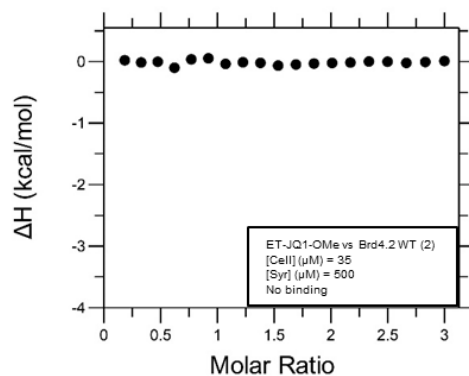
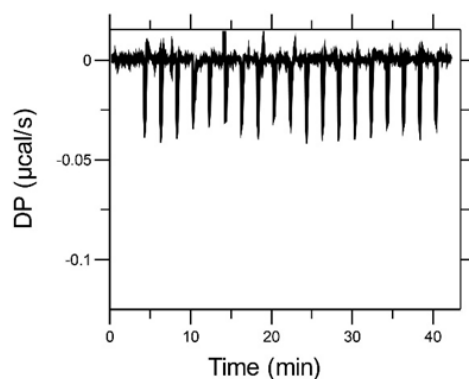
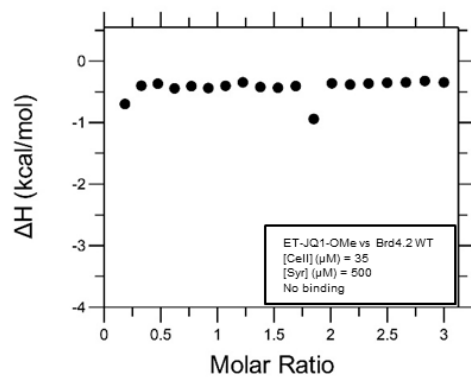
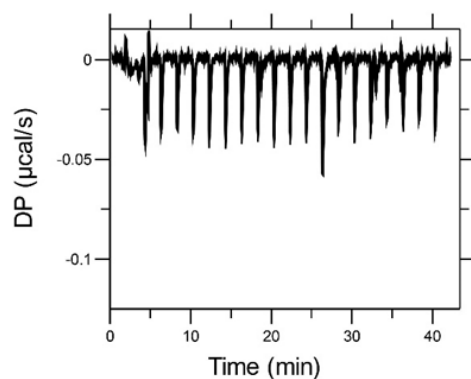
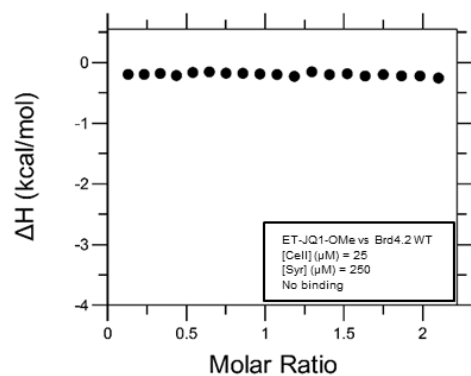
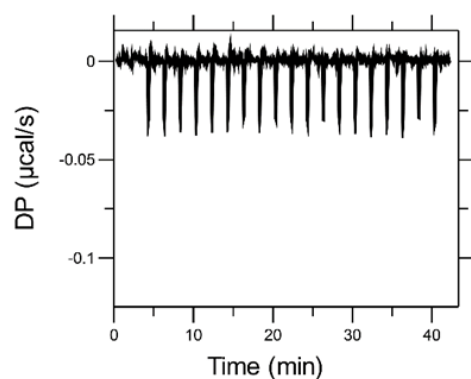
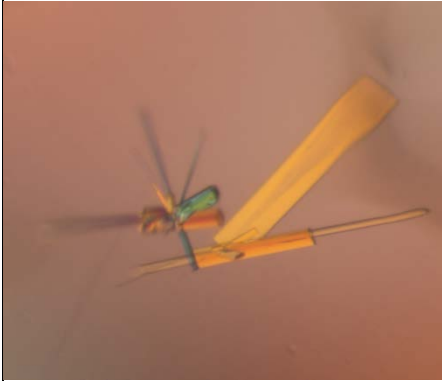


Figure S5. Titrations of ET-JQ1-OMe (**16**) into Brd4(2) wild-type construct. The experiment was performed in triplicate, each replicate is shown.

Table S1. X-ray data collection and refinement statistics.

Compound	ET-JQ1-OMe (16)
PDB code	6YTM
Resolution range	39.95 - 1.56 (1.616 - 1.56)
Space group	P 21 21 21
Unit cell	34.05 50.535 130.486 90 90 90
Total reflections	402700 (33778)
Unique reflections	32590 (3130)
Multiplicity	12.4 (10.7)
Completeness	98.71 (96.45)
(%)	
Mean $I/\sigma(I)$	14.08 (2.88)
Wilson B-factor	15.66
R-merge	0.1846 (2.556)
R-meas	0.1926 (2.689)
R-pim	0.0543 (0.8114)
CC_{1/2}	0.998 (0.55)
CC*	0.999 (0.843)
Reflections used in refinement	32557 (3129)
Reflections used for R-free	1589 (147)
R-work	0.1723 (0.2552)
R-free	0.2034 (0.2988)
CC(work)	0.962 (0.784)
CC(free)	0.943 (0.587)
Number of non-hydrogen atoms	2108
macromolecules	1846
ligands	76
solvent	186
Protein residues	218
RMS(bonds)	0.009

RMS(angles)	0.89
Ramachandran favored (%)	99.07
Ramachandran allowed (%)	0.93
Ramachandran outliers (%)	0.00
Rotamer outliers (%)	0.51
Clashscore	1.33
Average B-factor	23.40
macromolecules	22.51
ligands	24.84
solvent	31.68
Number of TLS groups	12
	

Biophysical Methods

All protein constructs used in this work were gifted by Dr. Kwok-Ho Chan and were expressed and purified using the same procedures described by Runcie et al..¹

X-ray Crystallography – Co-crystallisation of **16 with Brd2(2) L/V**

Purified Brd2(2) L383V protein at 18 mg/ml (≈ 1.3 mM) was mixed with an excess amount of **16** (2 mM) to give a 1:1.5 ratio of protein to ligand with a final DMSO concentration of 5%. This was incubated at 4°C for 30 min to allow for complex formation before mixing 1:1 (1 μ L:1 μ L) with the precipitation solution in sitting-drop vapour diffusion format. A 24-well plate was set up with conditions ranging from 0.1 M Tris pH 7.77 – 9.00 and varying concentrations of pentaerythritol propoxylate (5/4 PO/OH) 45 – 60%. Crystals formed after 16 h and were fully grown after 3-4 days.

Diffraction data was collected at Diamond Light Source beamline I24 using a Pilatus 6M detector at a wavelength of 0.9686 Å. Crystals grown in 0.1 M Tris pH 8.75 with 55% pentaerythritol propoxylate had the best diffraction of highest resolution. Data was taken from the Diamond Light Source autoPROC,² auto processing function. The structure was solved by molecular replacement in Phaser,³ using two copies of search models derived from the coordinates of 9-ET-1 with Brd2(2)^{L383V} (PDB entry 5O3D). The model was iteratively refined using PHENIX,⁴ and COOT. Ligand restraints were generated in eLBOW.⁵ The structure models have been deposited in the protein data bank (PDB) and data collection and refinement statistics are presented in the supplementary information. All figures were generated using PyMOL 2.3.0.

Isothermal Titration Calorimetry (ITC)

ITC titrations were performed on an ITC200 instrument (MicroCal™, GE Healthcare). Proteins and **16** were dissolved in ITC buffer (20 mM HEPES, 100 mM NaCl, pH 7.5). Protein samples underwent buffer exchange via dialysis using 6-8 kDa mini D-tubes (Millipore). ITC titrations were performed at 25°C and consisted of 20 titrations: 1 initial injection of 0.4 μ L over 0.8s, followed by 19 injections of 2 μ L over 4s, at 2 min intervals. Data was analysed using MicroCal PEAQ-ITC Analysis Software, using a single site binding model, to determine thermodynamic values such as K_d and enthalpy of binding ΔH .

For Brd4(2) L/A and L/V constructs, 250 μ M of **16** was titrated into 25 μ M of protein with a final DMSO concentration of 2.5%. This was repeated to provide triplicates. For Brd4(2) wild-type,

500 μM of **16** was titrated into 35 μM of protein with a final DMSO concentration of 2.5%. This was repeated to provide duplicates. A third experiment was performed with 250 μM of **16** titrating into 25 μM of protein with a final DMSO concentration of 2.5% to provide a comparison with data from mutant constructs.

Chemistry – Materials and Methods

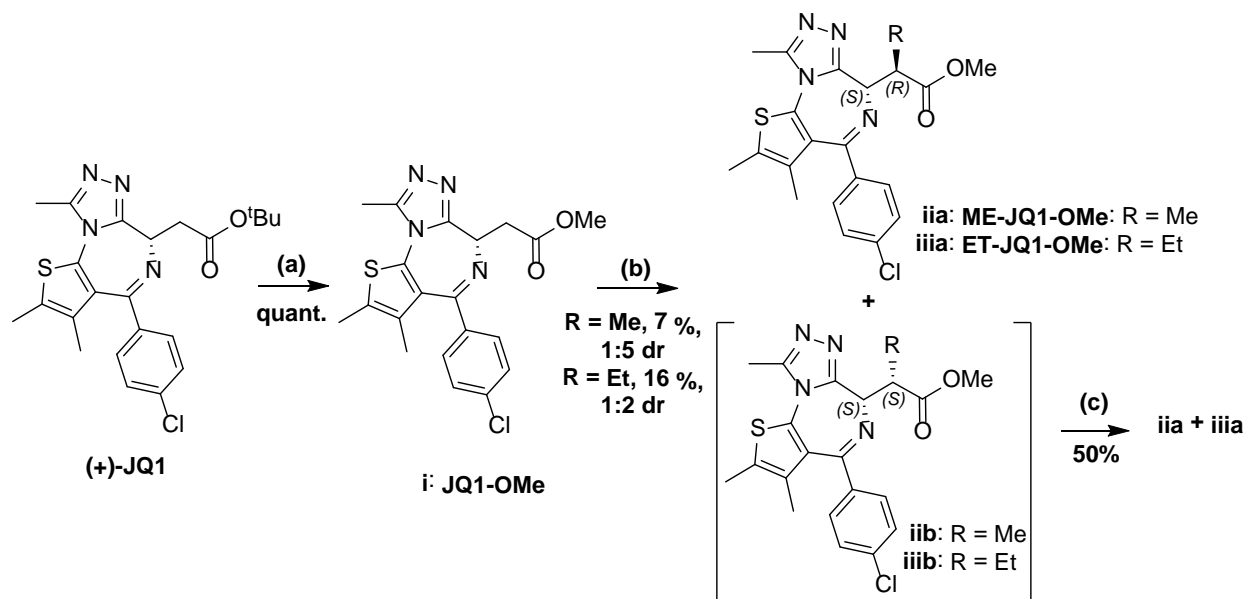
All chemicals, reagents and solvents used, unless stated otherwise, were obtained from commercial sources and used without further purification. Intermediates were purified by flash column chromatography using a Teledyne Isco Combiflash Rf or Rf200i, with Normal Phase RediSep Rf Disposable Columns or with Reverse Phase RediSep Rf Gold C18 Reusable Columns. Final compounds were purified by HPLC (High Performance Liquid Chromatography) using a Gilson Preparative HPLC System equipped with a Waters X-Bridge C18 column (100 mm x 19 mm; 5 μm particle size) using a gradient from 5% to 95% of acetonitrile in water containing 0.1% formic over 10 min at a flow rate of 25 mL/min unless stated otherwise.

Compound characterisation using NMR was performed either on a Bruker 500 Ultrashield or Bruker Ascend 400 spectrometers. The proton (^1H) and carbon (^{13}C) reference solvents used were as follows: d_1 -Chloroform – CDCl_3 ($\delta\text{H} = 7.26 \text{ ppm}$ / $\delta\text{C} = 77.15 \text{ ppm}$) and d_5 -Methanol – CD_3OD ($\delta\text{H} = 3.31 \text{ ppm}$ / $\delta\text{C} = 49.00 \text{ ppm}$). Signal patterns are described as singlet (s), doublet (d), triplet (t), quartet (q), multiplet (m), broad (br.), or a combination of the listed splitting patterns. NMR spectra for all compounds were processed using Bruker TopSpin 4.0.5.

Reactions were monitored using an Agilent Technologies 1200 series analytical HPLC connected to an Agilent Technologies 6130 quadrupole LC/MS containing an Agilent diode array detector and a Waters XBridge column (50 mm x 2.1 mm, 3.5 μm particle size). Samples were eluted with a 3 min gradient of 5% to 95% acetonitrile: water containing 0.1% formic acid at a flow rate of 0.7 mL/min. High resolution mass spectrometry (HRMS) data was performed on a Bruker microTOF. Chiral HPLC analysis was outsourced at Reach Separations Ltd, BioCity Nottingham, UK.

Chemistry – Experimental

Scheme S1: Alkylation of (+)-JQ1



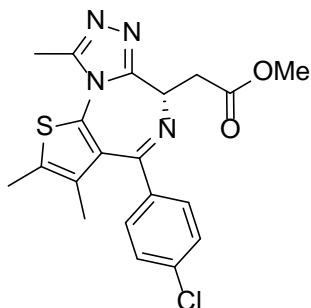
Conditions: (a) i) TFA, DCM, r.t., 2 h, ii) SOCl_2 , MeOH, r.t., 3 h; (b) i) KHMDS, THF, -78°C , 1 h, ii) MeI/EtI, -78°C to r.t., 16 h, iii) HPLC separation; (c) i) NaOMe, MeOH, 120°C M.W., 40 min, ii) HPLC separation.

General procedure for direct alkylation of (+)-JQ1

(+)-JQ1 (300 mg, 0.66 mmol) was dissolved in a 1:1 mixture of DCM (1.8 ml) to TFA (1.8 ml) and stirred at r.t. until complete conversion to the free acid was observed by LC-MS. The reaction was then concentrated *in vacuo* and freeze dried (x3) to remove excess TFA and leave a yellow solid. The solid was then immediately dissolved in MeOH (5 ml/mmol) and SOCl_2 (3 eq.) was added and left to stir at r.t. for 3 h. The reaction mixture was then concentrated *in vacuo* to afford JQ1-OMe (i) as a yellow solid in quantitative yields. JQ1-OMe (1 eq.) was then dissolved in THF (17.5 ml/mmol) and cooled to -78°C . A solution of 0.5 M KHMDS in toluene (1.4 eq.) was added dropwise to the flask and stirred at -78°C for 1 h. The appropriate alkyl iodide (1.4 eq) was then added and the reaction was left to warm to r.t. over 16 h. LCMS showed a 1:5 (methyl) or 1:2 (ethyl) ratio of diastereomers with the major (S,S) isomer eluting later on silica. The reaction was then quenched with AcOH and concentrated *in vacuo* and diastereomers were separated by HPLC using a linear gradient of 30% to 70% MeCN in 0.1% formic acid in water over 10 minutes affording diastereomers with total alkylation isolated yields of $\approx 20\%$. For epimerisation, major (S,S) diastereomers, iib and iiib, (1 eq., 50 μmol) and NaOMe (10 eq.) were dissolved in

anhydrous MeOH (4 ml) and heated to 120°C by microwave irradiation for 40 min. The reaction was acidified with AcOH (1 ml) at 60°C and then concentrated *in vacuo*. Diastereomers were separated by HPLC using a linear gradient of 30 to 70% MeCN in 0.1% formic acid in water over 10 minutes affording (S,S) and (S,R) isomers in a 1:1 ratio.

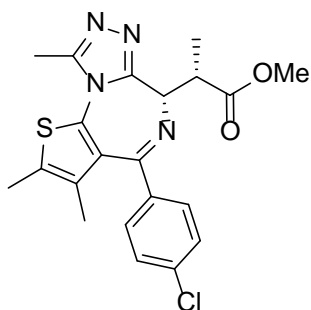
methyl (S)-2-(4-(4-chlorophenyl)-2,3,9-trimethyl-6H-thieno[3,2-f][1,2,4]triazolo[4,3-a][1,4]diazepin-6-yl)acetate (**JQ1-OMe (i)**)



¹H-NMR (500 MHz, CDCl₃): δ, ppm 7.41 (2H, d, *J* = 8.6 Hz), 7.33 (2H, d, *J* = 8.8 Hz), 4.62 (1H, dd, *J* = 6.1, 8.0 Hz), 3.78 (3H, s), 3.69 - 3.58 (2H, m), 2.68 (3H, s), 2.41 (3H, s), 1.70 (3H, s);

LC-MS *m/z* calc. for C₂₀H₂₀ClN₄O₂S [M+H]⁺ 415.1, found: 414.9.

methyl (S)-2-((S)-4-(4-chlorophenyl)-2,3,9-trimethyl-6H-thieno[3,2-f][1,2,4]triazolo[4,3-a][1,4]diazepin-6-yl)propanoate (**iib**)



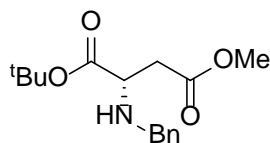
¹H-NMR (500 MHz, CDCl₃) δ, ppm: 7.43 (2H, d, *J* = 8.5 Hz), 7.33 (2H, d, *J* = 8.5 Hz), 4.31 (1H, d, *J* = 9.8 Hz), 3.88 (1H, qd, *J* = 7.2, 9.7 Hz), 3.72 (3H, s), 2.64 (3H, s), 2.41 (3H, s), 1.70 (1H, s), 1.62 (3H, d, *J* = 7.1 Hz);

¹³C-NMR (500 MHz, CDCl₃) δ, ppm: 176.1, 163.9, 155.5, 149.6, 136.95, 136.89, 132.7, 130.8, 130.4, 129.9, 129.8, 128.8, 58.5, 52.1, 41.2, 15.4, 14.5, 13.2, 11.9;

LC-MS *m/z* calc. for C₂₁H₂₂ClN₄O₂S [M+H]⁺ 429.1, found: 429.0.

Stereoselective Synthesis

1-(*tert*-butyl) 4-methyl benzyl-*L*-aspartate (2)



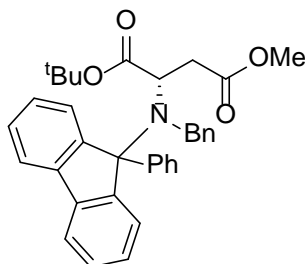
1-(*tert*-butyl) 4-methyl-*L*-aspartate hydrogen chloride (4.11 g, 17.1 mmol) was first converted to the free amine by dissolving in saturated NaHCO₃ (100 ml) and EtOAc (100 ml). After stirring at r.t. for 10 min, the aqueous layer was extracted with EtOAc (3 x 50 ml). The combined organic layers were dried with anhydrous MgSO₄ and concentrated *in vacuo* leaving a colourless oil with a mass of 2.86 g, 14.1 mmol. The free amine was subsequently dissolved in anhydrous DCM (70 ml) which contained a suspension of anhydrous MgSO₄ (3.39 g, 28.2 mmol). Freshly distilled benzaldehyde (2.70 g, 25.4 mmol) was then added and the reaction was left to stir at r.t. and monitored by NMR. After 2 h, NMR analysis showed the presence of the imine and excess benzaldehyde. MeOH (30 ml) was added and the reaction was then cooled to 0°C. NaBH₄ (1.07 g, 28.2 mmol) was added at once to the flask. After 10 min of stirring, the reaction was allowed to warm to r.t. and monitored by NMR. After 1 h the reaction mixture was filtered into a solution of saturated NaHCO₃ (200 ml) and stirred for 10 min. The aqueous phase was extracted with DCM (4 x 50 ml) and the combined organic layers were dried with MgSO₄ and concentrated *in vacuo*. The residue was purified by flash column chromatography (120 g silica column) using a linear gradient from 0% to 30% acetone in heptane to afford 1-(*tert*-butyl) 4-methyl benzyl-*L*-aspartate (2.72 g, 66%) as a colourless oil.

¹H-NMR (400 MHz, CDCl₃) δ, ppm: 7.34 - 7.28 (4H, m), 7.25 - 7.22 (1H, m), 3.88 (1H, d, *J* = 13.0 Hz), 3.72 (1H, d, *J* = 12.8 Hz), 3.68 (3H, s), 3.55 (1H, t, *J* = 6.5 Hz), 2.69 (1H, dd, *J* = 6.2, 15.5 Hz), 2.63 (1H, dd, *J* = 6.9, 15.5 Hz), 2.07 (1H, br. s), 1.47 (9H, s);

¹³C-NMR (400 MHz, CDCl₃) δ, ppm: 172.9, 171.6, 139.9, 128.5, 128.4, 127.2, 81.8, 57.9, 52.2, 51.9, 38.4, 28.2;

HRMS *m/z* calc. for C₁₆H₂₄NO₄ [M+H]⁺ 294.1705, found: 294.1708.

1-(*tert*-butyl) 4-methyl *N*-benzyl-*N*-(9-phenyl-9H-fluoren-9-yl)-L-aspartate (**3**)



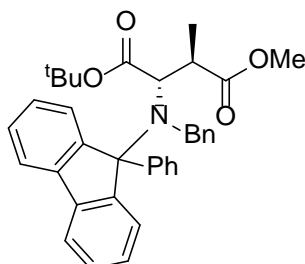
1-(*tert*-butyl) 4-methyl benzyl-*L*-aspartate (5.49 g, 18.7 mmol), 9-bromo-9-phenyl-9H-fluorene (7.59 g, 22.5 mmol), tribasic potassium phosphate (7.94 g, 37.4 mmol) and lead (II) nitrate (4.95 g, 14.96 mmol) were dissolved in MeCN (180 ml) and left to stir at r.t. TLC analysis confirmed that the reaction had gone to completion after 4 h. The mixture was then filtered through a celite pad and the solid was washed with DCM. The combined filtrate was then concentrated *in vacuo*. The residue was dissolved in diethyl ether (100 ml) and washed with 50 mM citric acid (2 x 100 ml) and then water (100 ml). The organic layer was dried with MgSO₄ and concentrated *in vacuo*. The residue was purified by flash column chromatography (crude split between 2 x 120 g silica columns) using a linear gradient from 5% to 15% MTBE in heptane to afford 1-(*tert*-butyl) 4-methyl *N*-benzyl-*N*-(9-phenyl-9H-fluoren-9-yl)-*L*-aspartate (7.91 g, 79%) as a fluffy white solid.

¹H-NMR (400 MHz, CDCl₃) δ , ppm: 7.82 (2H, d, J = 7.8 Hz), 7.73 (2H, t, J = 7.5 Hz), 7.69 (1H, d, J = 7.4 Hz), 7.56 (1H, d, J = 7.5 Hz), 7.47 (2H, d, J = 7.2 Hz), 7.37 (2H, dq, J = 1.1, 7.9 Hz), 7.31 - 7.27 (4H, m), 7.25 - 7.17 (3H, m), 4.21 (1H, d, J = 13.9 Hz), 3.91 - 3.84 (2H, m), 3.42 (3H, s), 2.54 (1H, dd, J = 10.8, 15.7 Hz), 1.94 (1H, dd, J = 2.9, 15.8 Hz), 1.14 (9H, s);

¹³C-NMR (400 MHz, CDCl₃) δ , ppm: 172.1, 171.4, 147.6, 146.5, 143.9, 140.9, 140.4, 139.1, 129.6, 128.74, 128.68, 128.5, 128.2, 127.7, 127.6, 127.4, 127.3, 127.1, 126.7, 120.5, 120.1, 80.8, 79.7, 57.8, 51.9, 51.5, 34.0, 27.8;

HRMS m/z calc. for C₃₅H₃₆NO₄ [M+H]⁺ 534.2644, found: 534.2658.

1-(*tert*-butyl) 4-methyl (2*S*,3*R*)-2-(benzyl(9-phenyl-9H-fluoren-9-yl)amino)-3-methylsuccinate (**4a**)



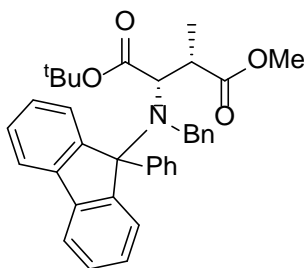
1-(*tert*-butyl) 4-methyl *N*-benzyl-*N*-(9-phenyl-9H-fluoren-9-yl)-*L*-aspartate (3.42 g, 6.41 mmol) was dissolved in anhydrous THF (50 ml) under an atmosphere of N₂ and cooled to -23°C. A solution of 1.0 M LHMDs in THF (9.62 ml, 9.62 mmol) was added dropwise to the flask and stirred at -23°C for 1 h. The solution turned orange. The reaction was then cooled to -78°C and methyl iodide (0.5 ml, 8.01 mmol) was added dropwise and left to warm to -40°C over 16h. LCMS showed a 1:6 ratio of diastereomers with the major isomer eluting later on silica. After completion, the reaction was quenched with saturated NH₄Cl solution and extracted with MTBE (3 x 50 ml). The combined organic layers were washed with brine (100 ml), dried with MgSO₄ and concentrated *in vacuo*. The residue was purified and diastereomers separated by flash column chromatography (crude split between 2 x 120 g silica columns) using a linear gradient from 0% to 15% MTBE in heptane to afford 1-(*tert*-butyl) 4-methyl (2*S*,3*R*)-2-(benzyl(9-phenyl-9H-fluoren-9-yl)amino)-3-methylsuccinate (2.28 g, 65%) as a fluffy white solid. This also afforded the minor (*S,S*) diastereomer (358 mg, 10%) as a fluffy white solid.

¹H-NMR (500 MHz, CDCl₃) δ, ppm: 7.94 - 7.88 (1H, m), 7.74 (1H, d, *J* = 7.5 Hz), 7.69 - 7.60 (4H, m), 7.51 (2H, d, *J* = 7.5 Hz), 7.42 (1H, dt, *J* = 0.8, 7.5 Hz), 7.32 - 7.27 (4H, m), 7.25 - 7.14 (5H, m), 4.67 (1H, d, *J* = 14.2 Hz), 4.31 (1H, d, *J* = 14.0 Hz), 3.87 (1H, d, *J* = 10.5 Hz), 3.56 (3H, s), 2.66 (1H, qd, *J* = 7.0, 10.4 Hz), 1.04 (1H, s), 0.73 (3H, d, *J* = 7.1 Hz);

¹³C-NMR (500 MHz, CDCl₃) δ, ppm: 174.8, 170.4, 147.3, 146.0, 145.5, 142.4, 141.9, 139.5, 129.5, 128.7, 128.4, 128.24, 128.20, 127.9, 127.75, 127.68, 127.54, 127.49, 127.1, 126.8, 120.3, 119.4, 80.9, 80.6, 64.2, 51.6, 51.3, 42.2, 27.7, 15.6;

HRMS *m/z* calc. for C₃₆H₃₈NO₄ [M+H]⁺ 548.2801, found: 548.2800.

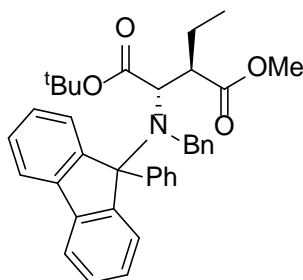
1-(*tert*-butyl) 4-methyl (2*S*,3*S*)-2-(benzyl(9-phenyl-9H-fluoren-9-yl)amino)-3-methylsuccinate (**4b**)



¹H-NMR (500 MHz, CDCl₃) δ, ppm: 7.77 - 7.71 (3H, m), 7.66 - 7.57 (5H, m), 7.45 (1H, t, *J* = 7.3 Hz), 7.34 - 7.27 (6H, m), 7.25 - 7.19 (3H, m), 4.39 (1H, d, *J* = 13.5 Hz), 4.31 (1H, d, *J* = 13.4 Hz), 3.60 (1H, d, *J* = 11.2 Hz), 3.36 (3H, s), 2.39 (1H, qd, *J* = 7.1, 11.2 Hz), 1.16 (3H, d, *J* = 7.1 Hz), 1.06 (9H, s);

^{13}C -NMR (500 MHz, CDCl_3) δ , ppm: 175.6, 170.9, 147.5, 146.7, 145.7, 142.0, 140.4, 129.8, 128.7, 128.5, 128.4, 128.0, 127.8, 127.6, 127.5, 127.3, 127.2, 126.8, 120.6, 120.1, 80.6, 63.9, 52.9, 51.4, 41.9, 27.6, 15.9;

1-(*tert*-butyl) 4-methyl (2*S*,3*R*)-2-(benzyl(9-phenyl-9H-fluoren-9-yl)amino)-3-ethylsuccinate (**5a**)

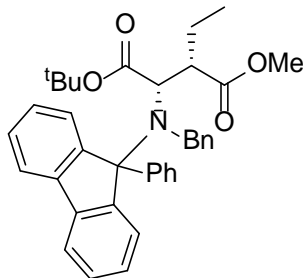


1-(*tert*-butyl) 4-methyl *N*-benzyl-*N*-(9-phenyl-9H-fluoren-9-yl)-*L*-aspartate (1.2 g, 2.25 mmol) was dissolved in anhydrous THF (6 ml) under an atmosphere of N_2 and cooled to -78°C . A solution of 1.0 M LHMDS in THF (4.38 ml, 4.38 mmol) was added dropwise to the flask and stirred at -78°C for 1 h. Ethyl iodide (1.09 ml, 13.5 mmol) was then added dropwise and the reaction was left to stir at -78°C for 16 h. The reaction was then warmed to between -23 and -30°C and stirred for 24 h until the starting material was consumed. LCMS showed a 1:2 ratio of diastereomers with the major isomer eluting later on silica. After completion, the reaction was quenched with saturated NH_4Cl solution and extracted with MTBE (3 x 20 ml). The combined organic layers were washed with brine (50 ml), dried with MgSO_4 and concentrated *in vacuo*. The residue was purified and diastereomers separated by flash column chromatography (40 g silica column) using a linear gradient from 5% to 15% MTBE in heptane to afford 1-(*tert*-butyl) 4-methyl (2*S*,3*R*)-2-(benzyl(9-phenyl-9H-fluoren-9-yl)amino)-3-ethylsuccinate (612 mg, 48%) as a fluffy white solid. This also afforded the minor (*S,S*) diastereomer (293 mg, 23%) as a fluffy white solid.

^1H -NMR (500 MHz, CDCl_3) δ , ppm: 7.93 - 7.89 (1H, m), 7.75 (1H, d, $J = 7.6$ Hz), 7.66 - 7.59 (4H, m), 7.53 (2H, d, $J = 7.6$ Hz), 7.45 (1H, t, $J = 7.5$ Hz), 7.33 - 7.14 (9H, m), 4.65 (1H, d, $J = 13.5$ Hz), 4.32 (1H, d, $J = 13.9$ Hz), 3.89 (1H, d, $J = 11.4$ Hz), 3.57 (3H, s), 2.57 (1H, ddd, $J = 3.9, 9.0, 11.0$ Hz), 1.20 - 1.11 (1H, m), 1.10 - 1.02 (1H, m), 1.02 (9H, s), 0.51 (3H, t, $J = 7.4$ Hz);

^{13}C -NMR (400 MHz, CDCl_3) δ , ppm: 173.8, 170.4, 147.3, 145.8, 145.7, 142.6, 141.5, 139.4, 130.0, 128.7, 128.4, 128.2, 127.8, 127.6, 127.5, 127.1, 126.9, 120.4, 119.3, 80.8, 80.7, 62.6, 51.6, 51.1, 48.8, 27.6, 23.0, 10.6;

1-(*tert*-butyl) 4-methyl (2*S*,3*S*)-2-(benzyl(9-phenyl-9H-fluoren-9-yl)amino)-3-ethylsuccinate (**5b**)



$^1\text{H-NMR}$ (500 MHz, CDCl_3) δ , ppm: 7.77 - 7.69 (3H, m), 7.65 - 7.61 (4H, m), 7.58 (1H, d, $J = 7.9$ Hz), 7.45 (1H, t, $J = 7.3$ Hz), 7.35 - 7.27 (6H, m), 7.26 - 7.19 (3H, m), 4.45 (1H, d, $J = 13.3$ Hz), 4.38 (1H, d, $J = 13.5$ Hz), 3.60 (1H, d, $J = 11.1$ Hz), 3.36 (3H, s), 2.29 - 2.16 (2H, m), 1.42 - 1.32 (1H, m), 0.44 (3H, t, $J = 7.4$ Hz);

$^{13}\text{C-NMR}$ (400 MHz, CDCl_3) δ , ppm: 174.9, 170.6, 147.5, 146.4, 145.6, 142.1, 140.7, 139.9, 129.7, 128.7, 128.4, 128.1, 127.8, 127.6, 127.5, 127.25, 127.17, 126.5, 120.5, 120.1, 80.5, 63.2, 52.2, 51.2, 49.6, 27.6, 23.1, 11.5;

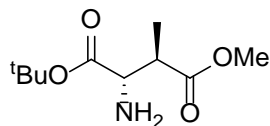
HRMS m/z calc. for $\text{C}_{37}\text{H}_{40}\text{NO}_4$ $[\text{M}+\text{H}]^+$ 562.2957, found: 562.2972.

General procedure for amino acid deprotection

Compounds **4a**, **5a**, **5b** were dissolved in acetic acid (6 L/mol) (MeOH was used as a co-solvent for the (*S,S*) diastereomer, **5b**) and a catalytic amount of Pd/C (15% wt/wt) was added. The reaction was left to stir under an atmosphere of hydrogen until no starting material was remaining by LC-MS analysis. The reaction was then filtered through PTFE syringe filters. The crude was *in vacuo* and the residue was partitioned between Et_2O and 1.0 M H_3PO_4 solution. The organic phase was extracted with 1.0 M H_3PO_4 solution (x 2) and the combined aqueous fractions were adjusted to pH 9 using solid K_2CO_3 . The basified solution was extracted with EtOAc (x 5) and the combined organic fractions were dried with MgSO_4 and concentrated *in vacuo* to afford free amines, **6**, **7** and **7*** in quantitative yields as colourless oils.

The resulting free amines were dissolved in a 1:1 mixture of DCM to TFA (1 ml/100 mg) and stirred for 1 h. The reaction was monitored by NMR to see the disappearance of the *tert*-butyl group. After completion the reaction mixture was concentrated *in vacuo*. The resulting TFA salt was then dissolved in 2.0 M HCl and freeze dried to convert the TFA salt to the HCl salt. This process was repeated 2-3 times to afford the amino acids **8**, **9** and **9*** as HCl salts in quantitative yields.

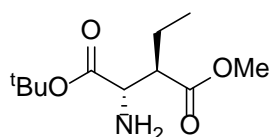
1-(*tert*-butyl) 4-methyl (2*S*,3*R*)-2-amino-3-methylsuccinate (**6**)



Yield: 561 mg (quant.); ¹H-NMR (500 MHz, CDCl₃) δ, ppm: 3.69 (3H, s), 3.55 (1H, d, *J* = 5.4 Hz), 2.89 (1H, dq, *J* = 5.5, 7.1 Hz), 1.62 (2H, s), 1.46 (9H, s), 1.21 (3H, d, *J* = 7.2 Hz);

¹³C-NMR (400 MHz, CDCl₃) δ, ppm: 174.4, 173.3, 81.7, 57.7, 51.8, 44.0, 28.1, 13.4;

1-(*tert*-butyl) 4-methyl (2*S*,3*R*)-2-amino-3-ethylsuccinate (**7**)

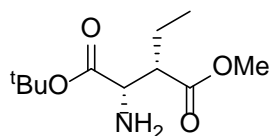


Yield: 451 mg (quant.); ¹H-NMR (500 MHz, CDCl₃) δ, ppm: 3.69 (3H, s), 3.50 (1H, d, *J* = 6.0 Hz), 2.70 (1H, td, *J* = 5.9, 8.9 Hz), 1.82 - 1.72 (1H, m), 1.65 - 1.55 (3H, m), 1.47 (9H, s), 0.96 (3H, t, *J* = 7.4 Hz);

¹³C-NMR (400 MHz, CDCl₃) δ, ppm: 174.1, 173.7, 81.6, 56.5, 51.6, 51.1, 28.1, 22.2, 12.2;

HRMS *m/z* calc. for C₁₁H₂₂NO₄ [M+H]⁺ 232.1549, found: 232.1552.

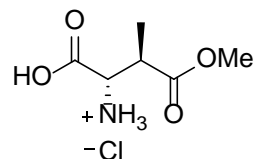
1-(*tert*-butyl) 4-methyl (2*S*,3*S*)-2-amino-3-ethylsuccinate (**7***)



Yield: 150 mg (quant.); ¹H-NMR (500 MHz, CDCl₃) δ, ppm: 3.71 (3H, s), 3.67 (1H, d, *J* = 5.6 Hz), 2.67 - 2.62 (1H, m), 1.84 - 1.74 (1H, m), 1.62 - 1.54 (1H, m), 1.53 (2H, s), 1.47 (9H, s), 0.95 (3H, t, *J* = 7.3 Hz);

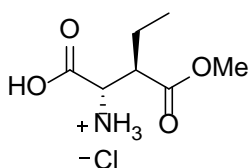
¹³C-NMR (500 MHz, CDCl₃) δ, ppm: 174.3, 173.3, 81.7, 56.4, 51.8, 51.0, 28.1, 20.8, 12.3;

(2S,3R)-2-amino-4-methoxy-3-methyl-4-oxobutanoic acid hydrogen chloride salt (**8**)



Yield: 607 mg (quant.); ¹H-NMR (500 MHz, MeOD) δ, ppm: 4.31 (1H, d, *J* = 4.2 Hz), 3.76 (3H, s), 3.31 - 3.25 (1H, m), 1.34 (3H, d, *J* = 7.4 Hz);

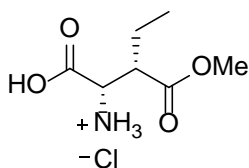
(2S,3R)-2-amino-3-(methoxycarbonyl)pentanoic acid hydrogen chloride salt (**9**)



Yield: 408 mg (quant.); ¹H-NMR (500 MHz, MeOD) δ, ppm: 4.23 (1H, d, *J* = 4.6 Hz), 3.76 (3H, s), 3.11 - 3.06 (1H, m), 1.94 - 1.82 (1H, m), 1.75 - 1.64 (1H, m), 1.06 (3H, t, *J* = 7.4 Hz);

¹³C-NMR (500 MHz, MeOD) δ, ppm: 173.5, 170.2, 54.4, 53.0, 47.7, 22.2, 12.3;

(2S,3S)-2-amino-3-(methoxycarbonyl)pentanoic acid hydrogen chloride salt (**9***)



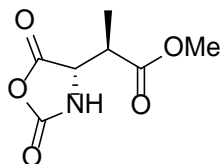
Yield: 128 mg (quant.) ¹H-NMR (400 MHz, MeOD) δ, ppm: 4.28 (1H, d, *J* = 4.3 Hz), 3.77 (3H, s), 3.03 - 2.95 (1H, m), 1.97 - 1.82 (1H, m), 1.79 - 1.66 (1H, m), 1.04 (3H, t, *J* = 7.3 Hz);

¹³C-NMR (400 MHz, MeOD) δ, ppm: 173.7, 170.1, 54.5, 53.0, 48.3, 22.7, 12.4;

General procedure for the synthesis of *N*-carboxyanhydrides (**10**, **11** and **11***)

Amino acids **8**, **9** and **9*** (1.0 eq.) were dissolved in anhydrous THF (3 L/mol). Triphosgene (0.67 eq.) was then added and the flask was flushed with N₂ and left to stir for 16 h in a closed vial. The reaction was monitored by ¹H-NMR. The flask was then concentrated *in vacuo* to afford *N*-carboxyanhydrides **10**, **11** and **11*** in quantitative yields as pale brown oils.

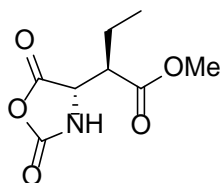
methyl (R)-2-((S)-2,5-dioxooxazolidin-4-yl)propanoate (10)



Yield: 575 mg (quant.); $^1\text{H-NMR}$ (400 MHz, CDCl_3) δ , ppm: 6.10 (1H, br. s), 4.36 (1H, d, $J = 7.0$ Hz), 3.77 (3H, s), 3.04 (1H, dq, $J = 7.2, 7.2$ Hz), 1.44 (3H, d, $J = 7.4$ Hz);

$^{13}\text{C-NMR}$ (400 MHz, CDCl_3) δ , ppm: 172.5, 167.9, 151.8, 59.1, 52.9, 42.0, 13.6;

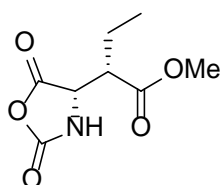
methyl (R)-2-((S)-2,5-dioxooxazolidin-4-yl)butanoate (11)



Yield: 386 mg (quant.); $^1\text{H-NMR}$ (400 MHz, CDCl_3) δ , ppm: 6.12 (1H, br. s), 4.45 (1H, d, $J = 6.7$ Hz), 3.76 (3H, s), 2.94 (1H, dt, $J = 6.5, 6.6$ Hz), 2.09 - 1.97 (1H, m), 1.91 - 1.80 (1H, m), 1.03 (3H, t, $J = 7.5$ Hz);

$^{13}\text{C-NMR}$ (400 MHz, CDCl_3) δ , ppm: 171.9, 168.3, 152.0, 57.1, 52.8, 48.4, 21.5, 11.1;

methyl (S)-2-((S)-2,5-dioxooxazolidin-4-yl)butanoate (11*)



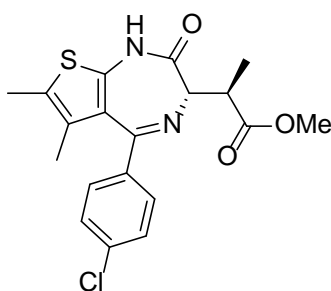
Yield: 121 mg (quant.) $^1\text{H-NMR}$ (400 MHz, MeOD) δ , ppm: 4.59 (1H, d, $J = 4.7$ Hz), 3.73 (3H, s), 2.87 - 2.81 (1H, m), 1.93 - 1.69 (2H, m), 1.02 (3H, t, $J = 7.5$ Hz);

$^{13}\text{C-NMR}$ (400 MHz, MeOD) δ , ppm: 173.9, 170.5, 154.2, 58.8, 52.8, 50.1, 22.4, 12.2;

General procedure for thienodiazepines (**13**, **14** and **14***)

(2-amino-4,5-dimethylthiophen-3-yl)(4-chlorophenyl)methanone (1 eq.) was suspended in toluene (830 mL/mol). 4 Å molecular sieves and TFA (2 eq.) were then added and stirred at r.t. for 5 min. *N*-carboxyanhydrides, **10**, **11** and **11***, (1.2 eq.) were dissolved in toluene (210 mL/mol) (DCM for compound **10**) and subsequently added to the flask which was then heated at 60°C for 1 h. The conversion of the amino ketone was monitored by LC-MS. TEA (2.5 eq.) was then added and the reaction was heated to 80°C and stirred for 2 h. The mixture was then cooled to r.t. and concentrated *in vacuo*. The residue was purified by flash column chromatography (12 g silica column) using a linear gradient from 0% to 40% EtOAc in heptane to afford **13**, **14** and **14*** in 29 – 51% yields.

methyl (R)-2-((S)-5-(4-chlorophenyl)-6,7-dimethyl-2-oxo-2,3-dihydro-1H-thieno[2,3-e][1,4]diazepin-3-yl)propanoate (**13**)

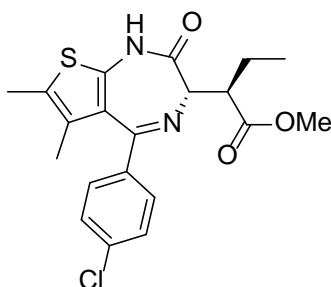


Yield: 228 mg (44%); ¹H-NMR (400 MHz, CDCl₃) δ, ppm: 9.64 (1H, s), 7.33 (2H, d, *J* = 8.7 Hz), 7.29 (2H, d, *J* = 8.9 Hz), 3.86 (1H, d, *J* = 10.1 Hz), 3.78 (3H, s), 3.71 (1H, qd, *J* = 6.8, 10.2 Hz), 2.28 (3H, s), 1.58 (3H, s), 1.38 (3H, d, *J* = 6.9 Hz);

¹³C-NMR (400 MHz, CDCl₃) δ, ppm: 176.0, 168.0, 164.7, 141.1, 136.9, 136.5, 130.3, 129.8, 128.7, 127.9, 126.9, 67.1, 51.7, 42.0, 15.1, 14.5, 13.0;

LC-MS *m/z* calc. for C₁₉H₂₀ClN₂O₃S [M+H]⁺ 391.1, found: 391.1.

methyl (R)-2-((S)-5-(4-chlorophenyl)-6,7-dimethyl-2-oxo-2,3-dihydro-1H-thieno[2,3-e][1,4]diazepin-3-yl)butanoate (14)

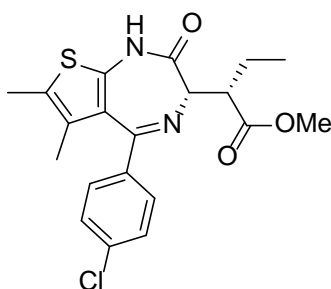


Yield: 119 mg (51%); $^1\text{H-NMR}$ (500 MHz, CDCl_3) δ , ppm: 9.64 (1H, s), 7.31 (2H, d, $J = 8.6$ Hz), 7.28 (2H, d, $J = 8.6$ Hz), 3.83 (1H, d, $J = 10.4$ Hz), 3.80 (3H, s), 3.64 (1H, dt, $J = 3.7, 10.6$ Hz), 2.27 (3H, s), 1.99 (3H, s), 1.95 - 1.85 (1H, m), 1.64 - 1.54 (4H, m), 1.02 (3H, t, $J = 7.5$ Hz);

$^{13}\text{C-NMR}$ (400 MHz, CDCl_3) δ , ppm: 175.5, 167.7, 164.8, 141.0, 136.8, 136.5, 130.3, 129.9, 128.7, 127.9, 126.9, 66.4, 51.6, 49.5, 23.5, 14.6, 13.0, 12.0;

LC-MS m/z calc. for $\text{C}_{20}\text{H}_{22}\text{ClN}_2\text{O}_3\text{S}$ $[\text{M}+\text{H}]^+$ 405.1, found: 405.1.

methyl (S)-2-((S)-5-(4-chlorophenyl)-6,7-dimethyl-2-oxo-2,3-dihydro-1H-thieno[2,3-e][1,4]diazepin-3-yl)butanoate (14*)



Yield: 35 mg (29%); $^1\text{H-NMR}$ (400 MHz, CDCl_3) δ , ppm: 9.55 (1H, s), 7.42 (2H, d, $J = 8.6$ Hz), 7.33 (2H, d, $J = 8.2$ Hz), 3.99 (1H, d, $J = 11.1$ Hz), 3.77 (3H, s), 3.47 (1H, ddd, $J = 4.0, 8.9, 10.7$ Hz), 2.27 (3H, s), 2.18 - 2.06 (1H, m), 1.81 - 1.68 (1H, m), 1.59 (3H, s), 0.96 (3H, t, $J = 7.5$ Hz);

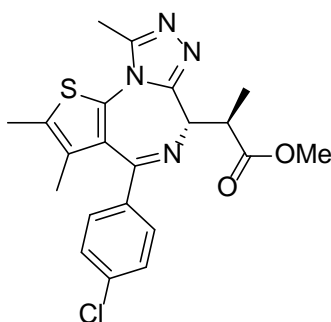
$^{13}\text{C-NMR}$ (400 MHz, CDCl_3) δ , ppm: 175.7, 169.5, 165.3, 141.6, 137.2, 136.5, 130.3, 129.6, 128.7, 127.5, 126.7, 65.0, 51.7, 47.3, 22.6, 14.5, 12.9, 11.0;

LC-MS m/z calc. for $\text{C}_{20}\text{H}_{20}\text{ClN}_2\text{O}_3\text{S}$ $[\text{M}+\text{H}]^+$ 405.1, found: 405.1.

General procedure for triazolothienodiazepines (**15**, **16** and **16***)

Thienodiazepines **13**, **14** and **14***, were dissolved in THF (5 L/mol) and cooled to -78°C. 1.0 M KO^tBu in THF (1.5 eq.) was added dropwise and stirred at -78°C for 1 h. Diethyl chlorophosphate (1.5 eq.) was added dropwise and left to warm to -10°C over 2 h. Conversion to the phosphorylimidate intermediate was monitored by LC-MS. Acetyl hydrazine (2 eq.) was then added and left to stir at r.t. for 1 h. *n*-Butanol (7.6 L/mol) was added and the reaction was heated to 90°C and stirred for 2 h. The mixture was then cooled to r.t. and concentrated *in vacuo*. The residue was purified by reverse phase flash column chromatography (50 g C18 gold column) using a linear gradient from 30% to 75% MeCN in 0.1% formic acid in water to afford **15**, **16** and **16*** in 12 – 39% yields as pale yellow sticky solids.

methyl (R)-2-((S)-4-(4-chlorophenyl)-2,3,9-trimethyl-6H-thieno[3,2-*f*][1,2,4]triazolo[4,3-*a*][1,4]diazepin-6-yl)propanoate (**ME-JQ1-OMe** (**15**))

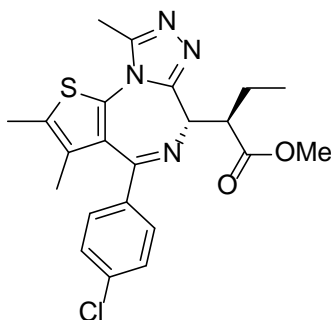


Yield: 98 mg (39%); ¹H-NMR (500 MHz, CDCl₃) δ, ppm: 7.32 (2H, d, *J* = 8.3 Hz), 7.28 (2H, d, *J* = 8.3 Hz), 4.23 (1H, d, *J* = 10.7 Hz), 4.07 - 3.98 (1H, m), 3.80 (3H, s), 2.65 (3H, s), 2.39 (3H, s), 1.66 (3H, s), 1.48 (3H, d, *J* = 7.0 Hz);

¹³C-NMR (500 MHz, CDCl₃) δ, ppm: 175.8, 163.2, 154.3, 149.8, 136.8, 136.5, 131.9, 131.1, 130.9, 130.7, 129.9, 128.7, 60.2, 51.8, 42.5, 15.3, 14.4, 13.1, 11.7;

LC-MS *m/z* calc. for C₂₁H₂₂ClN₄O₂S [M+H]⁺ 429.1, found: 429.1.

methyl (R)-2-((S)-4-(4-chlorophenyl)-2,3,9-trimethyl-6H-thieno[3,2-f][1,2,4]triazolo[4,3-a][1,4]diazepin-6-yl)butanoate (ET-JQ1-OMe (16))



Enantiomeric excess of 99.0% (determined with chiral SFC).

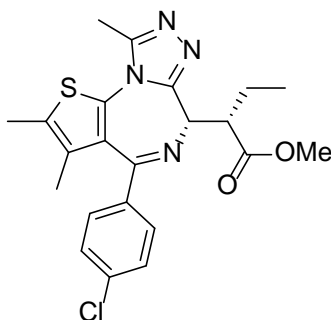
Column Details	Amy SA (4.6mm x 250mm, 5um)
Column Temperature	40°C
Flow Rate	4 mL/min
Isocratic Conditions	25:75 MeOH:CO ₂ (0.2% v/v NH ₃)

Yield: 45 mg (35%); ¹H-NMR (500 MHz, CDCl₃) δ, ppm: 7.31 (2H, d, *J* = 8.9 Hz), 7.28 (2H, d, *J* = 8.6 Hz), 4.22 (1H, d, *J* = 10.9 Hz), 3.97 (1H, ddd, *J* = 10.7, 10.7, 3.6 Hz), 3.82 (3H, s), 2.64 (3H, s), 2.39 (3H, s), 2.22 - 2.11 (1H, m), 1.72 - 1.60 (4H, m), 1.00 (3H, t, *J* = 7.4 Hz);

¹³C-NMR (500 MHz, CDCl₃) δ, ppm: 175.4, 163.2, 154.5, 149.8, 136.8, 136.6, 132.2, 131.0, 130.9, 130.5, 129.9, 128.7, 59.5, 51.6, 49.7, 23.3, 14.5, 13.2, 11.9, 11.7;

HRMS *m/z* calc. for C₂₂H₂₄ClN₄O₂S [M+H]⁺ 443.1308, found: 443.1303.

methyl (S)-2-((S)-4-(4-chlorophenyl)-2,3,9-trimethyl-6H-thieno[3,2-f][1,2,4]triazolo[4,3-a][1,4]diazepin-6-yl)butanoate (16*)

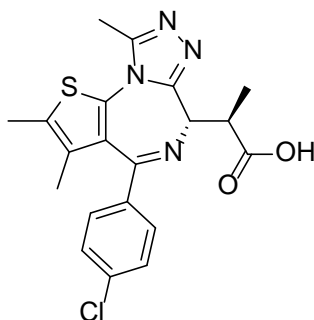


Yield: 4.5 mg (12%); ¹H-NMR (400 MHz, CDCl₃) δ, ppm: 7.43 (2H, d, *J* = 8.6 Hz), 7.34 (2H, d, *J* = 8.7 Hz), 4.31 (1H, d, *J* = 10.9 Hz), 3.84 (1H, ddd, *J* = 3.8, 9.3, 10.9 Hz), 3.73 (3H, s), 2.64 (3H, s), 2.42 (3H, s), 2.38 - 2.27 (1H, m), 1.93 - 1.81 (1H, m), 1.70 (3H, s), 1.06 (3H, t, *J* = 7.5 Hz);

¹³C-NMR (400 MHz, CDCl₃) δ, ppm: 175.5, 163.9, 155.5, 149.6, 136.95, 136.91, 132.7, 130.81, 130.75, 130.3, 129.9, 128.8, 57.6, 51.9, 47.6, 23.4, 14.5, 13.2, 12.0, 11.2;

HRMS *m/z* calc. for C₂₂H₂₄ClN₄O₂S [M+H]⁺ 443.1308, found: 443.1305.

(*R*)-2-((*S*)-4-(4-chlorophenyl)-2,3,9-trimethyl-6H-thieno[3,2-*f*][1,2,4]triazolo[4,3-*a*][1,4]diazepin-6-yl)propanoic acid (**ME-JQ1-OH (17)**)



Methyl (*R*)-2-((*S*)-6-(4-chlorophenyl)-9-methoxy-1-methyl-4H-benzo[*f*][1,2,4]triazolo[4,3-*a*][1,4]diazepin-4-yl)propanoate (133 mg, 0.31 mmol) was dissolved in THF (4.59 ml). LiOH (15 mg, 0.62 mmol) was subsequently dissolved in water (1.15 ml) and added to the flask. The flask was heated to 30°C and stirred for 48 h. The conversion of the ester to the acid was monitored by LC-MS. Water (0.25 ml) was added at regular intervals (every 12 h) to assist with the conversion. After 100% conversion, the solution was neutralised with 2.0 M HCl solution and freeze dried. Slight epimerisation of the carbon adjacent to the carbonyl had occurred so the residue was purified by HPLC using a linear gradient of 35 to 75% MeCN in 0.1% formic acid in water over 10 minutes to afford (*R*)-2-((*S*)-4-(4-chlorophenyl)-2,3,9-trimethyl-6H-thieno[3,2-*f*][1,2,4]triazolo[4,3-*a*][1,4]diazepin-6-yl)propanoic acid (isolated yield of 77 mg, 61%) as a white solid with an enantiomeric excess of 98.7% (determined with chiral SFC).

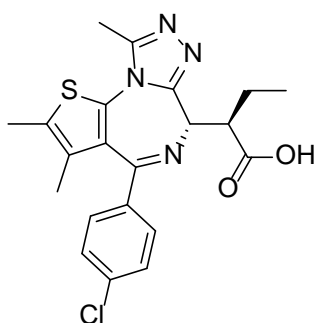
Column Details	Chiralpak IG (4.6mm x 250mm, 5um)
Column Temperature	40°C
Flow Rate	4 mL/min
Isocratic Conditions	45:55 MeOH:CO ₂ (0.2% v/v NH ₃)

$^1\text{H-NMR}$ (500 MHz, CDCl_3) δ , ppm: 7.39 (2H, d, $J = 8.2$ Hz), 7.28 (2H, d, $J = 8.1$ Hz), 4.22 (1H, d, $J = 8.0$ Hz), 3.93 (1H, dq, $J = 7.2, 7.2$ Hz), 2.68 (3H, s), 2.41 (3H, s), 1.69 (3H, s), 1.54 (3H, d, $J = 6.9$ Hz);

$^{13}\text{C-NMR}$ (500 MHz, CDCl_3) δ , ppm: 177.1, 164.0, 154.7, 150.0, 137.2, 136.2, 132.1, 131.4, 131.1, 130.6, 130.1, 128.8, 59.6, 41.9, 15.7, 14.6, 13.2, 11.8;

HRMS m/z calc. for $\text{C}_{20}\text{H}_{20}\text{ClN}_4\text{O}_2\text{S}$ $[\text{M}+\text{H}]^+$ 415.0995, found: 415.1009.

(*R*)-2-((*S*)-4-(4-chlorophenyl)-2,3,9-trimethyl-6H-thieno[3,2-*f*][1,2,4]triazolo[4,3-*a*][1,4]diazepin-6-yl)butanoic acid (ET-JQ1-OH (18))



Methyl (*R*)-2-((*S*)-4-(4-chlorophenyl)-2,3,9-trimethyl-6H-thieno[3,2-*f*][1,2,4]triazolo[4,3-*a*][1,4]diazepin-6-yl)butanoate (60 mg, 0.14 mmol) was dissolved in THF (2.0 ml). LiOH (8 mg, 0.34 mmol) was subsequently dissolved in water (0.5 ml) and added to the flask. The flask was heated to 45°C and stirred for 6 days. The conversion of the ester to the acid was monitored by LC-MS. Water (0.25 ml) and 0.65 M LiOH solution (0.25 ml) was added at regular intervals (every 12 h) to assist with the conversion. After 100% conversion, the solution was neutralised with 2.0 M HCl solution and freeze dried. Slight epimerisation of the carbon adjacent to the carbonyl had occurred so the residue was purified by HPLC using a linear gradient of 35 to 75% MeCN in 0.1% formic acid in water over 10 minutes to afford (*R*)-2-((*S*)-4-(4-chlorophenyl)-2,3,9-trimethyl-6H-thieno[3,2-*f*][1,2,4]triazolo[4,3-*a*][1,4]diazepin-6-yl)butanoic acid (isolated yield of 48 mg, 83%) as a white solid with an enantiomeric excess of 99.0% (determined with chiral SFC).

Column Details	Amy SA (4.6mm x 250mm, 5um)
Column Temperature	40°C
Flow Rate	4 mL/min
Isocratic Conditions	35:65 EtOH:CO ₂ (0.2% v/v NH ₃)

$^1\text{H-NMR}$ (400 MHz, CDCl_3) δ , ppm: 7.38 (2H, d, $J = 8.5$ Hz), 7.26 (2H, d, $J = 8.6$ Hz), 4.25 (1H, d, $J = 8.2$ Hz), 3.81 (1H, ddd, $J = 4.6, 4.6, 13.1$ Hz), 2.67 (3H, s), 2.40 (3H, s), 2.12 - 2.00 (1H, m), 1.93 - 1.80 (1H, m), 1.68 (3H, s), 1.07 (3H, t, $J = 7.4$ Hz);

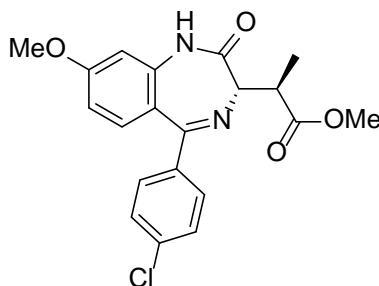
$^{13}\text{C-NMR}$ (400 MHz, CDCl_3) δ , ppm: 176.6, 164.1, 154.7, 150.0, 137.1, 136.2, 132.2, 131.4, 131.1, 130.4, 130.1, 128.8, 58.5, 49.0, 23.5, 14.5, 13.2, 11.77, 11.75;

HRMS m/z calc. for $\text{C}_{21}\text{H}_{22}\text{ClN}_4\text{O}_2\text{S}$ $[\text{M}+\text{H}]^+$ 429.1152, found: 429.1137.

General procedure for benzodiazepines (**20** and **21**)

(2-amino-4-methoxyphenyl)(4-chlorophenyl)methanone (1 eq.) was suspended in toluene (830 mL/mol). 4 Å molecular sieves and TFA (2 eq.) were then added and stirred at r.t. for 5 min. *N*-carboxyanhydrides, **10** and **11** (1.2 eq.) were dissolved in toluene (210 mL/mol) (DCM for compound **10**) and subsequently added to the flask which was then heated at 60°C for 2 h. The conversion of the amino ketone was monitored by LC-MS. TEA (2.5 eq) was then added and the reaction was heated to 80°C and stirred for 2 h. The mixture was then cooled to r.t. and concentrated *in vacuo*. The residue was purified by HPLC using a linear gradient of 35 to 75% MeCN in 0.1% formic acid in water over 10 minutes to afford **20** and **21** with isolated yields of 30 and 50% yields respectively.

methyl (R)-2-((S)-5-(4-chlorophenyl)-8-methoxy-2-oxo-2,3-dihydro-1H-benzo[e][1,4]diazepin-3-yl)propanoate (**20**)

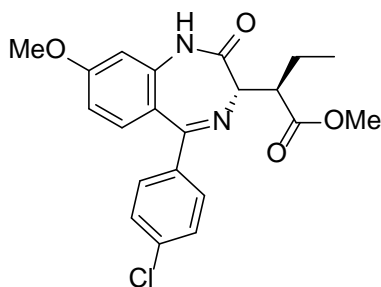


Yield: 14 mg (30%); $^1\text{H-NMR}$ (500 MHz, CDCl_3): δ , ppm: 9.09 (1H, s), 7.36 (2H, d, $J = 8.4$ Hz), 7.30 (2H, d, $J = 8.3$ Hz), 7.20 (1H, d, $J = 8.8$ Hz), 6.72 (1H, dd, $J = 2.1, 8.8$ Hz), 6.63 (1H, d, $J = 2.2$ Hz), 3.88 (3H, s), 3.81 - 3.77 (4H, m), 3.71 (1H, qd, $J = 6.7, 10.2$ Hz), 1.39 (3H, d, $J = 6.7$ Hz);

$^{13}\text{C-NMR}$ (500 MHz, CDCl_3) δ , ppm: 176.0, 169.6, 167.9, 162.4, 139.9, 137.8, 136.6, 132.9, 131.3, 128.5, 120.3, 111.0, 105.4, 66.3, 55.8, 51.8, 42.1, 15.0;

LC-MS m/z calc. for $\text{C}_{20}\text{H}_{20}\text{ClN}_2\text{O}_4$ $[\text{M}+\text{H}]^+$ 387.1, found: 387.0.

methyl (R)-2-((S)-5-(4-chlorophenyl)-8-methoxy-2-oxo-2,3-dihydro-1H-benzo[e][1,4]diazepin-3-yl)butanoate (21)



Yield: 14.8 mg (50%); $^1\text{H-NMR}$ (400 MHz, CDCl_3): δ , ppm: 8.50 (1H, s), 7.36 (2H, d, $J = 8.6$ Hz), 7.31 (2H, d, $J = 8.6$ Hz), 7.21 (1H, d, $J = 8.8$ Hz), 6.73 (1H, dd, $J = 2.5, 8.8$ Hz), 6.60 (1H, d, $J = 2.4$ Hz), 3.88 (3H, s), 3.81 (3H, s), 3.76 (1H, d, $J = 10.6$ Hz), 3.64 (1H, dt, $J = 3.6, 10.5$ Hz), 1.97 - 1.86 (1H, m), 1.63 - 1.51 (1H, m);

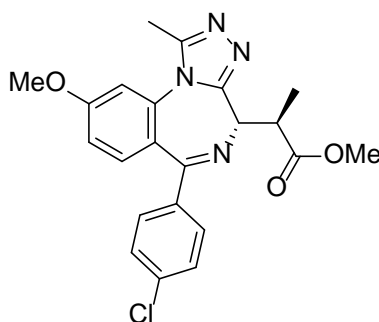
$^{13}\text{C-NMR}$ (400 MHz, CDCl_3) δ , ppm: 175.5, 169.2, 167.9, 162.4, 139.7, 137.8, 136.7, 133.0, 131.3, 128.5, 120.3, 111.0, 105.3, 65.7, 55.8, 51.6, 49.6, 23.5, 12.0;

LC-MS m/z calc. for $\text{C}_{21}\text{H}_{22}\text{ClN}_2\text{O}_4$ $[\text{M}+\text{H}]^+$ 401.1, found: 401.1.

General procedure for triazolobenzodiazepines (**22** and **23**)

Benzodiazepines **20** and **21**, were dissolved in THF (5 L/mol) and cooled to -78°C. 1.0 M KO^tBu in THF (1.5 eq.) was added dropwise and stirred at -78°C for 1 h. Diethyl chlorophosphate (3 eq.) was added dropwise and left to warm to -10°C over 2 h. Conversion to the phosphorylimidate intermediate was monitored by LC-MS. Acetyl hydrazine (3 eq.) was then added and left to stir at r.t. for 1 h. *n*-Butanol (7.6 L/mol) was added and the reaction was heated to 90°C and stirred for 2 h. The mixture was then cooled to r.t. and concentrated *in vacuo*. The residue was purified by HPLC using a linear gradient of 5 to 95% MeCN in 0.1% formic acid in water over 15 minutes to afford **22** and **23** in isolated yields of 11% and 8% respectively, with enantiomeric excess of 99.0% (determined with chiral SFC).

methyl (R)-2-((S)-6-(4-chlorophenyl)-9-methoxy-1-methyl-4H-benzof[1,2,4]triazolo[4,3-a][1,4]diazepin-4-yl)propanoate (**9-ME-1 (22)**)



Enantiomeric excess of 99.0% (determined with chiral SFC).

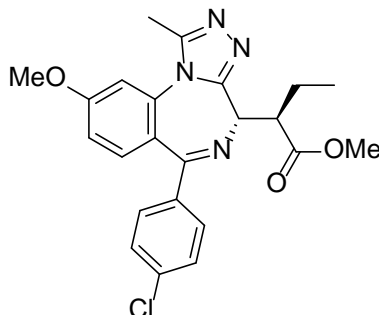
Column Details	Lux C1 (4.6mm x 250mm, 5um)
Column Temperature	40°C
Flow Rate	4 mL/min
Isocratic Conditions	30:70 EtOH:CO ₂ (0.2% v/v NH ₃)

Yield: 1.7 mg (11%); ¹H-NMR (400 MHz, CDCl₃): δ, ppm: 7.39 (2H, d, *J* = 8.5 Hz), 7.36 (1H, d, *J* = 8.8 Hz), 7.31 (2H, d, *J* = 8.7 Hz), 6.98 (1H, dd, *J* = 2.5, 8.7 Hz), 6.94 (1H, d, *J* = 2.4 Hz), 4.24 (1H, d, *J* = 10.7 Hz), 4.07 (1H, qd, *J* = 6.9, 10.7 Hz), 3.95 (3H, s), 3.82 (3H, s), 2.64 (3H, s), 1.49 (3H, d, *J* = 6.9 Hz);

¹³C-NMR (400 MHz, CDCl₃) δ, ppm: 176.2, 165.8, 161.8, 155.2, 150.3, 137.6, 136.9, 135.0, 133.5, 131.0, 128.6, 121.6, 112.9, 109.6, 59.8, 56.1, 51.9, 42.6, 15.4, 12.5;

LC-MS m/z calc. for C₂₂H₂₂ClN₄O₃ [M+H]⁺ 425.1, found: 425.0.

Methyl (*R*)-2-((*S*)-6-(4-chlorophenyl)-9-methoxy-1-methyl-4H-benzof[*f*][1,2,4]triazolo[4,3-*a*][1,4]diazepin-4-yl)butanoate (9-ET (23))



Enantiomeric excess of 99.1% (determined with chiral SFC).

Column Details	Lux C1 (4.6mm x 250mm, 5μm)
Column Temperature	40°C
Flow Rate	4 mL/min
Isocratic Conditions	25:75 EtOH:CO ₂ (0.2% v/v NH ₃)

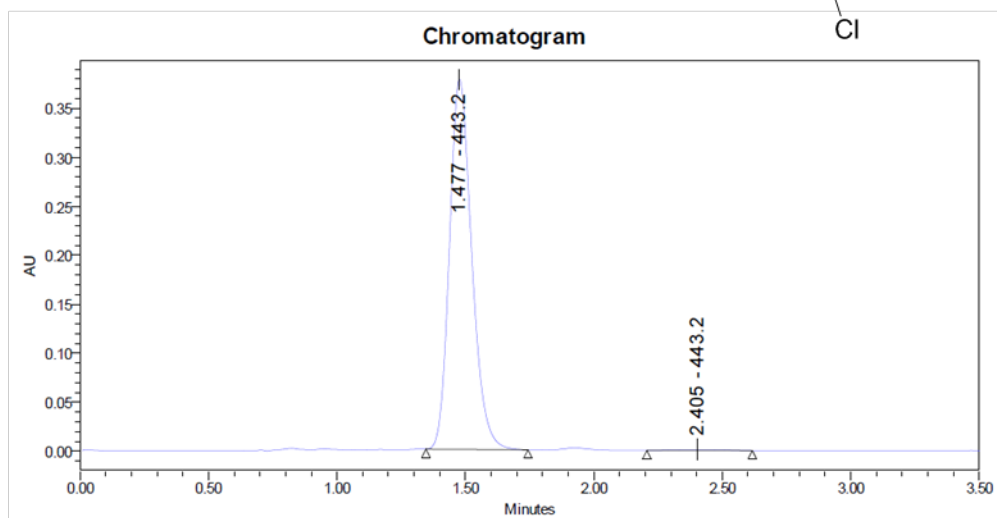
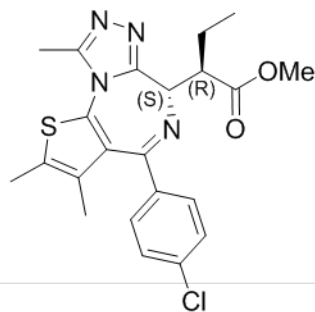
Yield: 1.6 mg (8%); ¹H-NMR (400 MHz, CDCl₃): δ, ppm: 7.39 - 7.33 (3H, m), 7.30 (2H, d, *J* = 8.7 Hz), 6.98 (1H, dd, *J* = 2.5, 8.8 Hz), 6.93 (1H, d, *J* = 2.5 Hz), 4.23 (1H, d, *J* = 11.0 Hz), 3.99 (1H, dt, *J* = 3.7, 10.8 Hz), 3.95 (3H, s), 3.84 (3H, s), 2.63 (3H, s), 2.24 - 2.12 (1H, m), 1.70 - 1.60 (1H, m), 1.01 (3H, t, *J* = 7.4 Hz);

¹³C-NMR (400 MHz, CDCl₃) δ, ppm: 175.7, 165.9, 161.7, 155.2, 150.4, 137.5, 136.9, 134.9, 133.6, 131.0, 128.5, 121.5, 112.8, 109.6, 58.9, 56.1, 51.7, 49.8, 23.3, 12.5, 11.7;

LC-MS m/z calc. for C₂₃H₂₄ClN₄O₃ [M+H]⁺ 439.2, found: 439.0.

Chiral HPLC Chromatograms

ET-JQ1-OMe (16)



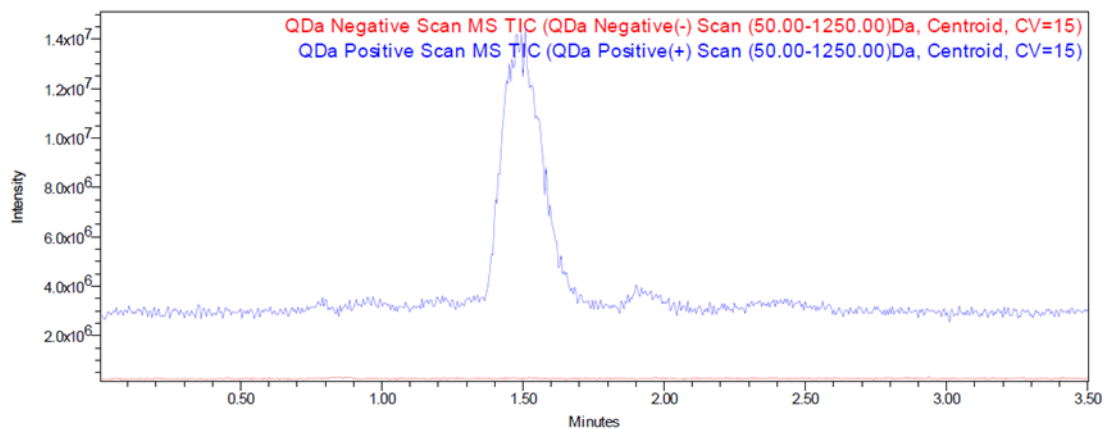
Peak Results				
	Retention Time (min)	Area ($\mu V \cdot sec$)	% Area	Width @ 50%
1	1.48	2275544	99.5	0.09195
2	2.40	11025	0.5	0.19363

Peak #1 - 1.477 - Q...

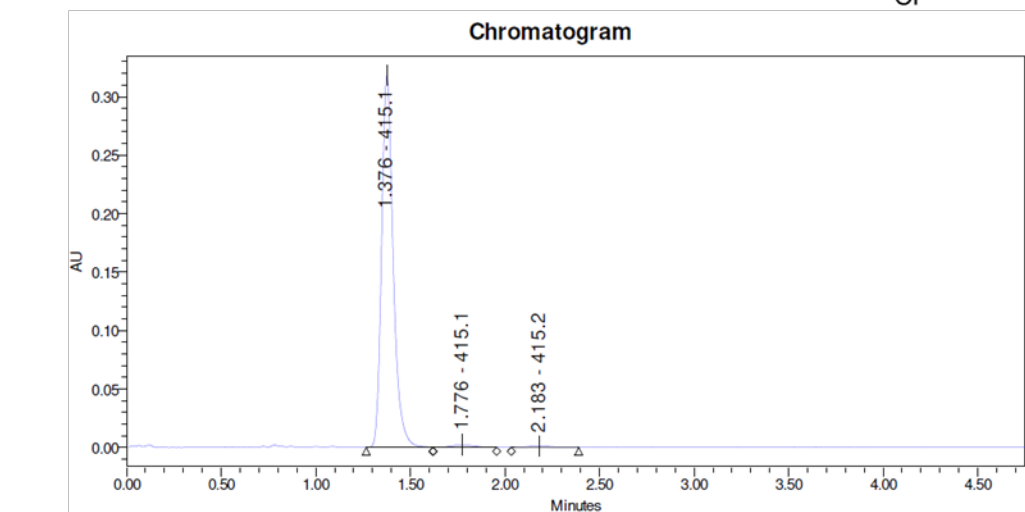
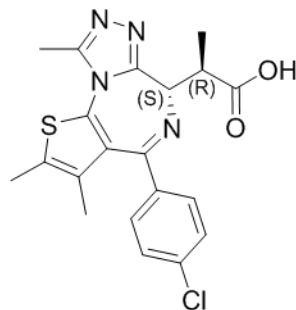
Apex

Peak #2 - 2.405 - Q...

Apex

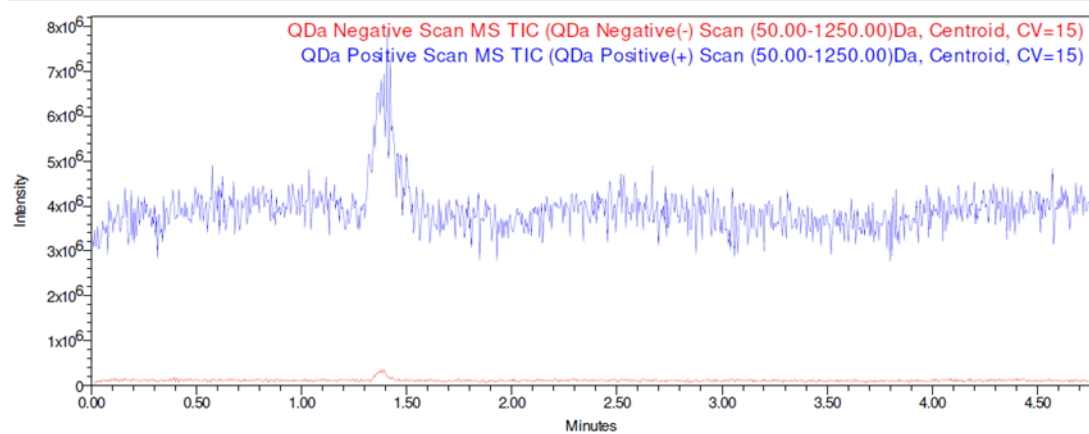
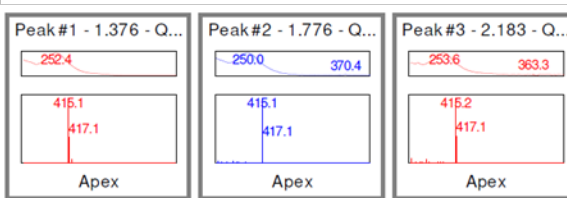


Me-JQ1-OH (17)

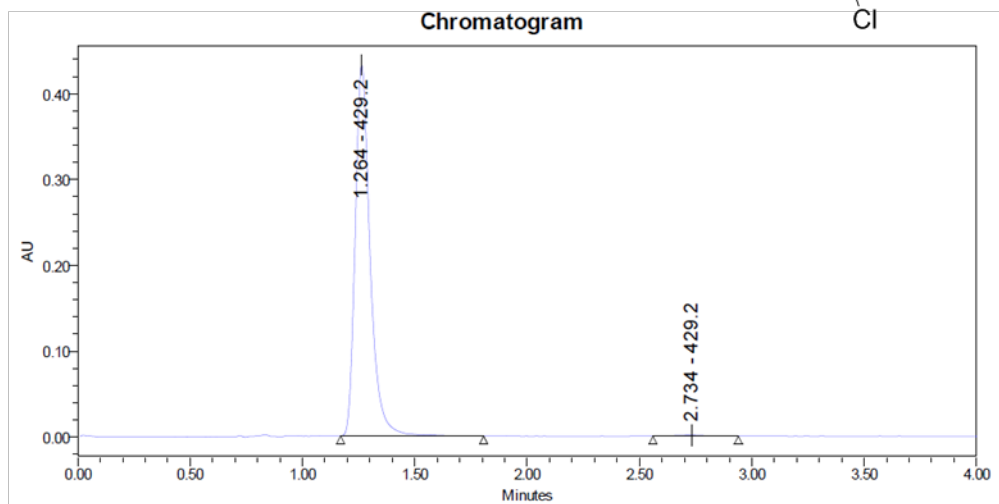
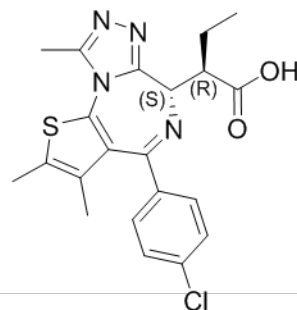


Peak Results

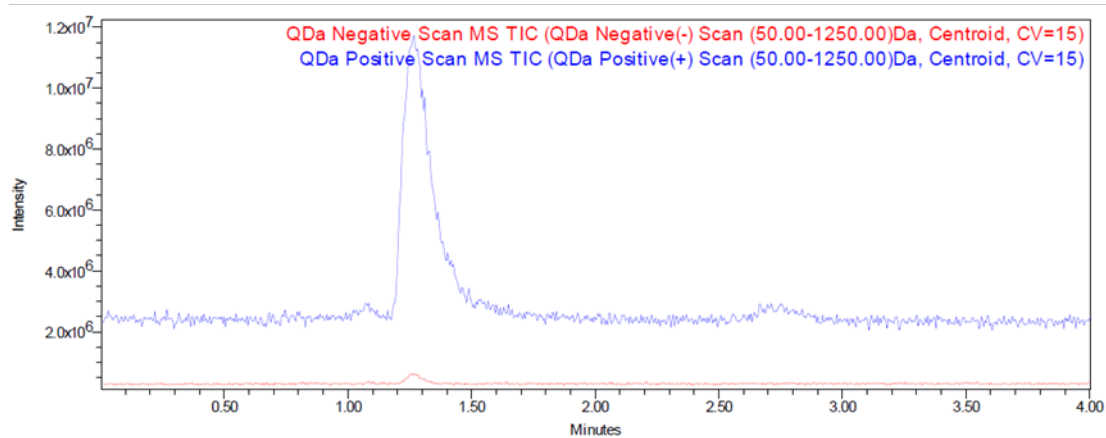
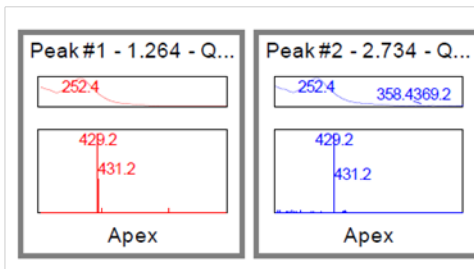
	Retention Time (min)	Area ($\mu\text{V}\cdot\text{sec}$)	% Area	Width @ 50%
1	1.38	1351725	98.0	0.06316
2	1.78	18099	1.3	0.11841
3	2.18	9703	0.7	0.13129



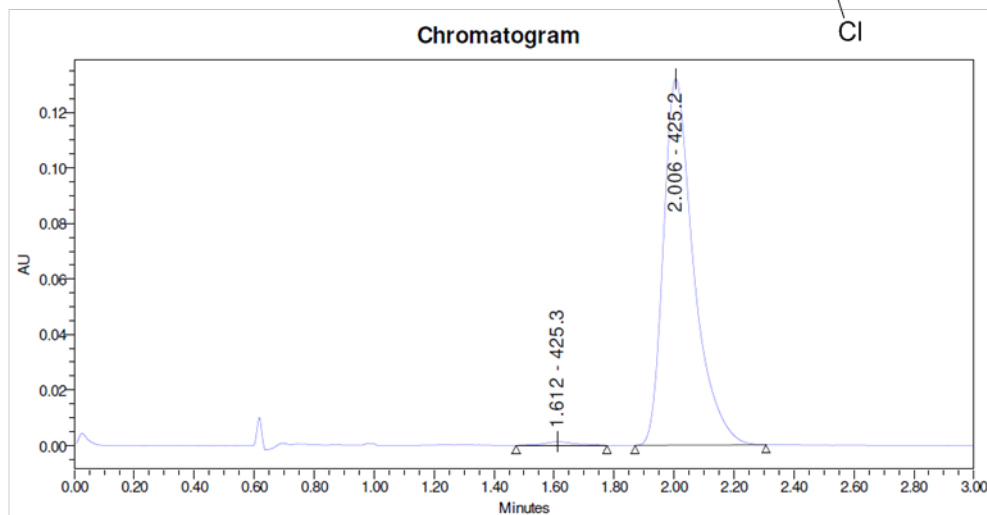
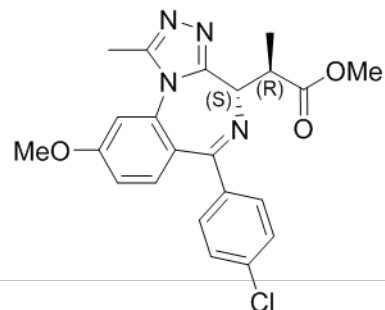
ET-JQ1-OH (18)



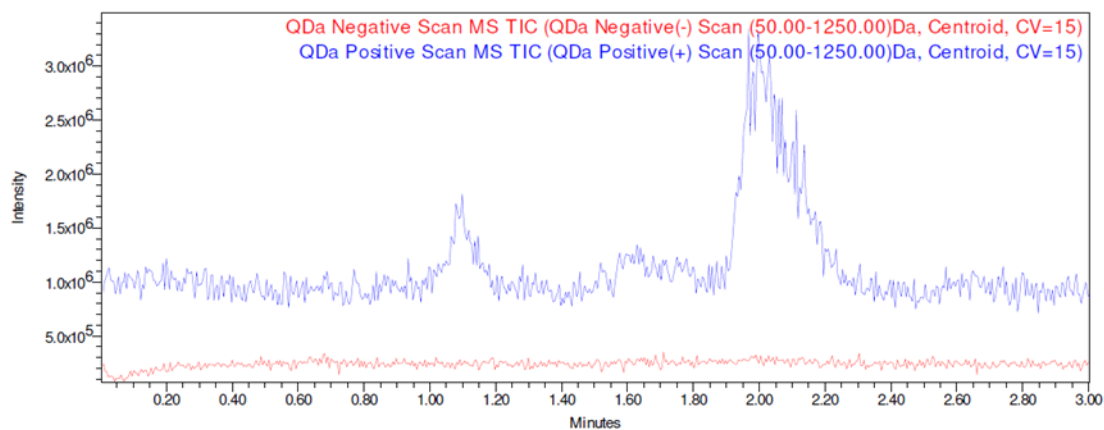
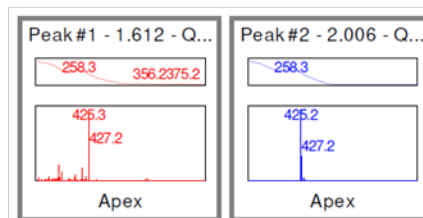
Peak Results				
	Retention Time (min)	Area (μV*sec)	% Area	Width @ 50%
1	1.26	1996022	99.5	0.06743
2	2.73	11033	0.5	0.17091



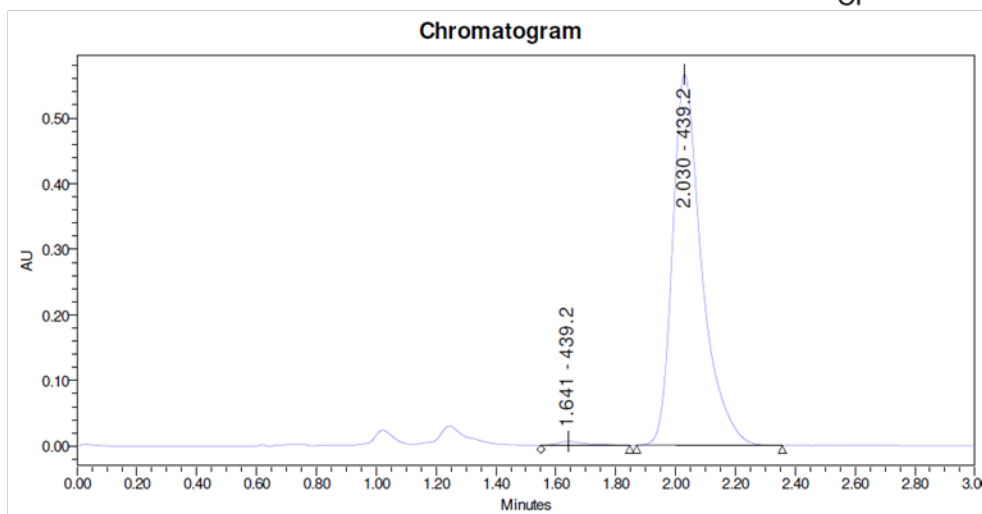
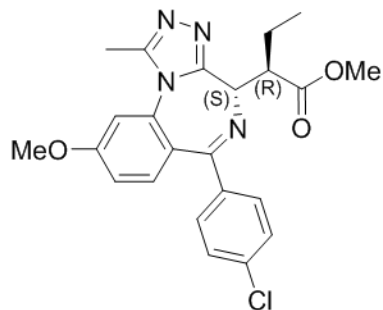
9-ME-1 (22)



Peak Results				
	Retention Time (min)	Area (μV*sec)	% Area	Width @ 50%
1	1.61	9770	1.0	0.10312
2	2.01	925436	99.0	0.10238



9-ET-1 (23)



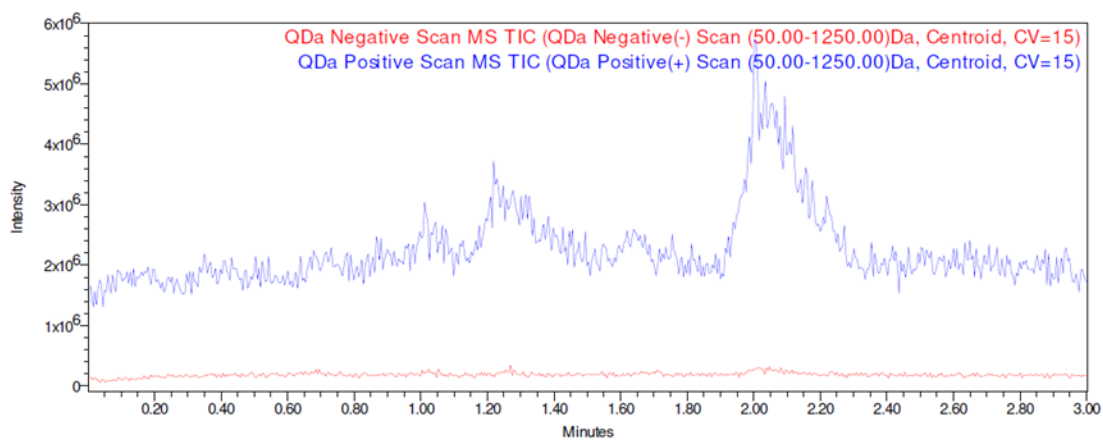
Peak Results				
	Retention Time (min)	Area ($\mu V \cdot sec$)	% Area	Width @ 50%
1	1.64	36447	0.9	0.08902
2	2.03	3824661	99.1	0.09786

Peak #1 - 1.641 - Q...

Apex

Peak #2 - 2.030 - Q...

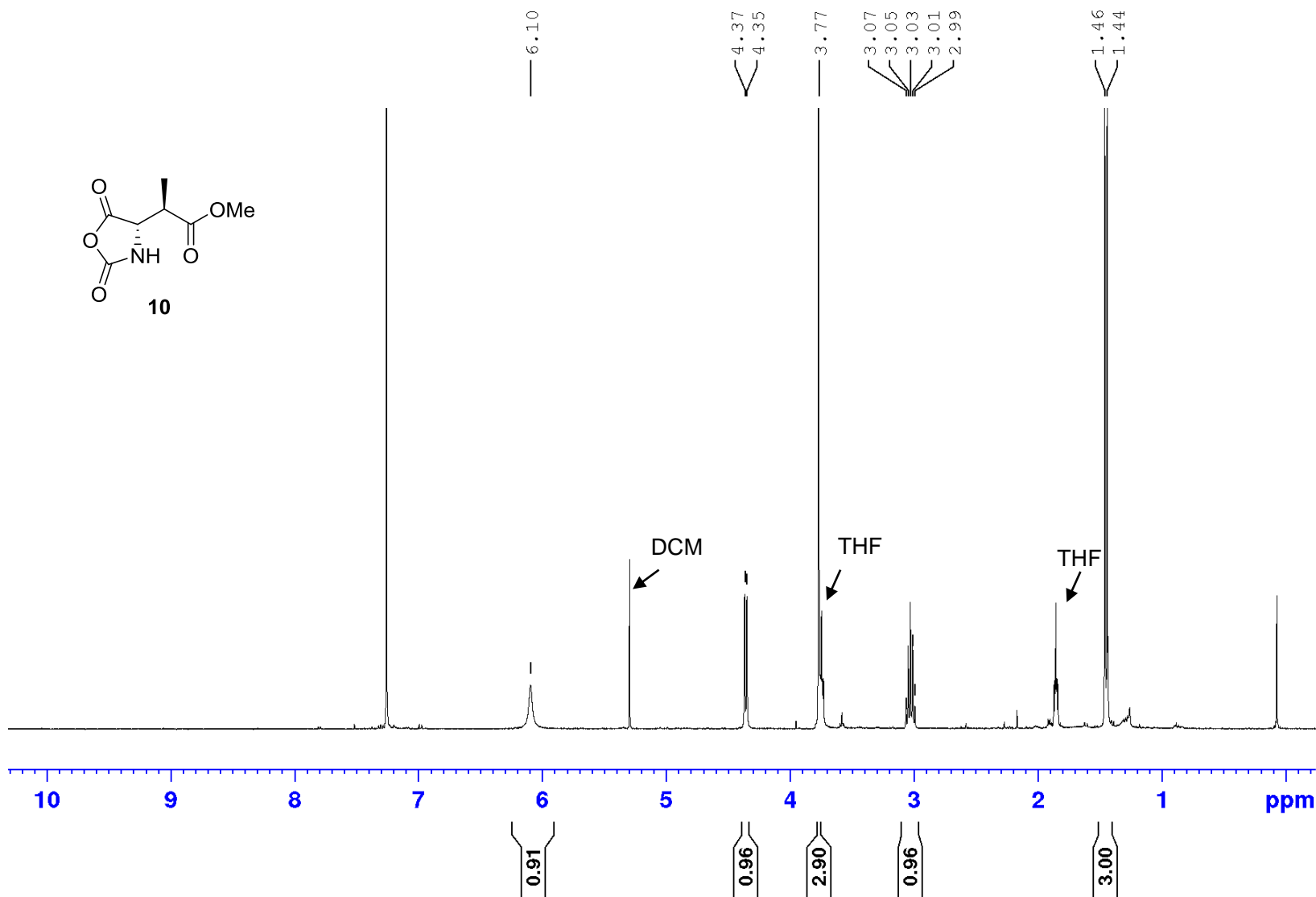
Apex



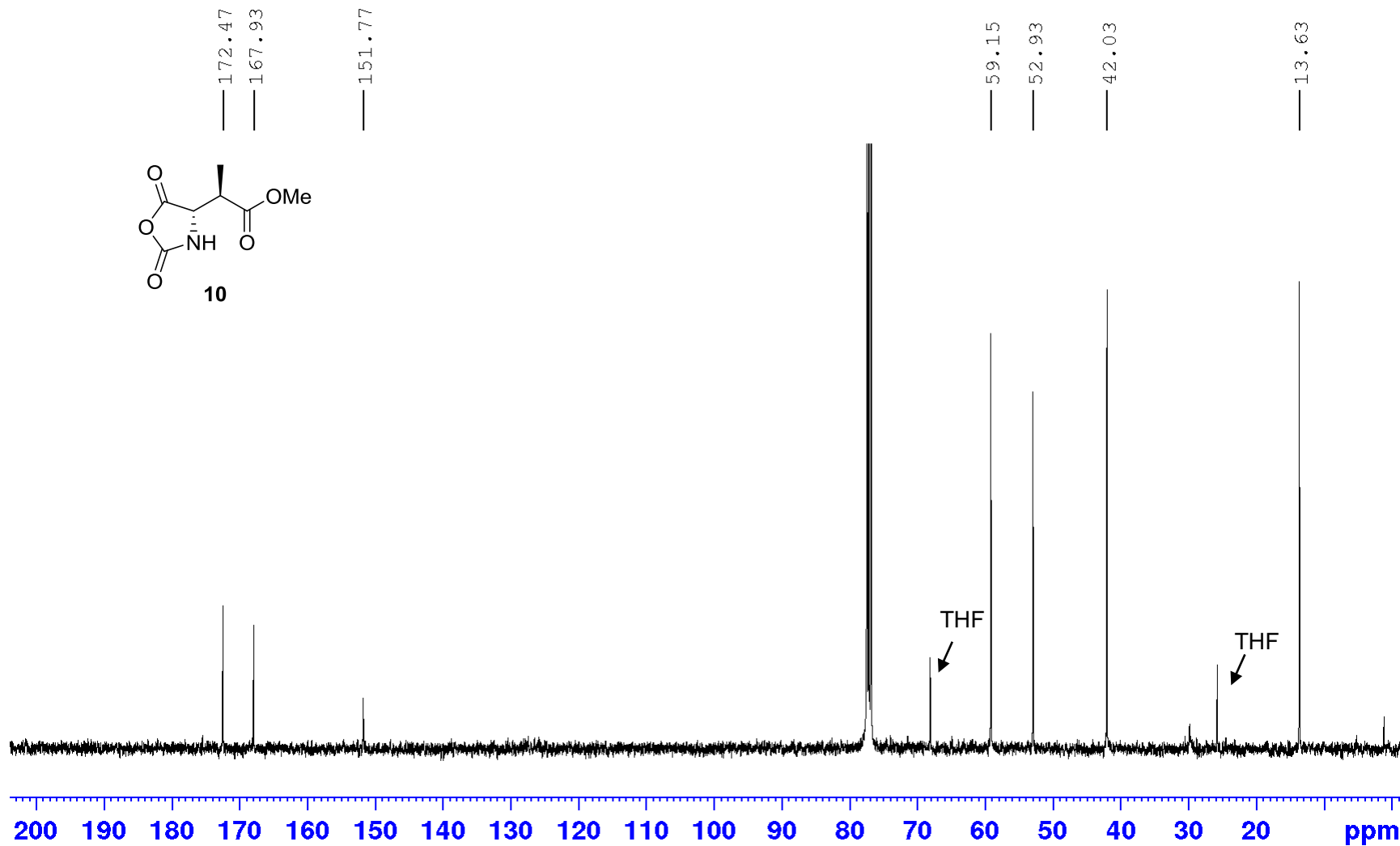
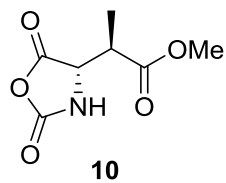
References

1. Runcie, A. C.; Zengerle, M.; Chan, K. H.; Testa, A.; van Beurden, L.; Baud, M. G. J.; Epemolu, O.; Ellis, L. C. J.; Read, K. D.; Coulthard, V.; Brien, A.; Ciulli, A., Optimization of a “bump-and-hole” approach to allele-selective BET bromodomain inhibition. *Chem Sci.* **2018**, 9 (9), 2452-2468.
2. Vonrhein, C.; Flensburg, C.; Keller, P.; Sharff, A.; Smart, O.; Paciorek, W.; Womack, T.; Bricogne, G., Data processing and analysis with the autoPROC toolbox. *Acta Crystallogr D Biol Crystallogr.* **2011**, 67, 293-302.
3. McCoy, A. J.; Grosse-Kunstleve, R. W.; Adams, P. D.; Winn, M. D.; Storoni, L. C.; Read, R. J., Phaser crystallographic software. *J Appl Crystallogr.* **2007**, 40 (4), 658-674.
4. Liebschner, D.; Afonine, P. V.; Baker, M. L.; Bunkoczi, G.; Chen, V. B.; Croll, T. I.; Hintze, B.; Hung, L.-W.; Jain, S.; McCoy, A. J.; Moriarty, N. W.; Oeffner, R. D.; Poon, B. K.; Prisant, M. G.; Read, R. J.; Richardson, J. S.; Richardson, D. C.; Sammito, M. D.; Sobolev, O. V.; Stockwell, D. H.; Terwilliger, T. C.; Urzhumtsev, A. G.; Videau, L. L.; Williams, C. J.; Adams, P. D., Macromolecular structure determination using X-rays, neutrons and electrons: recent developments in Phenix. *Acta Crystallogr D Struct Biol.* **2019**, 75 (10), 861-877.
5. Moriarty, N. W.; Grosse-Kunstleve, R. W.; Adams, P. D., electronic Ligand Builder and Optimization Workbench (eLBOW): a tool for ligand coordinate and restraint generation. *Acta Crystallogr D Biol Crystallogr.* **2009**, 65 (10), 1074-1080.

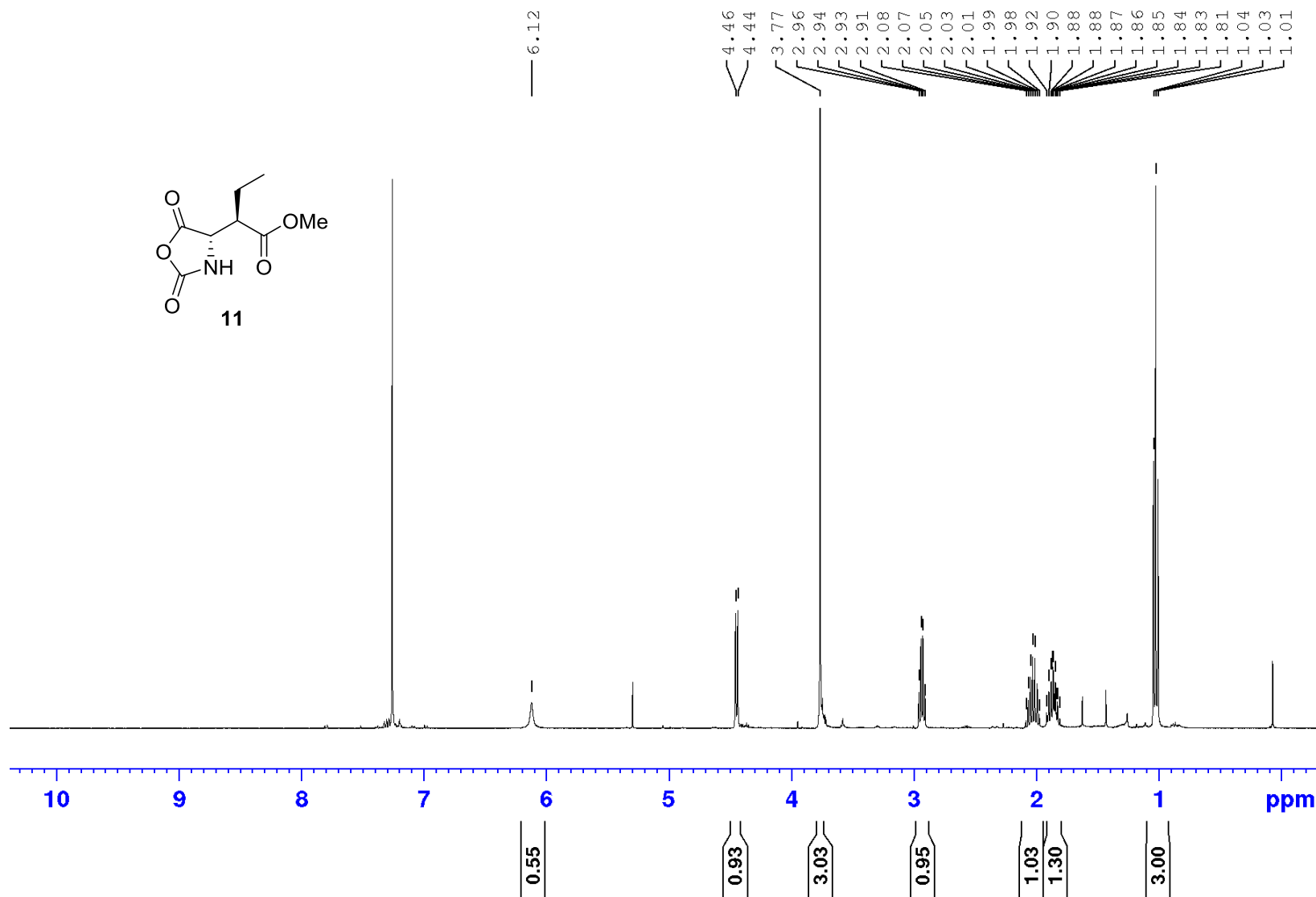
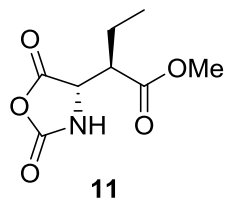
$^1\text{H-NMR}$, CDCl_3



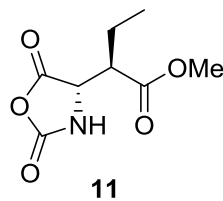
^{13}C -NMR, CDCl_3



$^1\text{H-NMR}$, CDCl_3



^{13}C -NMR, CDCl_3



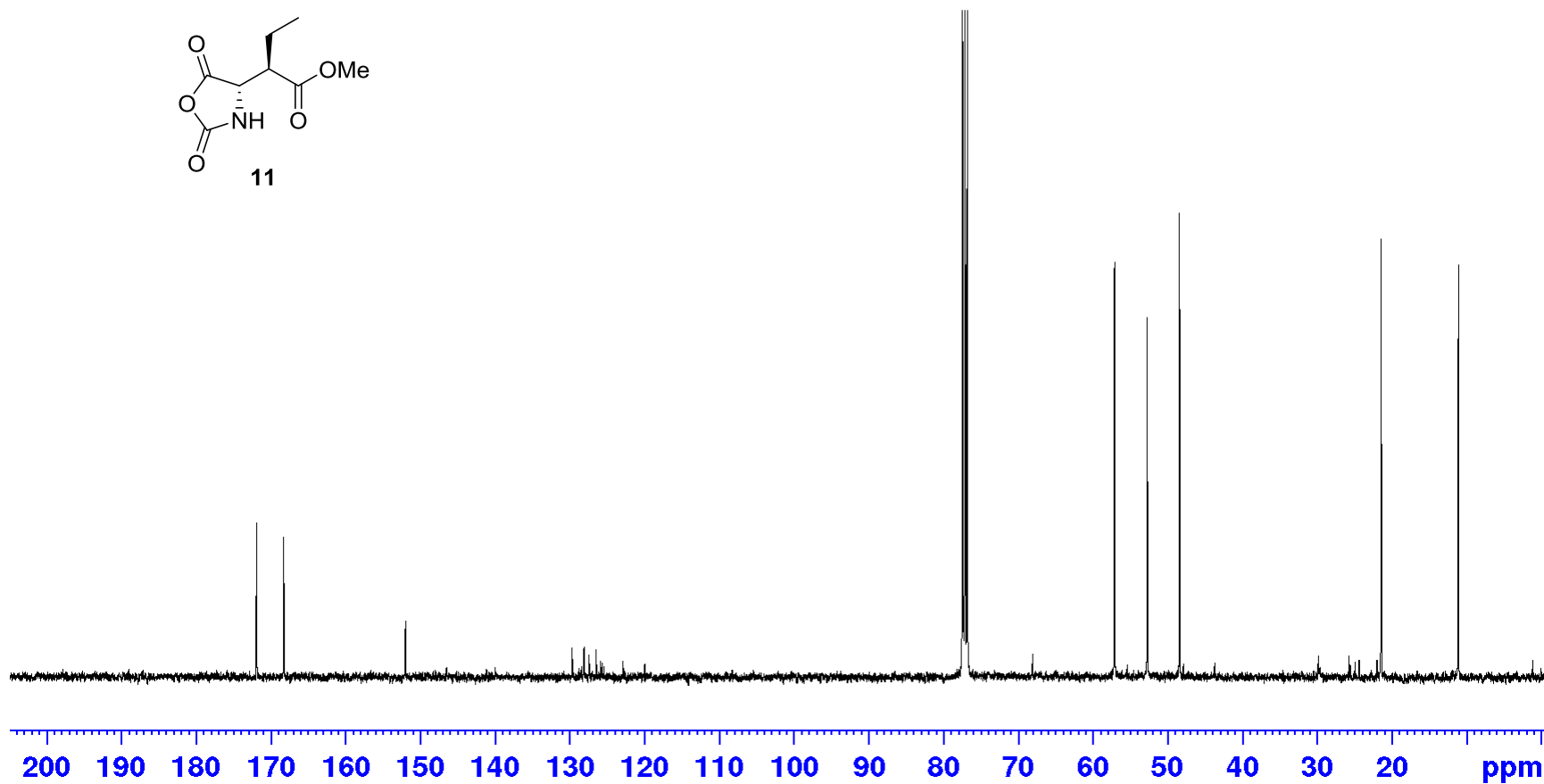
— 171.93
— 168.30

— 152.02

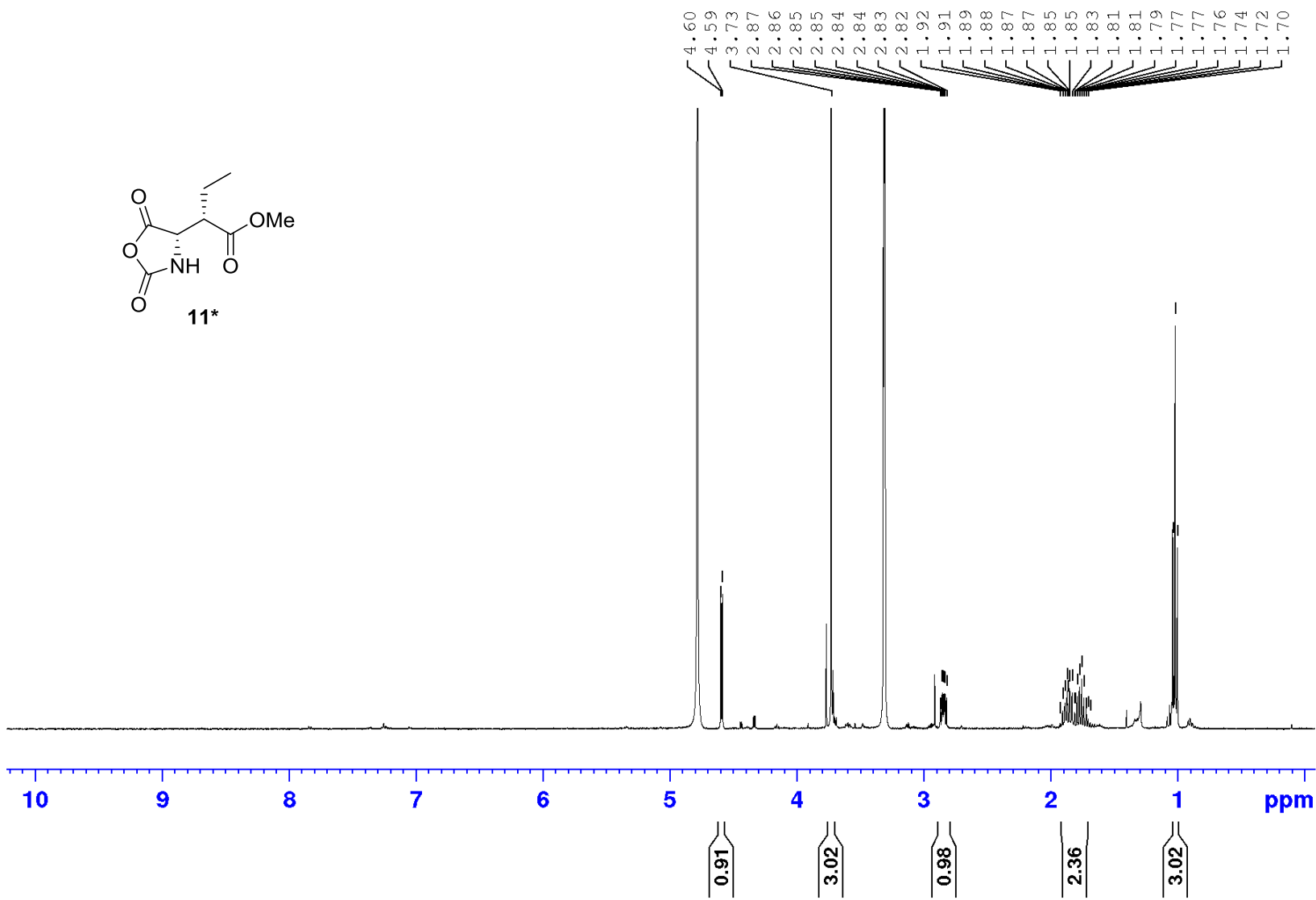
— 57.14
— 52.76
— 48.43

— 21.46

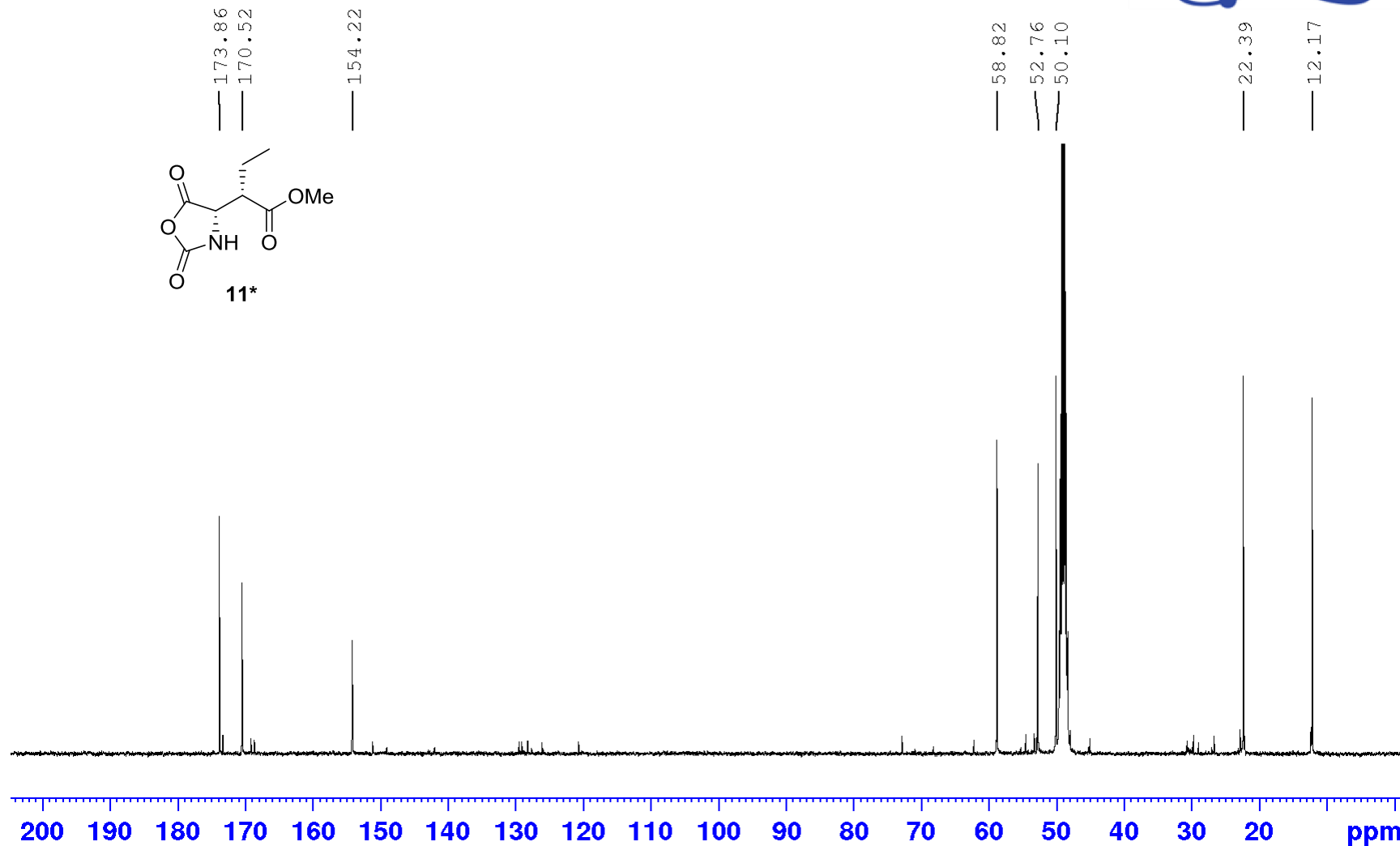
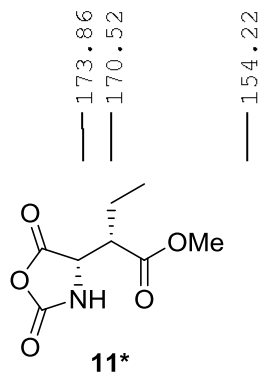
— 11.13



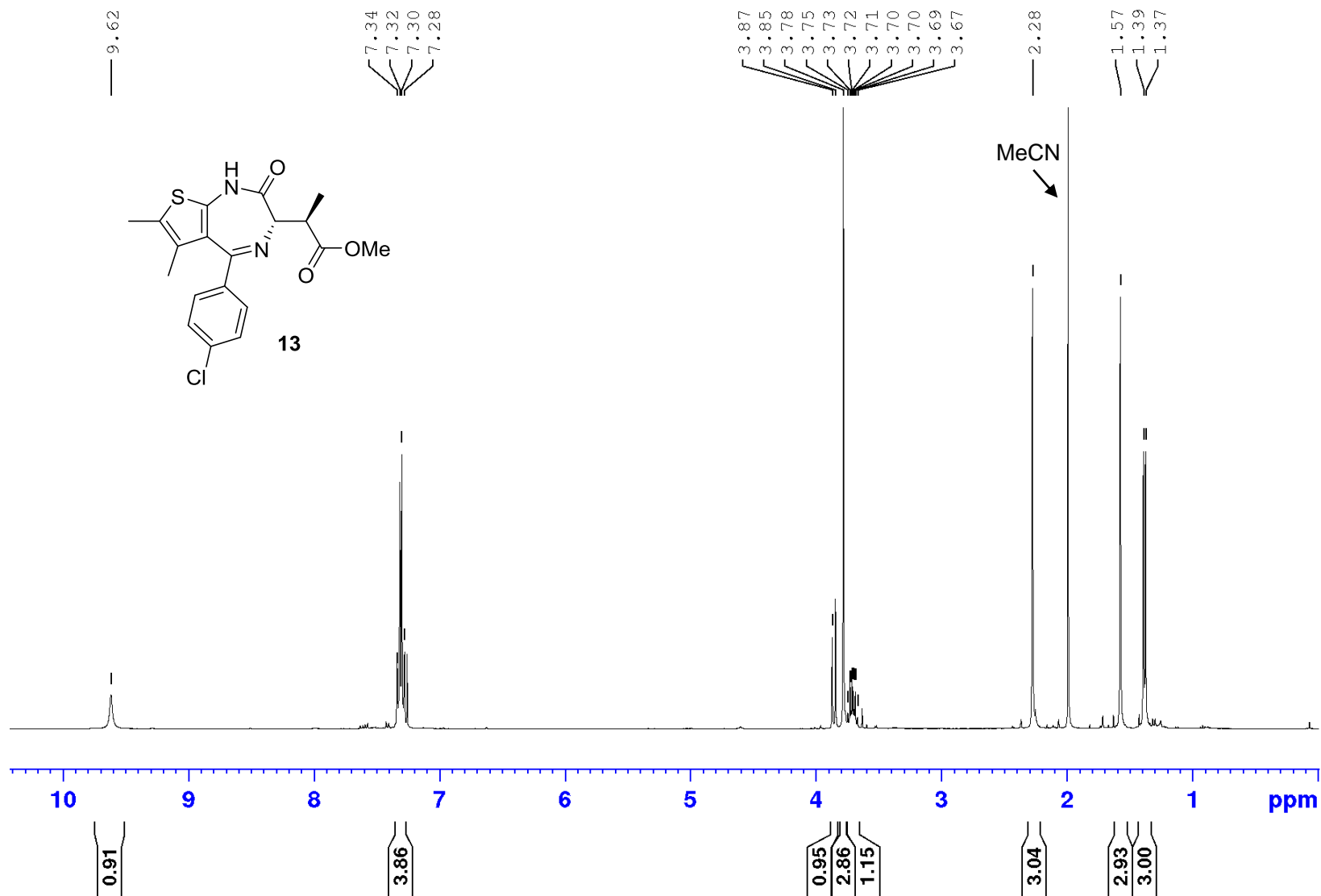
^1H -NMR, MeOD



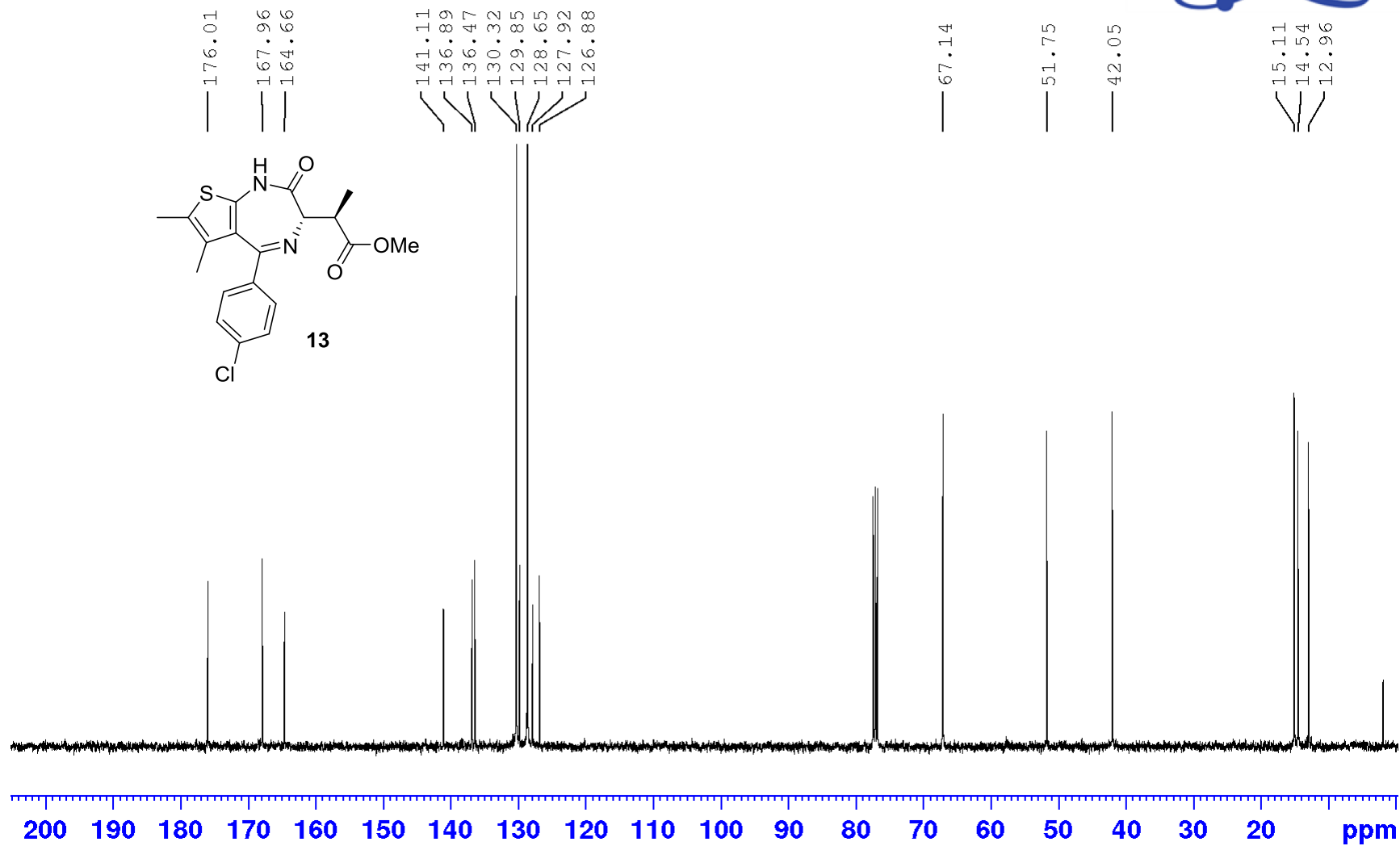
^{13}C -NMR, MeOD



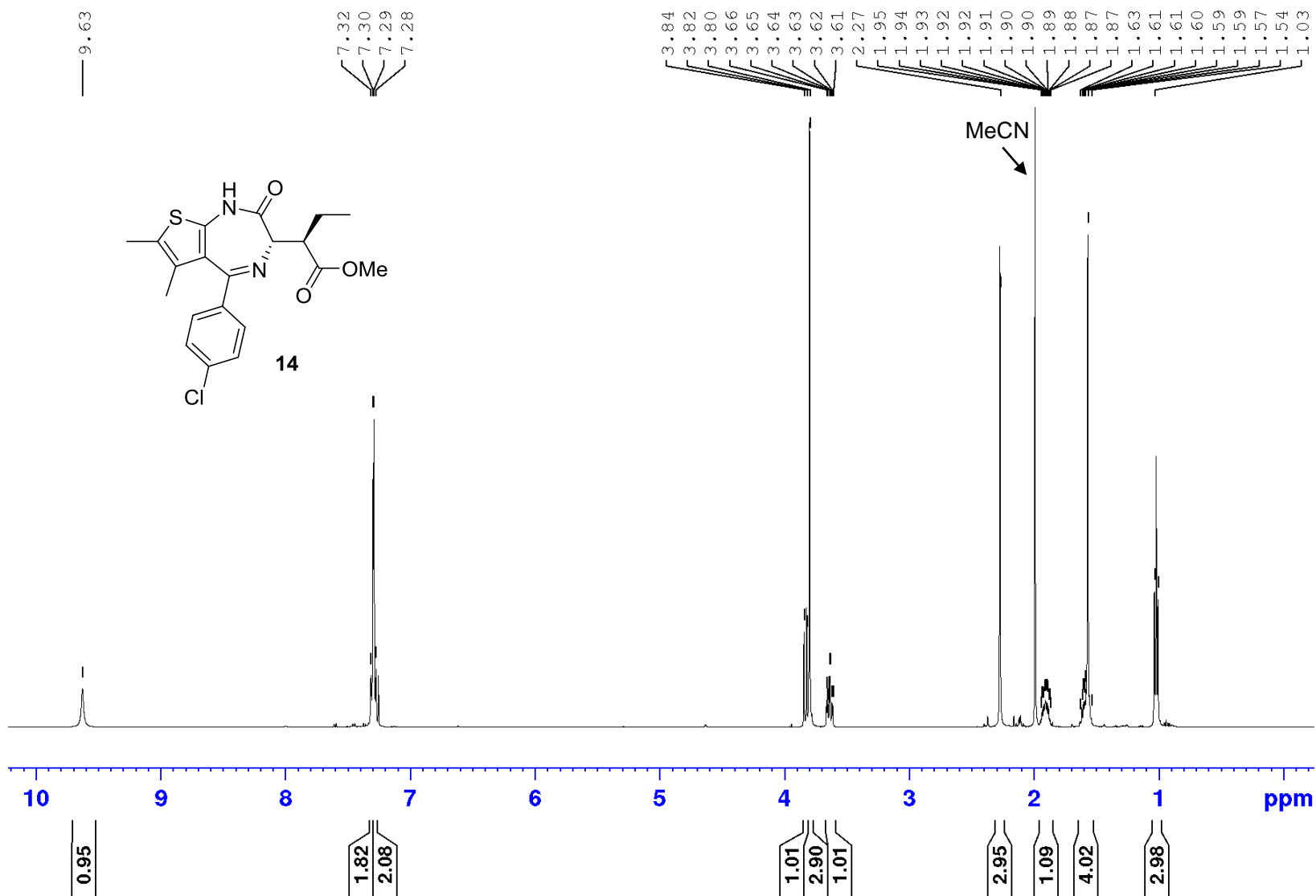
$^1\text{H-NMR}$, CDCl_3



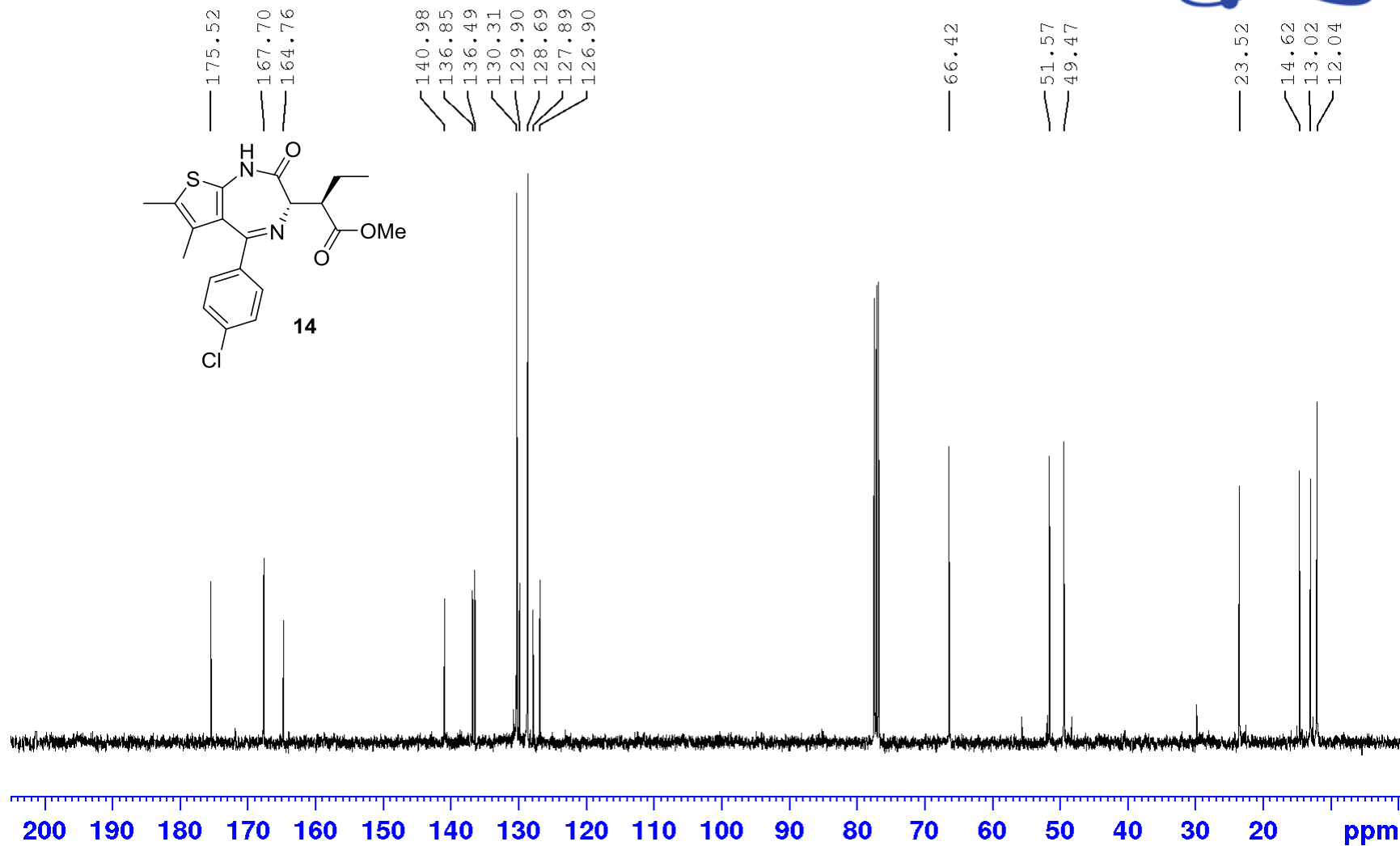
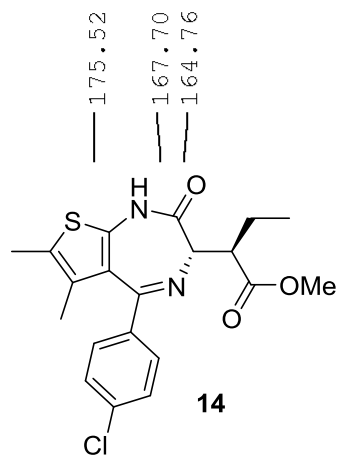
^{13}C -NMR, CDCl_3

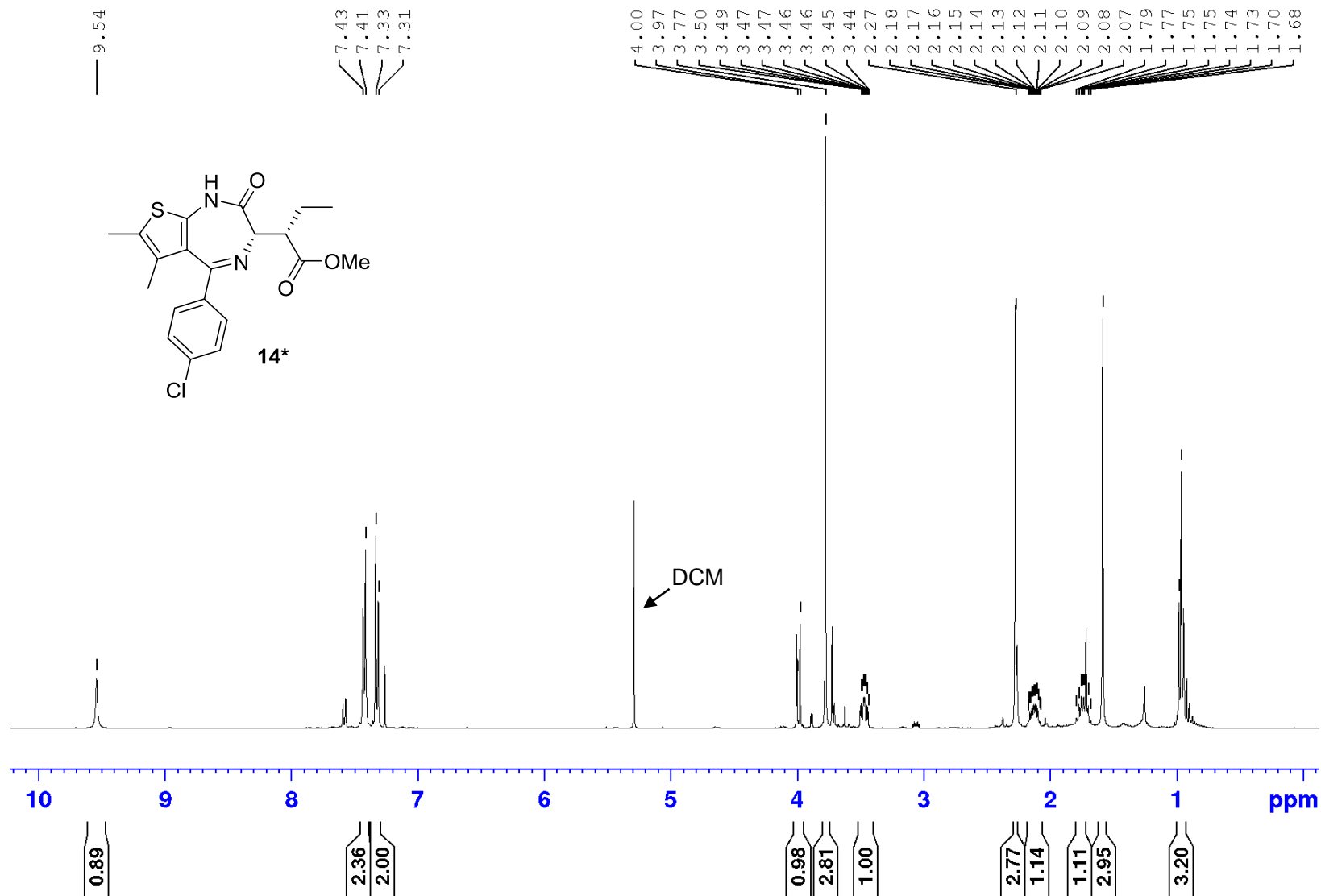


$^1\text{H-NMR}$, CDCl_3

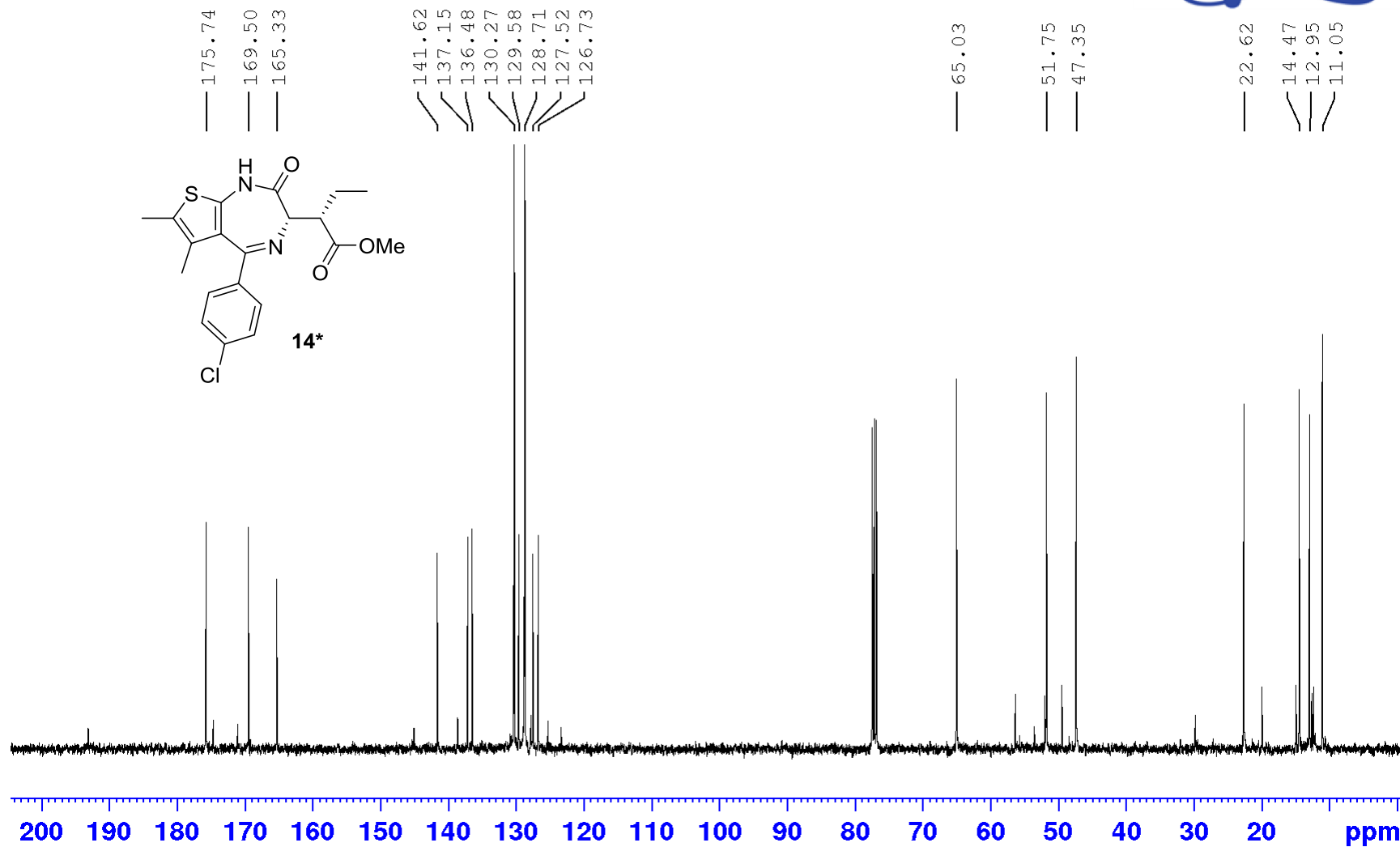


^{13}C -NMR, CDCl_3

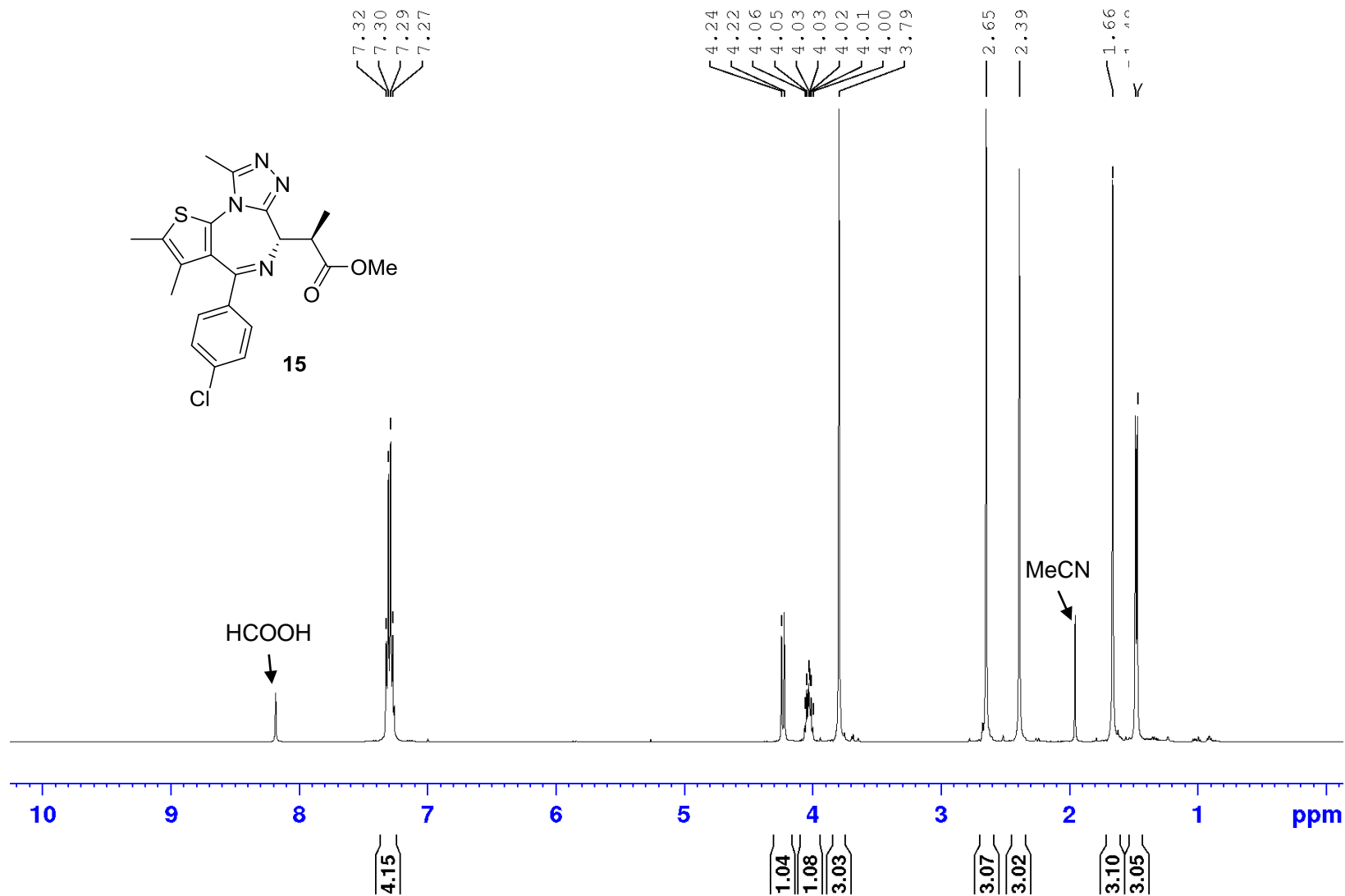




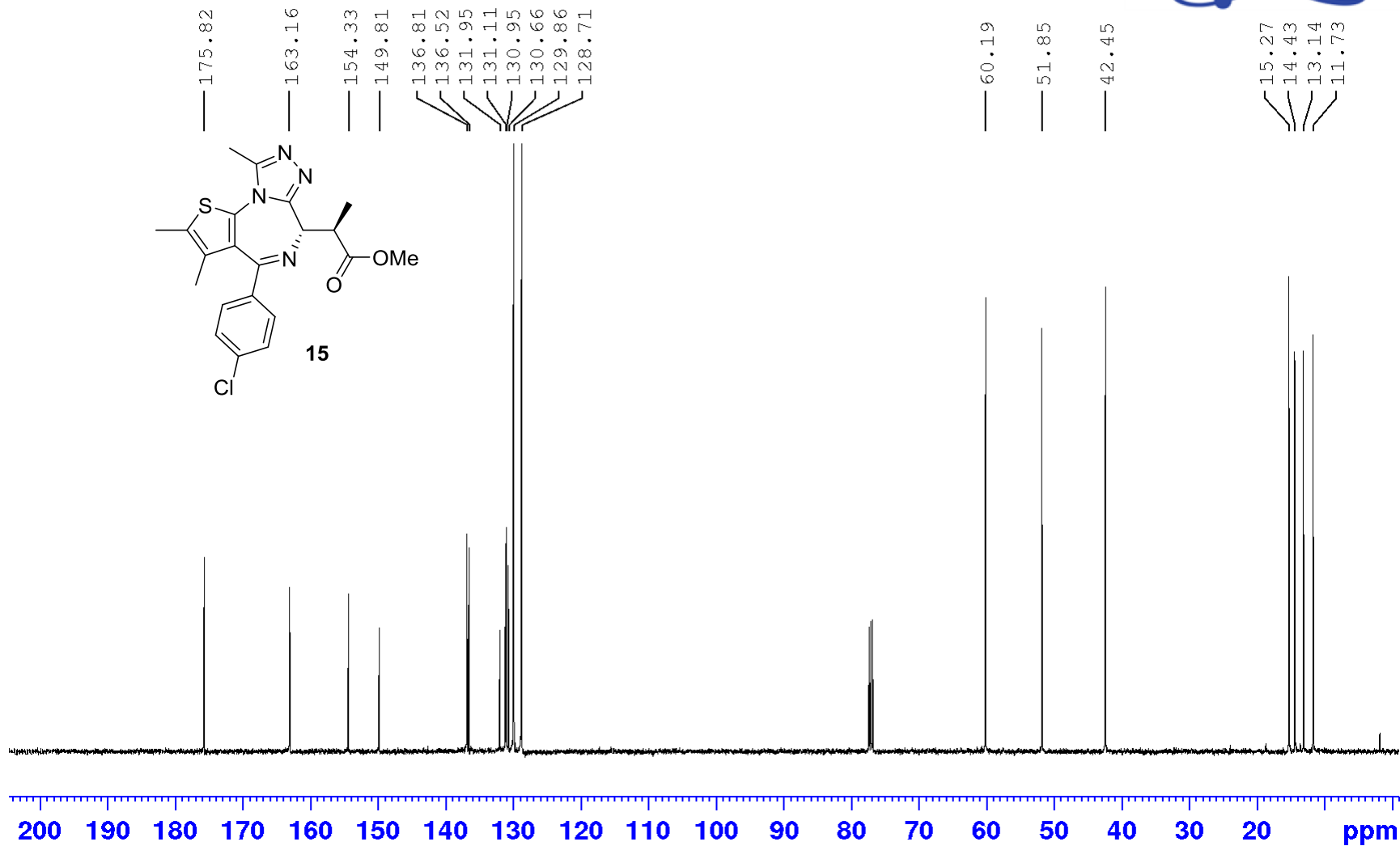
^{13}C -NMR, CDCl_3



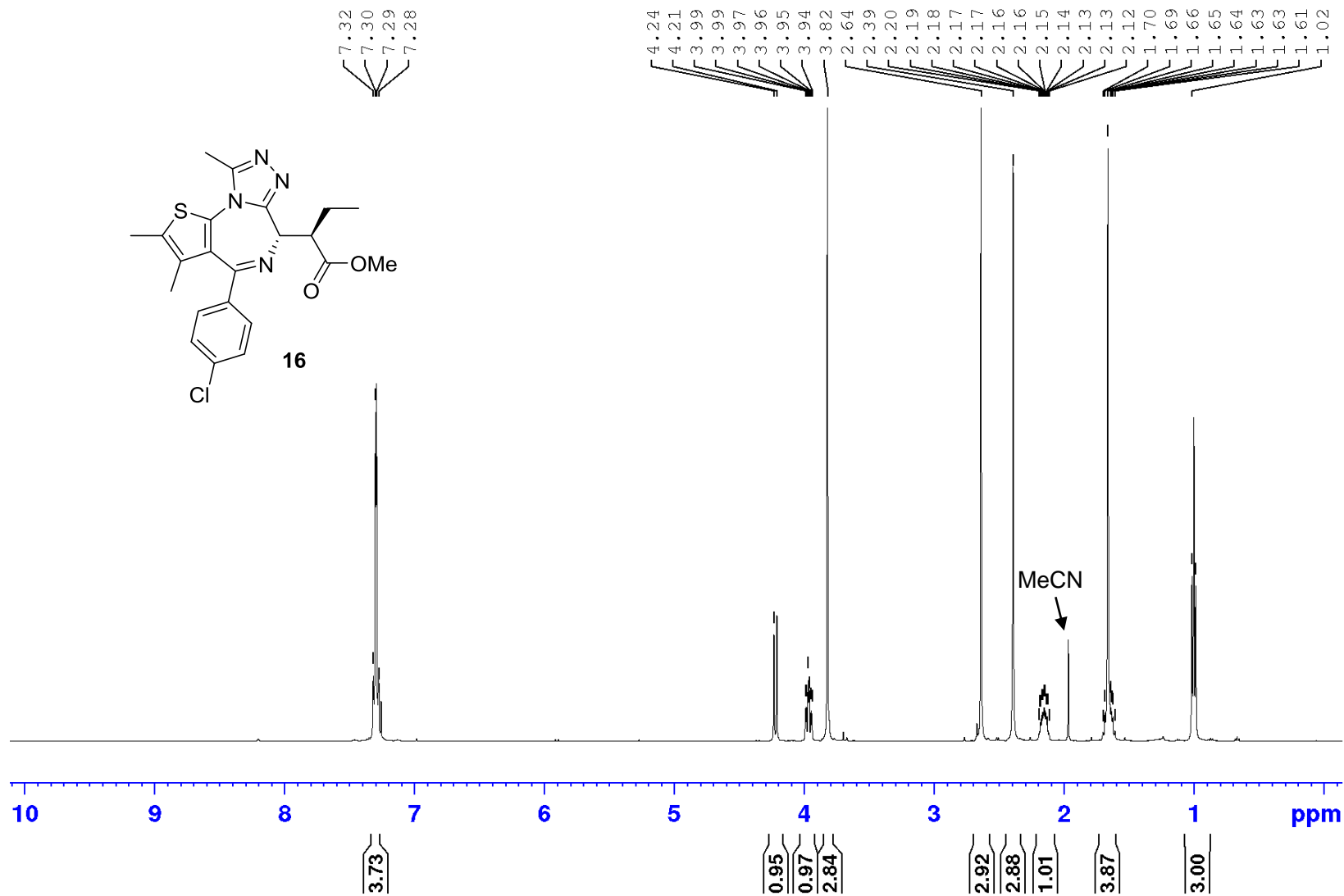
$^1\text{H-NMR}$, CDCl_3



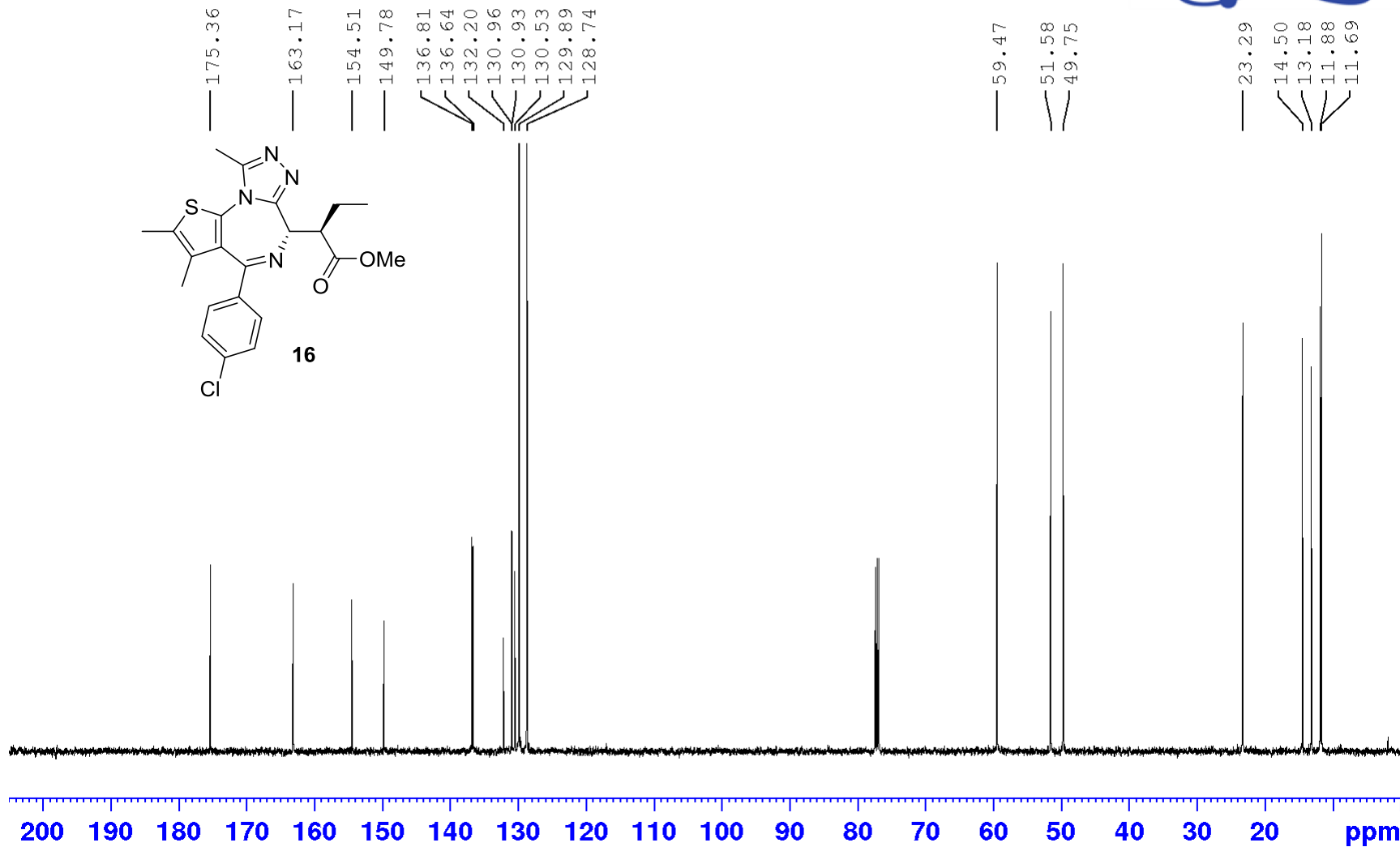
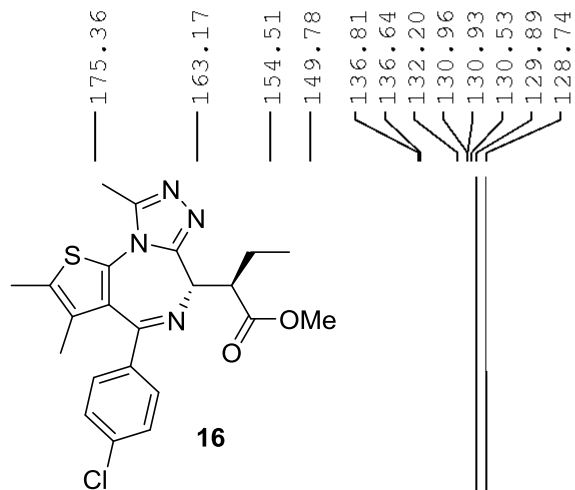
^{13}C -NMR, CDCl_3



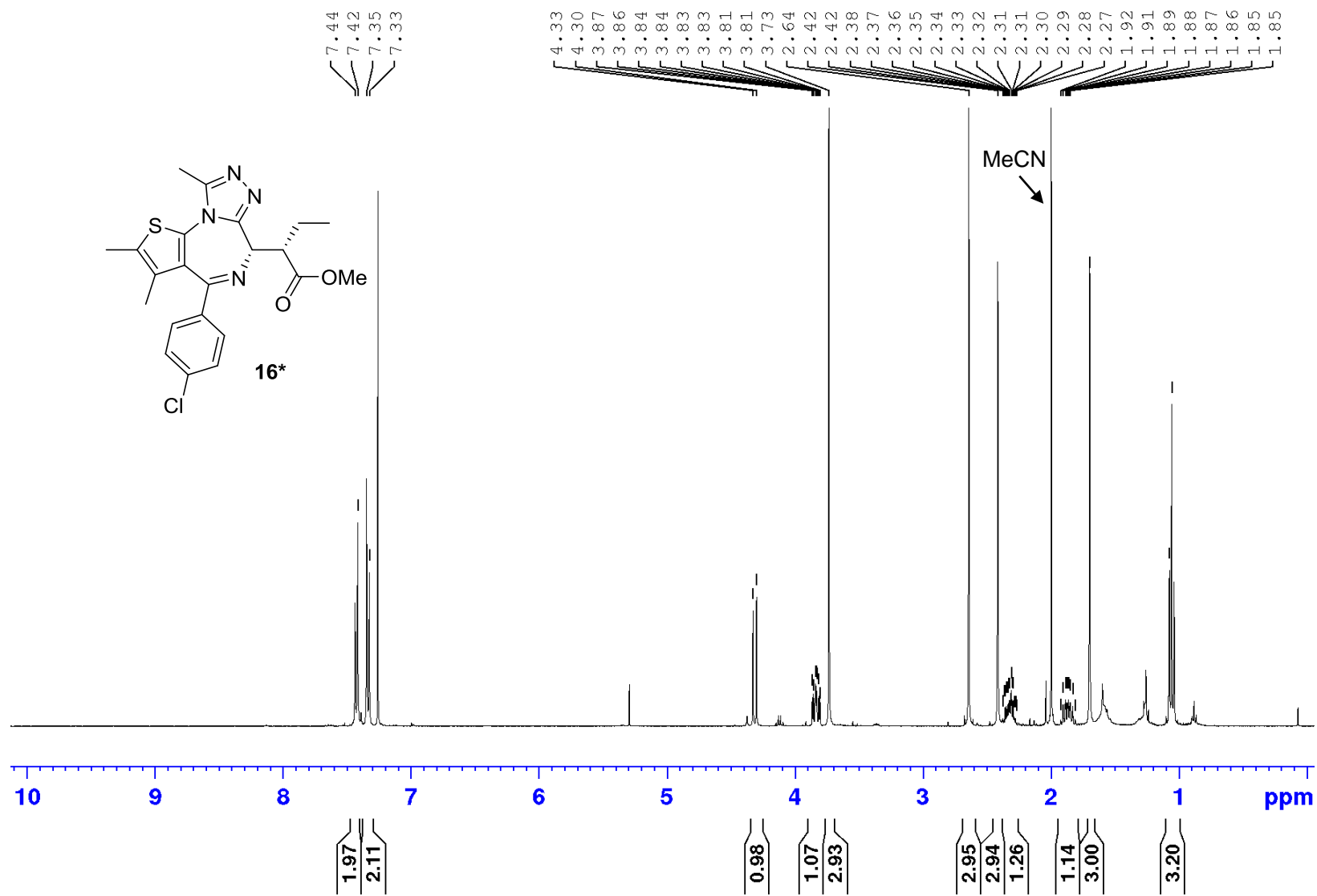
$^1\text{H-NMR}$, CDCl_3



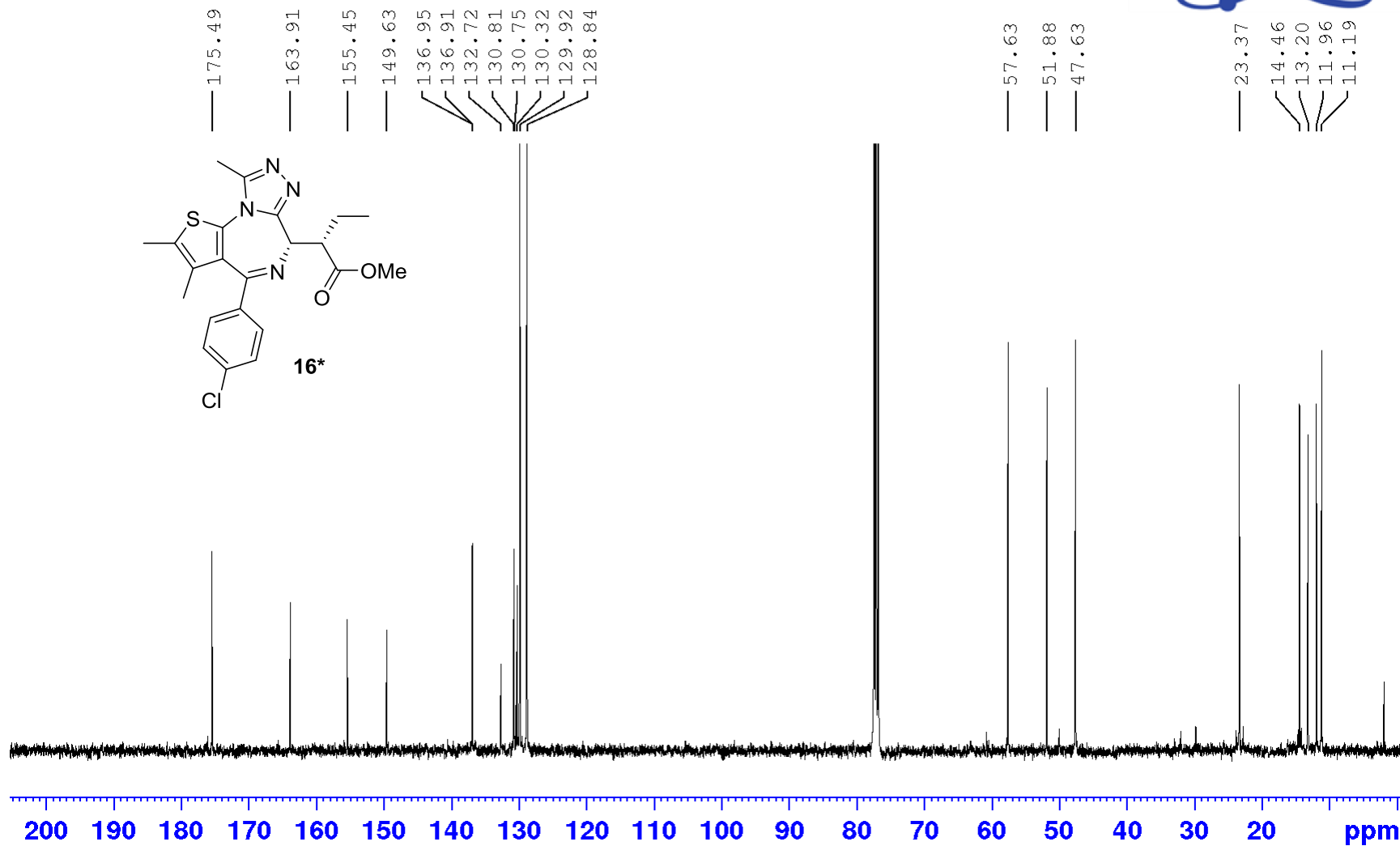
^{13}C -NMR, CDCl_3



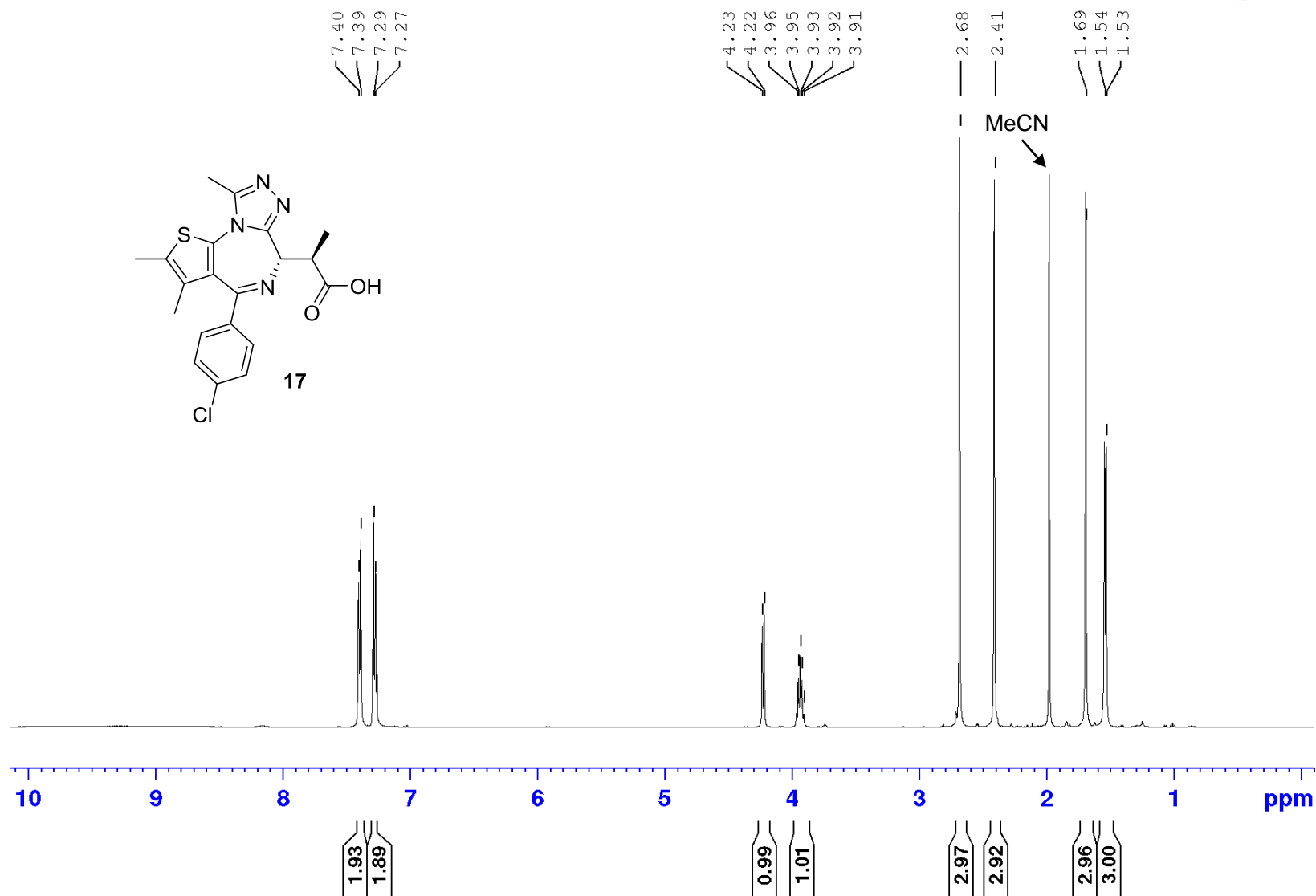
$^1\text{H-NMR}$, CDCl_3



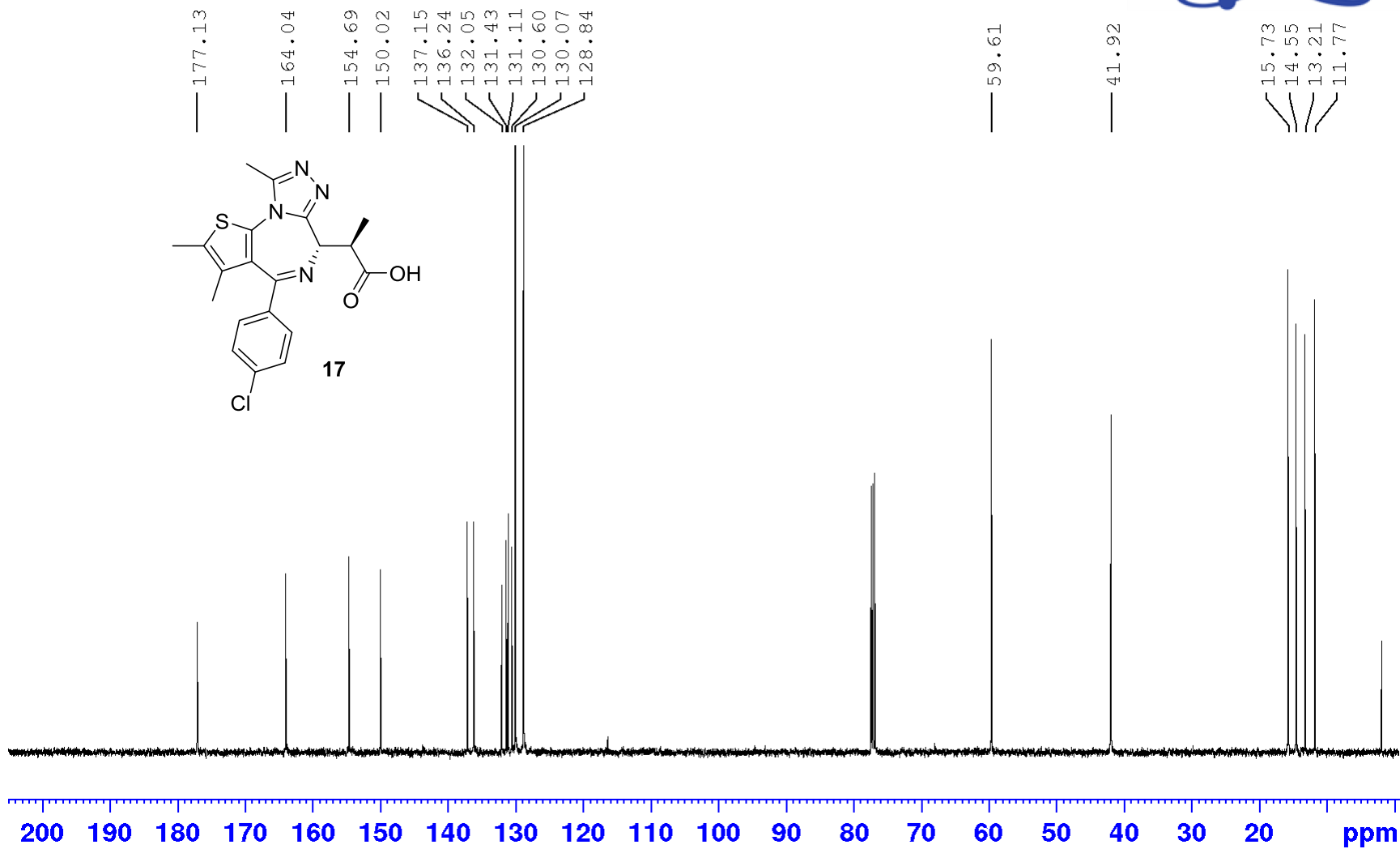
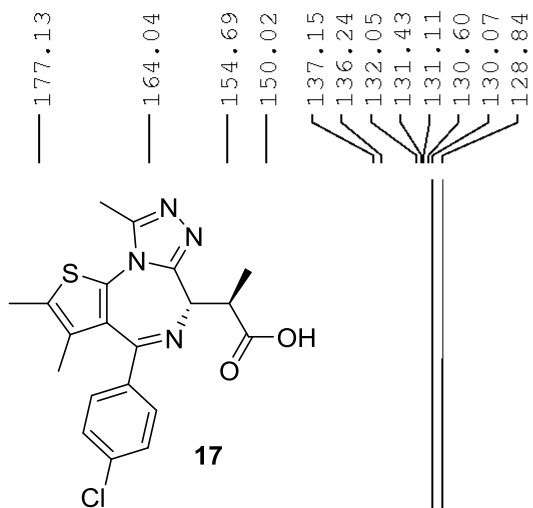
^{13}C -NMR, CDCl_3



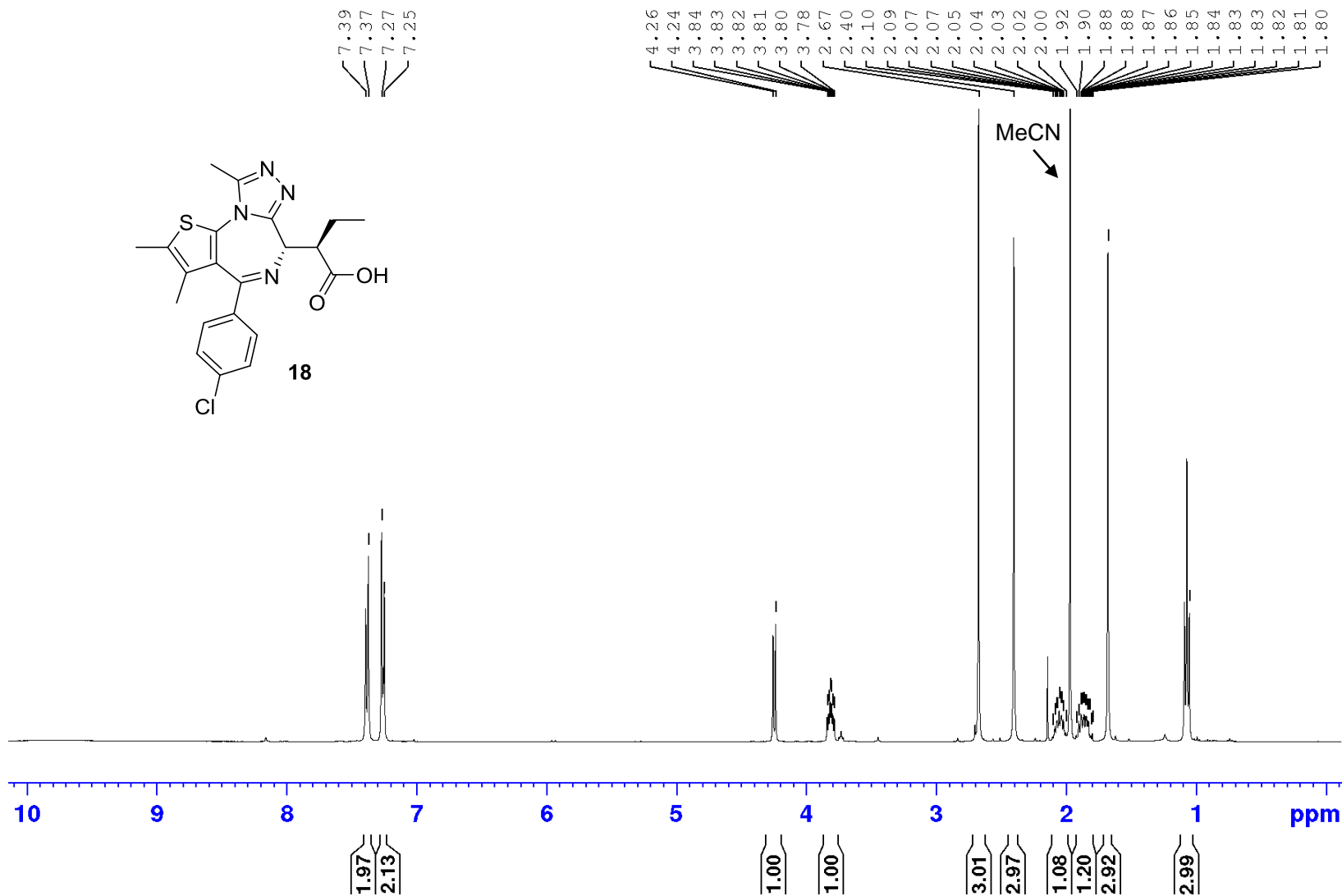
$^1\text{H-NMR}$, CDCl_3



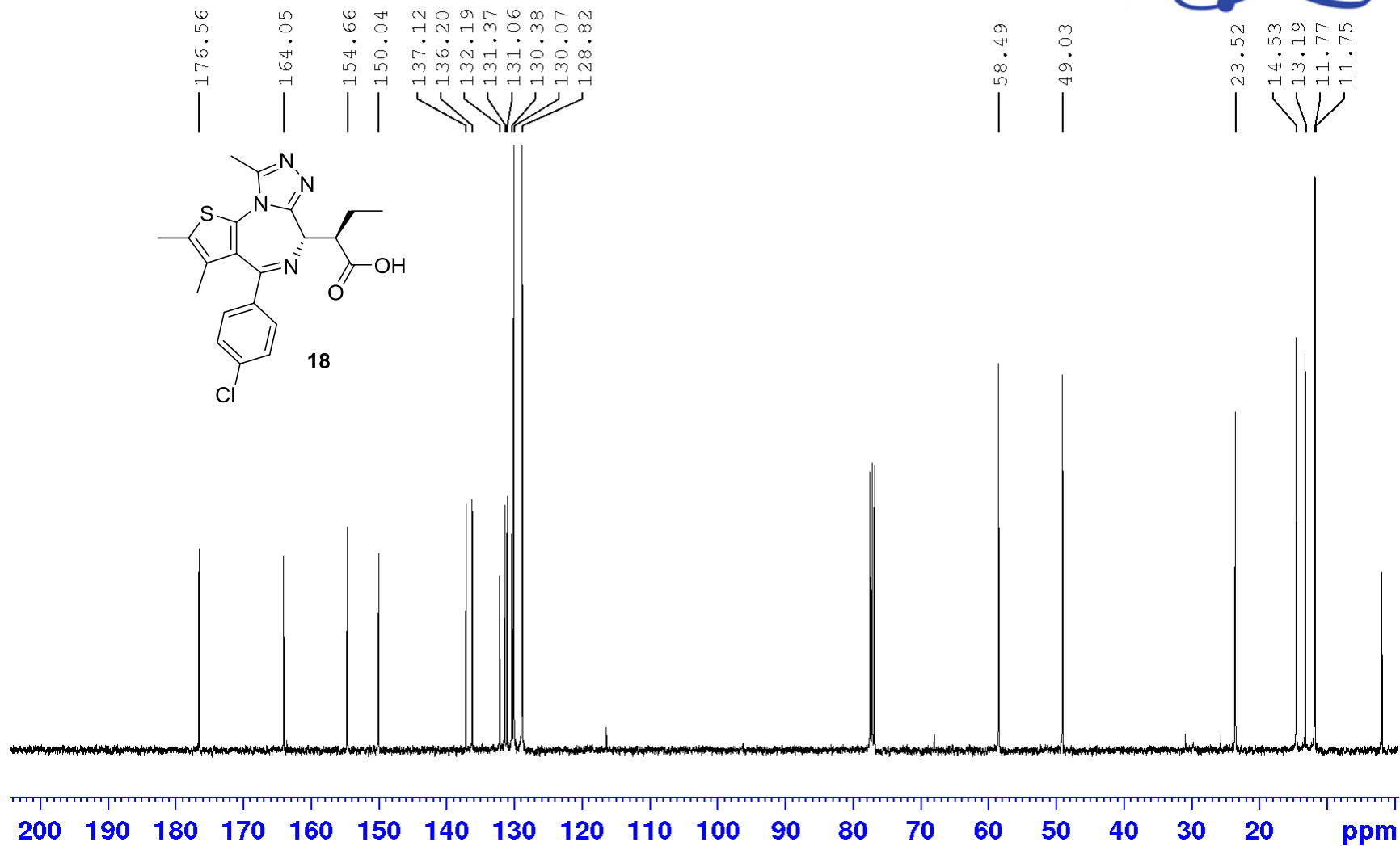
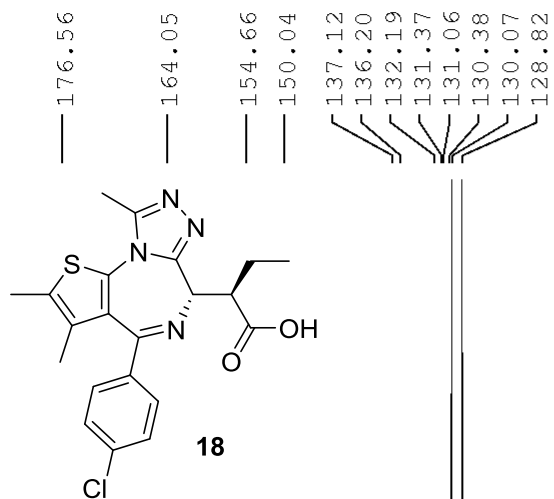
^{13}C -NMR, CDCl_3



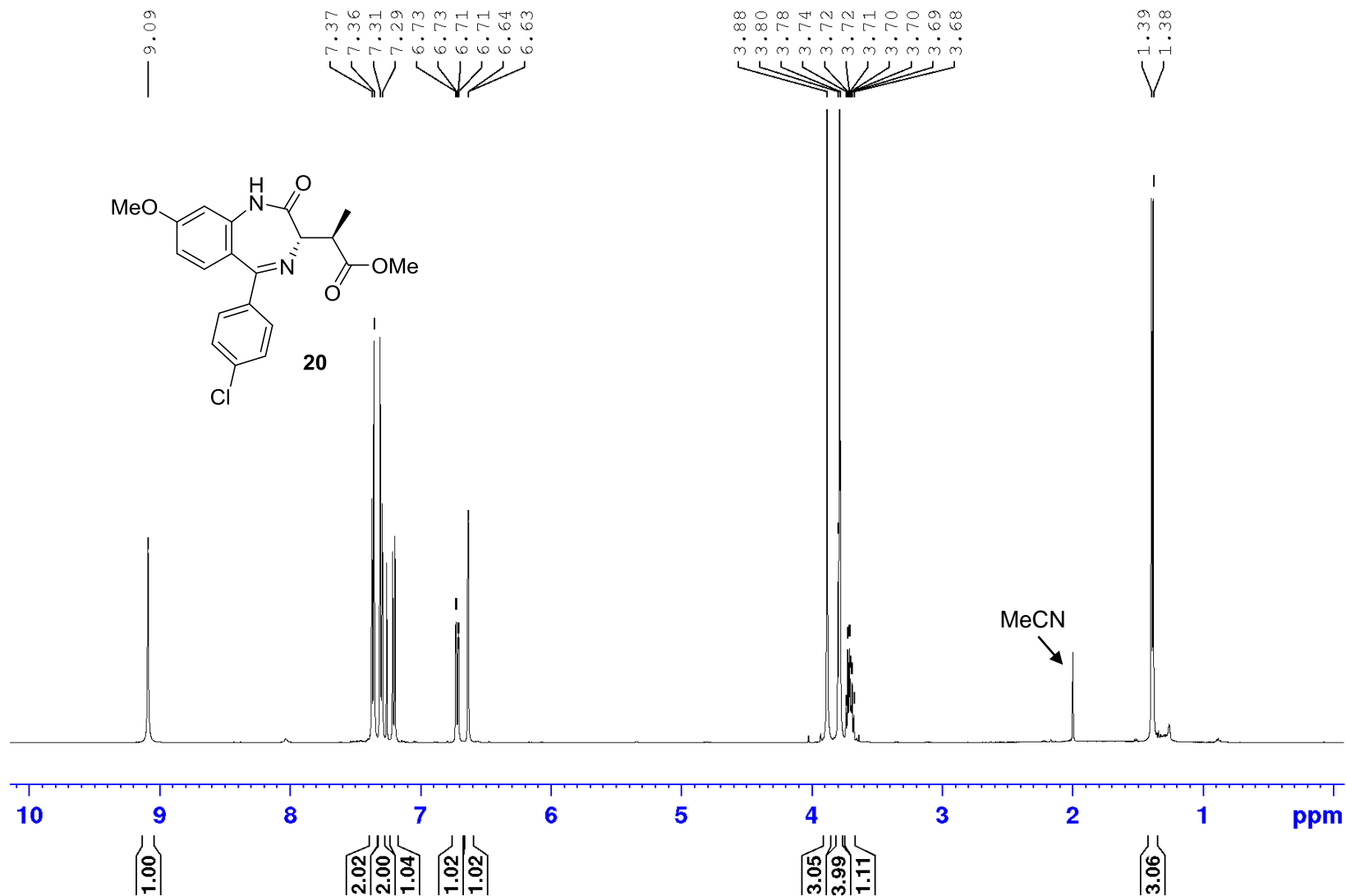
$^1\text{H-NMR}$, CDCl_3



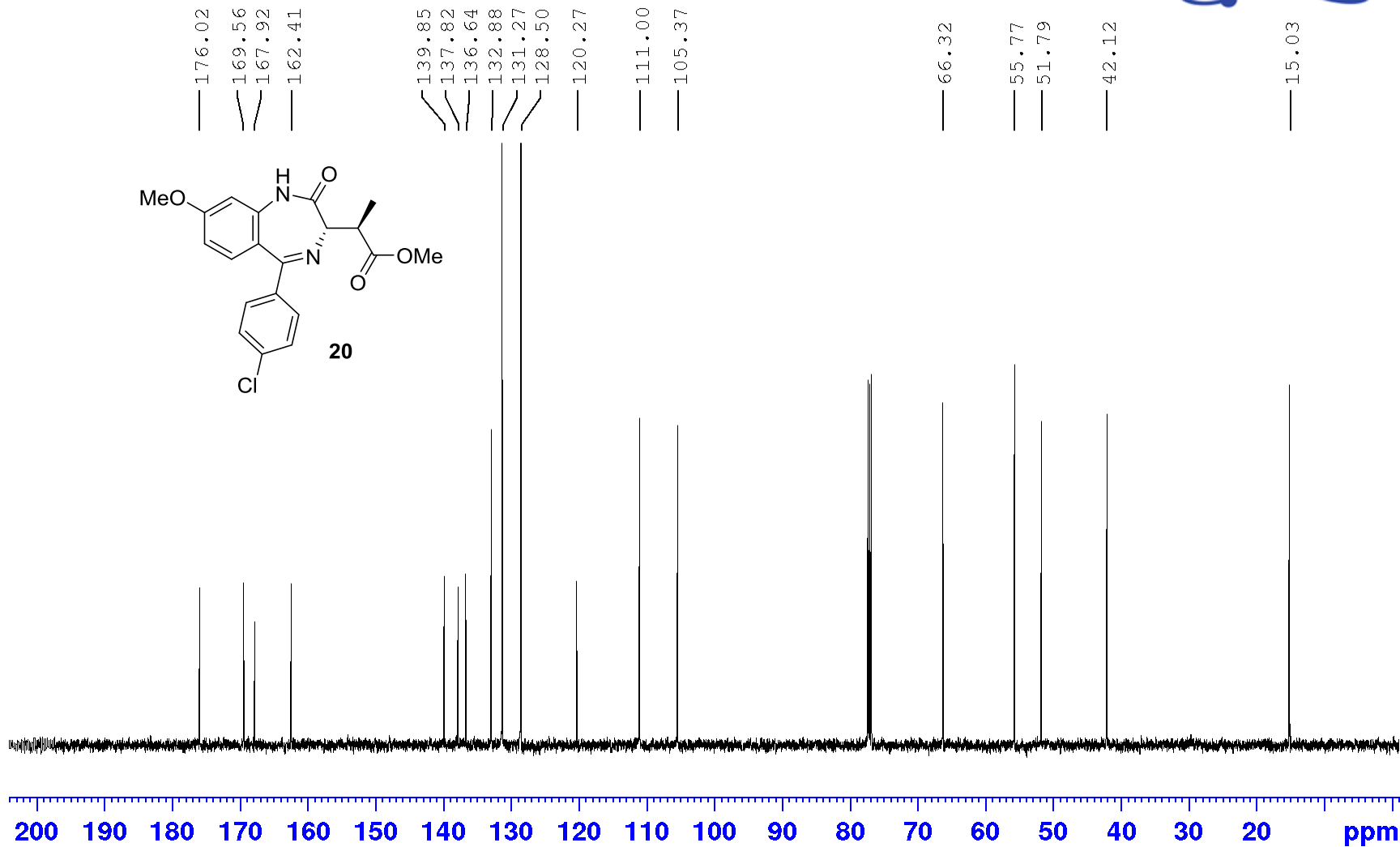
^{13}C -NMR, CDCl_3



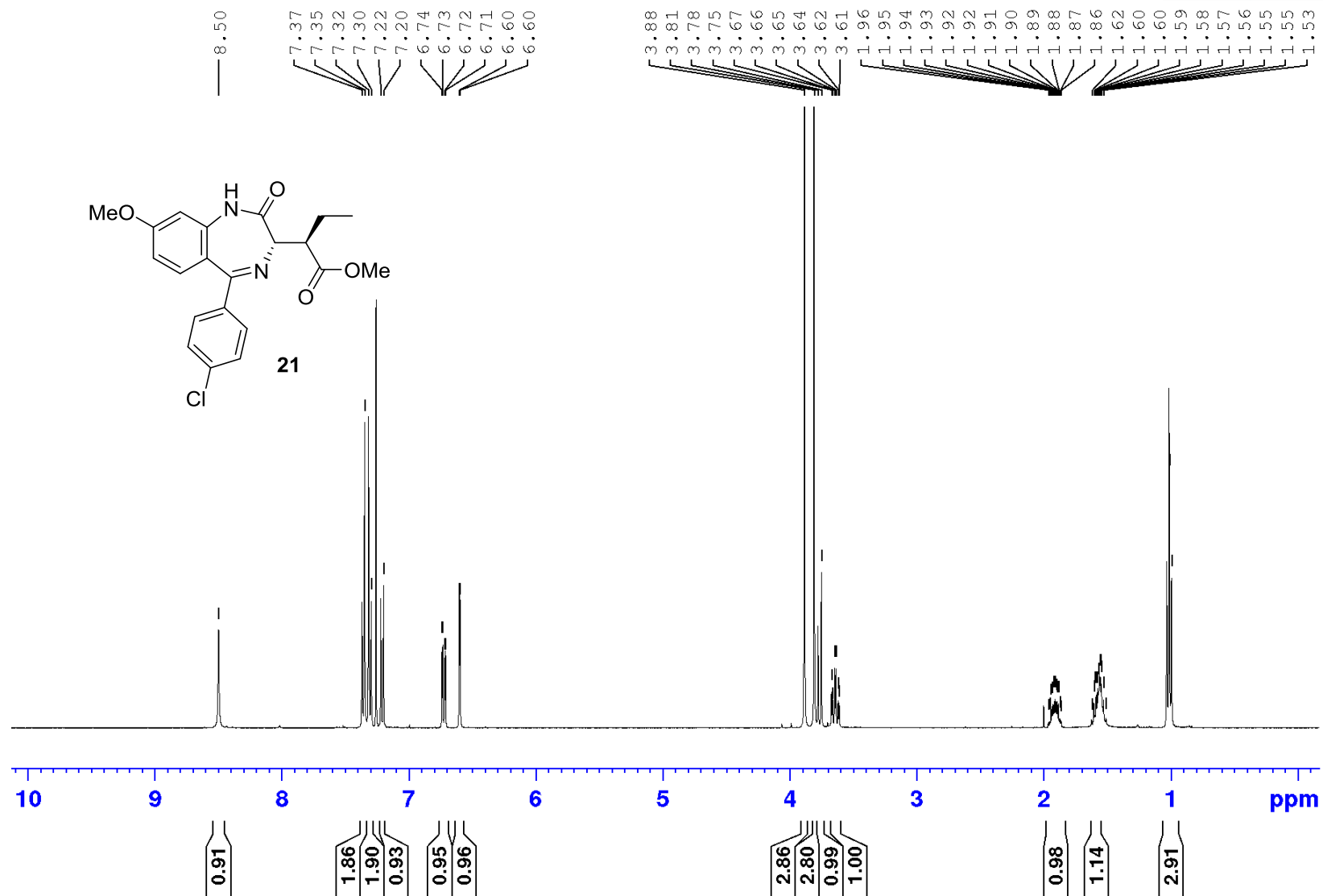
$^1\text{H-NMR}$, CDCl_3



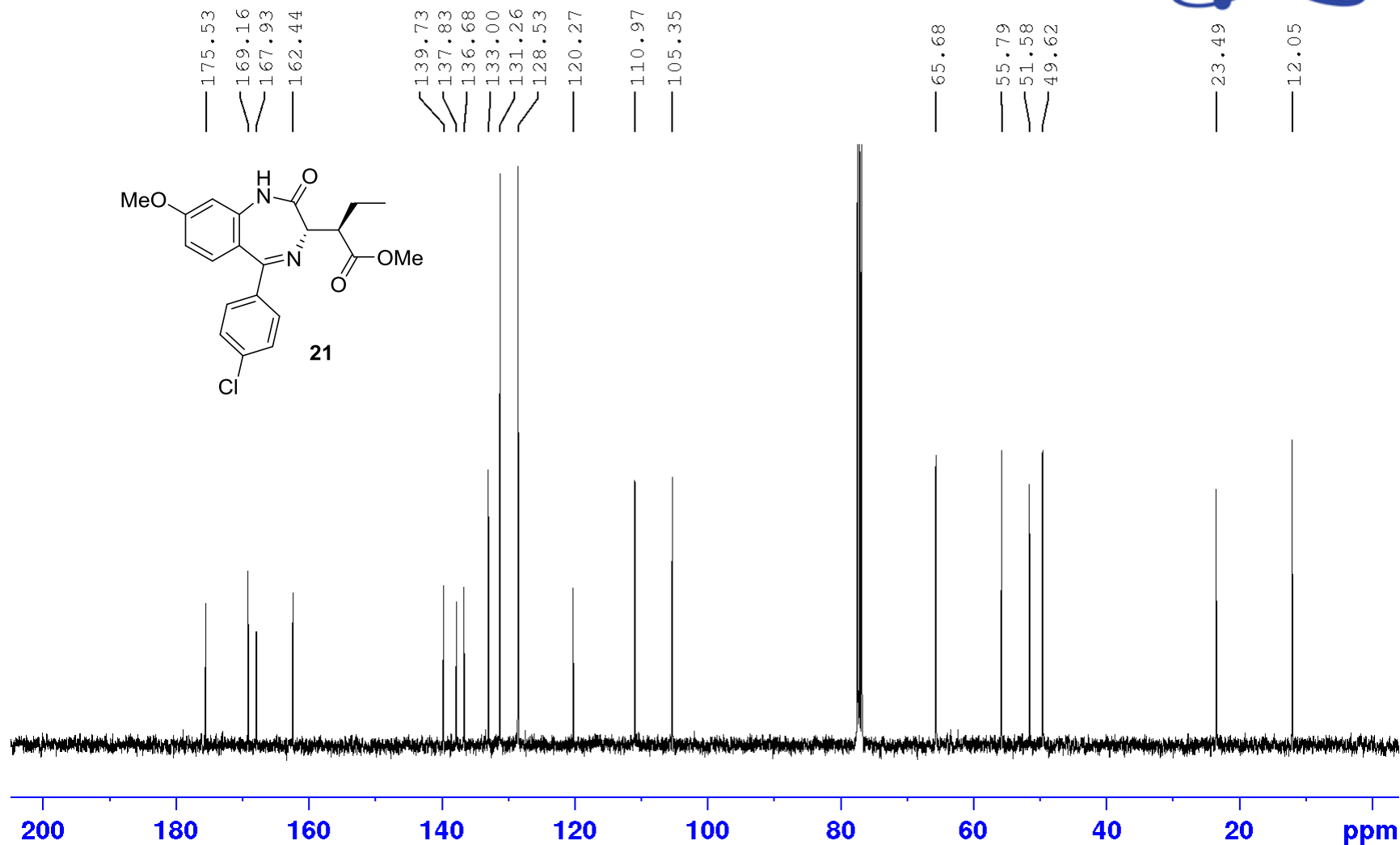
^{13}C -NMR, CDCl_3



$^1\text{H-NMR}$, CDCl_3



^{13}C -NMR, CDCl_3



Merged Supporting Information 2.pdf (3.41 MiB)

[view on ChemRxiv](#) • [download file](#)
